ENVIRONMENTAL CHAMBER STUDIES OF VOC SPECIES IN ARCHITECTURAL COATINGS AND MOBILE SOURCE EMISSIONS

Final Report to the

South Coast Air Quality Management District
Contract No. 03468

By

William P. L. Carter, Irina L. Malkina, David R. Cocker III, and Chen Song

July 5, 2005

Center for Environmental Research and Technology
College of Engineering
University of California
Riverside, California 92521

ABSTRACT

Environmental chamber experiments were carried out to assess the atmospheric ozone and particle matter (PM) impacts of selected representative VOCs emitted from architectural coatings. The UCR EPA environmental chamber was employed for the ozone and PM impact experiments, and most consisted of incremental reactivity experiments carried out at NO_x levels of 25-30 ppb and at ambient surrogate ROG/NO_x ratios representing maximum incremental reactivity (MIR) and NO_x-limited conditions. The compounds studied included the representative water-based coatings VOCs ethylene and propylene glycol, 2-(2-butoxyethoxy)-ethanol (DGBE), and benzyl alcohol. In addition, measurements of PM formation were made in experiments for these compounds and also in experiments with Texanol® (isobutyrate monoesters of 2,2,4-trimethyl-1,3-pentanediol), and several representative hydrocarbon solvents that were carried out for a separate project for the California Air Resources Board. Information was also obtained about PM background effects in the environmental chamber experiments.

The results of the chamber experiments were used to evaluate the predictions of the SAPRC-99 mechanism. The existing mechanism for DGBE was found to simulate the ozone reactivity data adequately, and a new mechanism for benzyl alcohol was developed that simulated the chamber data as well as mechanisms for other aromatics. The existing mechanisms for ethylene and propylene glycols were found to underpredict their ozone impacts by ~20% and 25-30% in some, but not all, experiments, but no scientifically acceptable basis was found to modify the mechanisms to improve these predictions. It is possible that that this is due to problems with the mechanisms for the aromatics present in the base ROG. The results of the experiments were also used to derive rate constants for the reactions of OH radicals with DGBE and benzyl alcohol relative to that for m-xylene, of 5.04×10^{-11} and 2.56×10^{-11}, respectively. The rate constant for DGBE is in good agreement with the estimated value used by SAPRC-99, and that for benzyl alcohol is in good agreement with another measurement in the literature.

In terms of PM impacts in the incremental reactivity experiments, the relative ordering was found to be benzyl alcohol >> DGBE > petroleum distillates > a synthetic hydrocarbon solvent consisting mainly of branched alkanes ≈ Texanol® > ethylene and propylene glycols. The benzyl alcohol was found to have a surprisingly high PM impact compared to other aromatics, and the glycols were found to actually reduce PM levels in the experiments, probably due to reducing rates of reactions of other VOCs present in the incremental reactivity experiment. No clear correlation between aromatic content and PM formation potential in the hydrocarbon solvents was seen. Background PM formation was observed in the chamber that will need to be characterized before these data can be used for PM model evaluation. Exploratory availability experiments were carried out to assess whether the presence of $(NH_4)2SO_4$ and NH_4HSO_4 seed aerosol at levels up to ~10 μg/m^3 and humidity up to ~10% RH affected the gas-phase loss rates or ozone formation potentials of ethylene and propylene glycol, but effects were seen.

Experiments with updated ambient reactive organic gas (ROG) surrogate mixtures that represents current emissions from mobile and other sources were also planned for this project, but they could not be carried out because of a lack of time and resources to derive a target composition for a new ROG surrogate within the timescale needed for this project.

ACKNOWLEDGEMENTS AND DISCLAIMERS

TABLE OF CONTENTS

LIST OF TABLES

LIST OF FIGURES

EXECUTIVE SUMMARY

Background

When emitted into the atmosphere, volatile organic compounds (VOCs) react in sunlight in the presence of oxides of nitrogen (NO_x) to contribute to the formation of ground-level ozone (O_3), and secondary particulate matter (PM) pollution, which are important air pollution problems in California. Emissions from architectural coatings are an important component of total VOC emissions into urban areas, as are emissions from mobile sources. In light of this, and as a part of the 1999 amendments to Rule 1113 – Architectural Coatings, the California South Coast Air Quality Management District (SCAQMD) Board approved a resolution, directing the SCAQMD staff to assess the reactivity and availability of solvents typically used in the formulation of architectural coatings. In addition, the SCAQMD staff desires to further understand the roles of various architectural coating emissions and mobile emission sources on ozone and particulate matter (PM) formation. Previous research has shown that different types of volatile organic compounds (VOCs) can differ significantly in their effects on ozone and PM formation, but significant uncertainties remain, particularly for compounds whose ozone and PM impacts have not been previously studied in environmental chamber experiments.

The California Air Resources Board (CARB), along with the SCAQMD, contracted the College of Engineering Center for Environmental Research and Technology (CE-CERT) at the University of California at Riverside to utilize the new UCR EPA environmental chamber to improve reactivity assessments of some solvent species found in architectural coatings. The new environmental chamber was recently constructed under U.S. EPA funding to permit well-characterized mechanism evaluation data to be obtained under more controlled conditions and at lower reactant than had previously been possible. To assess coatings VOC impacts, the CARB funded a subset of VOCs most commonly used in solvent-based coating formulations as well as the water-based coating solvent Texanol®[1], whereas the SCAQMD funding was used exclusively for the other common VOC species used in waterborne formulation, and also for studying PM impacts of the various solvents. An additional component of the SCAQMD-funded project was to investigate the utility of the UCR EPA chamber in availability studies of coatings VOCs, specifically to determine whether the presence of aerosols affects the gas-phase reactivities and availabilities of glycols.

Another component of the SCAQMD-funded project as proposed was to conduct environmental chamber experiments with reactive organic gas (ROG) surrogates representing current ambient emissions and concentrations in order to determine the most appropriate set of "base case" experiments to use in incremental reactivity assessment experiments and in experiments and model calculations to evaluate atmospheric impacts of motor vehicle emissions. However, after discussions with the CARB and SCAQMD staff, we were unable to address this objective because of insufficient time and resources to analyze the available data and derive an atmospheric composition to use as the basis for developing new atmospheric ROG surrogates during the time frame necessary for this project. Instead, environmental chamber experiments were conducted to study an additional water-based coatings compound.

The objectives, approach, results, discussion and conclusions for the work carried out for the SCAQMD project are summarized below. Relevant conclusions drawn from the CARB-funded portion of coatings VOC reactivity project are summarized as well.

---

[1] Texanol is a registered trademark of Eastman Chemical Company. It is used throughout this executive summary rather than the generic chemical name for simplicity.

Environmental Chamber Experiments for Ozone Mechanism Evaluation

The major task in this project was to conduct environmental chamber experiments to evaluate the ability of chemical mechanisms to predict atmospheric ozone impacts of the coatings solvents ethylene and propylene glycols, 2-(2-butoxy-ethoxy) ethanol or dipropylene glycol butyl ether (DGBE), and benzyl alcohol. The type of environmental chamber experiments carried out were "incremental reactivity" experiments, which involved determining the effect of adding the solvent to standard reactive organic gas (ROG) surrogate - NO_x experiments designed to simulate the chemical conditions of polluted urban atmospheres. (This is referred to as the "Base ROG" in the discussion in this report.) Experiments at two different ROG and NO_x levels were employed to represent different conditions of NO_x availability, to provide a more comprehensive test of the mechanisms under differing chemical conditions that affect reactivity. The total NO_x levels employed were in the 25-30 ppb range, which is designed to be representative of those in urban areas in California and which are lower than employed in previous reactivity chamber studies.

This approach was the same as used for the experiments carried out for the CARB-funded portion of the coatings VOC reactivity project, except in that case the compounds studied were the water-based coatings solvent Texanol® and representatives of different six different types of hydrocarbon solvents used in coatings. Together, these two projects cover the major types of coatings VOCs where environmental chamber data were needed to reduce uncertainties in model predictions of ground-level ozone impacts.

The compounds and solvents studied in the environmental chamber experiments for these two projects are summarized in Table E-1. The experiments were used to evaluate the reactivity predictions of the SAPRC-99 mechanism (Carter, 2000a), which is the mechanism used to derive the current version of the MIR scale used in California, and represents the current state of the art in this regard. The results of the evaluation against this mechanism are also summarized in Table E-1, and are discussed further below. (The table also includes a summary of the PM results, which are discussed in the following section.)

It is important to recognize that the ozone mechanism evaluation results are somewhat uncertain because the SAPRC-99 mechanism tends to underpredict rates of O_3 formation in the experiments that represent MIR conditions (Carter, 2004a). We believe that this is due to problems with the aromatics mechanisms that have not yet been addressed. In order to remove or at least assess this potential source of bias in the evaluation, evaluation calculations were also carried out with an adjusted version of the aromatics mechanism where the tendency to underpredict O_3 in the MIR simulation experiments was removed. This is not a "better" aromatics mechanism because it still has problems and its predictions are not consistent with results of experiments used to develop the current mechanism. For ethylene and propylene glycol experiments were carried out using a special base ROG surrogate where the aromatics have been removed, to assess the role of aromatic mechanism uncertainty in the evaluation results for these glycols.

The ozone mechanism evaluation results for the specific compounds studied for this project are briefly discussed below. The results for the compounds studied for the CARB project are discussed in more detail in the separate report and executive summary for that project (Carter and Malkina, 2005) (see also Table E-1).

Ethylene and Propylene Glycols. The atmospheric chemical mechanisms for these compounds appear to be reasonably well understood, and the measured relative consumption rates for these glycols in the chamber experiments for these compounds were consistent with their currently accepted OH radical rate constants. Nevertheless, the SAPRC-99 mechanism appears to have a tendency to underpredict the ozone impacts of these compounds in some in the chamber experiments at low concentrations and with

Table E-1.   Summary of solvents studied in the environmental chamber experiments and the overall conclusions from the evaluation results.

Compound or Mixture	MIR [a]		PM Impact or Approximate SOA Yields [b]	Discussion of Mechanism Evaluation Results [c]
	Previous	Revised		
Water Based Coatings VOCs				
Ethylene Glycol	3.36	3.63	Lower PM than base case	The glycolaldehyde product now represented explicitly. This mechanism still underpredicts glycol reactivity by 25-30% in experiments with aromatics in the base ROG surrogate, but there is no chemical justification for glycol mechanism adjustments
Propylene Glycol	2.74	No change	Lower PM than base case	This mechanism underpredicts glycol reactivity by ~20% in experiments with aromatics in the base ROG surrogate, but there is no chemical justification for glycol mechanism adjustments
Texanol® (Isobutyrate monoesters of 2,2,4-tri-methyl-1,3-pentanediol) [d]	0.88	No change	No net effect on PM formed evident	Experimental results for Texanol® and DGBE generally consistent with chamber data. The OH radical rate constants found to be in good agreement with the estimated values used in the mechanism.
2-(2-butoxyethoxy)-ethanol (DGBE)	2.86	No change	14 - 26%	
Benzyl Alcohol	None	4.89	~30%	Mechanism developed for this project and adjusted to fit the chamber data. Mechanism performance comparable to that for other aromatic compounds.
Hydrocarbon Solvents Studied for CARB Project [e]				
VMP Naphtha, Primarily C_7-C_9 mixed alkanes	1.41	1.35	0.1 - 0.7%	The experimental results for the primarily alkane, petroleum distillate-derived hydrocarbon solvents were generally consistent with the chamber data.
Dearomatized Mixed Alkanes, Primarily C_{10}-C_{12} (ASTM-1C)	0.91	0.96	~0.2%	
Reduced Aromatics Mineral Spirits, Primarily C_{10}-C_{12} mixed alkanes with 6% aromatics (ASTM-1B)	1.21	1.26	0.6 - 0.7%	

3

Table E-1 (continued)

Compound or Mixture	MIR [a] Previous	MIR [a] Revised	PM Impact or Approximate SOA Yields [b]	Discussion of Mechanism Evaluation Results [c]
Regular mineral spirits, Primarily C_{10}-C_{12} mixed alkanes with 19% aromatics (ASTM-1A)	1.82	1.97	0.3 - 0.8%	The experimental results were generally consistent with the chamber data.
Synthetic isoparaffinic alkanes, primarily C_{10}-C_{12} branched alkanes (ASTM-3C1)	0.81	1.1 - 1.5 [f]	No net effect on PM formed evident	Data not well simulated by the model. Model probably underpredicts atmospheric ozone formation by 25-75%, depending on the cause of the discrepancy.
Aromatic 100 (Primarily C_9-C_{10} alkylbenzenes)	7.51	7.70	0.3 - 0.4%	Experimental results representing MIR conditions generally consistent with model predictions. But model underpredicted O_3 inhibition in low NO_x conditions and has other problems.

[a] Maximum incremental reactivity in gm O_3 per gm VOC. Calculated as described by Carter (1994a,b). Values in "Previous" column are the MIR values incorporated in CARB regulations. The values for the compounds were from the most recent complete MIR tabulation given by Carter (1003). The values for the hydrocarbon solvents were derived using the CARB Bin assignments developed by Kwok et al (2000). No mechanism or MIR value previously existed for benzyl alcohol. Values in the "Revised" column are the best estimate MIRs based on the results of the current study. The changes in MIRs that may result when the mechanism is updated are unknown.

[b] For compounds with measurable positive PM impacts, the secondary organic aerosol (SOA) yields were derived from differences between PM volume levels in the base case and added test compound incremental reactivity experiments after 5 hours of irradiation. These approximate yields were estimated based on assuming same molecular weight for SOA as the starting material, assuming that the PM formed has the same density as water, and using approximate corrections for PM wall losses and approximate estimates of amounts of test compound or hydrocarbon solvent constituents reacted.

[c] Ozone prediction evaluation results are applicable to the SAPRC-99 mechanism (Carter, 2000a).

[d] Texanol was studied for the CARB project; see Carter and Malkina (2005) for details. Texanol is a registered trademark of Eastman Chemical Company.

[e] See Carter and Malkina (2005) for a discussion of the experimental and calculated data for the hydrocarbon solvent reactivities. The ASTM designations are based on the D 235-02 specification (ASTM, 2003).

[f] Range of MIRs for alternative mechanisms adjusted to fit the chamber data with this solvent. The available data are inadequate to distinguish between these mechanisms. See Carter and Malkina (2005).

aromatic-containing base ROG surrogates. as indicated on Table E-1. On the other hand, the model predictions were consistent with results of the experiments with these two glycols using a ROG surrogate with the aromatics removed, and also with results of higher concentration surrogate experiments carried out previously for Philip Morris (Carter et al, 1997). This suggests that the problem may not necessarily be the glycol mechanisms but may be in the mechanisms for the aromatics in the base surrogate. Given that the mechanisms and rate constants for these compounds are reasonably well established, and the results do not appear to be highly sensitive to uncertainties in the mechanisms for the glycol oxidation products, it is unclear what modifications to the mechanism for these compounds would be appropriate to improve the fits to these data.

The recommendation in this regard is to continue to use the current mechanism for these glycols to predict their atmospheric ozone impacts for the time being, but to re-examine them using the data from this project when the aromatics mechanisms have been updated. A project to update and hopefully address the problems with current aromatics mechanisms is underway for the CARB. When the mechanisms are re-evaluated using improved aromatics mechanisms that, for example, correctly predict radical levels and the effects of added CO, the reactivity data from this project can be used to indicate whether there are indeed problems with the glycol mechanisms that need further study. The updated data will then be made available to the SCAQMD, CARB, and others. If the problems persist, then there will be a need to verify the currently assumed product yields from these glycols, and to study the atmospheric reactivities of these products.

2-(2-Butoxyethoxy)-ethanol (DGBE). Despite the fact that there are no known kinetic and product data concerning the atmospheric reactions of DGBE, and that the current representation of this compound in the SAPRC-99 mechanism is based entirely on estimates, the results of the experiments for this project were entirely consistent with the predictions of the mechanism. This is true not only for predictions of its ozone impacts, but also for its OH radical rate constant, where the rate constant derived from the data in from this project was only 17% higher than the estimated rate constant used in the mechanism. Therefore, the data obtained in this project tended to validate the mechanism already used for this compound, and indicated no need to change the mechanism or its estimated reactivity in the MIR scale.

A similar result was observed in our previous experiments with the Texanol® isomers, where the OH radical rate constant and reactivity data derived from our experiments were entirely consistent with predictions of the estimated mechanism. Together, these data tend to support the predictive capabilities of mechanisms derived using the SAPRC-99 mechanism estimation and generation methods (Carter, 2000a), at least for these higher molecular weight glycol ethers and esters. However, the estimated mechanisms for these compounds are relatively complex, having many modes of reaction and competing processes involved in their photooxidations. Therefore, the relatively good performance in predicting rate constants and reactivities for these compounds may be due, at least in part, to cancellations of errors in the estimations of the many branching ratios and rate constants that go into the derivations of these mechanisms.

Benzyl Alcohol. This project resulted in the development of a new mechanism for the atmospheric reactions of benzyl alcohol, a compound that was not previously represented in the SAPRC mechanisms. Benzyl alcohol appears to be similar to other aromatic hydrocarbons in having relatively large internal radical sources and tending to enhance O_3 formation under MIR conditions, but inhibiting, or at least not enhancing, O_3 when NO_x is limited. As with other aromatics, many of the details of its atmospheric reactions are uncertain and difficult to estimate, but a suitably modified version of the existing parameterized SAPRC-99 mechanism for toluene was found to simulate the data at least as well

as mechanisms for other aromatics. The relative consumption rate of benzyl alcohol in the reactivity experiments indicated an OH radical rate constant of 2.56 x 10^{-11} cm^3 $molec^{-1}$ s^{-1}, which is in good agreement with the previously reported value of 2.29 x 10^{-11} that is used in the mechanism.

Since the new benzyl alcohol mechanism is reasonably consistent with the data obtained in this project and is consistent with the representation used for other aromatics, it represents our current best estimate for the purpose of calculating atmospheric ozone impacts of this compound. However, it suffers from the same problems as aromatic mechanisms in general, which use simplifying assumptions to represent many uncertain mechanistic details, and which do not correctly simulate certain aspects of the available environmental chamber data. Therefore, this mechanism will also need to be updated when we have new mechanisms for aromatics that can serve as a better basis for deriving a more explicit mechanism for this compound. The data obtained in this project will then be useful for evaluating and if necessary improving the updated mechanism for this compound once it is developed.

Investigation of PM Formation Potentials of Coatings VOCs

The second major objective of this project was to obtain measurements of PM impacts of the representative coatings VOCs that were studied for this and the CARB coatings reactivity project. As far as we are aware, there are no previous environmental chamber data concerning PM impacts of these particular compounds or solvents, nor are we aware of PM impact data for any VOCs under conditions as closely approximating atmospheric pollutant levels as these experiments and that also sufficiently well characterized for gas-phase mechanism evaluation.

Because of limited funding, the approach used in this task was not co carry out separate experiments to assess PM impacts of the coatings compounds or solvents, but to measure PM formation in the incremental reactivity environmental chamber experiments carried out primarily for ozone mechanism evaluation, as discussed above. The difference in PM formation between the base case ROG - NO_x irradiation with and without the added test VOC was used to provide an indication of the PM impacts of the test compounds.

In order to utilize chamber data for quantitative assessments of PM impacts, it is necessary to characterize background PM levels in the chamber. Therefore, experiments to address this were carried out as part of this project, and also under separate EPA funding. A small amount of background PM formation was observed in pure air and propene - NO_x irradiations, typically ~0.5 $\mu g/m^3$ in one reactor and ~0.1 $\mu g/m^3$ in the other, though no background PM was observed in dark experiments or in CO - NO_x or CO - air irradiations. The fact that the presence of CO inhibits background PM indicates that it is probably due to some background PM precursor reacting with OH radicals to form condensable products, but the source of the background material and the reason the background was always higher in one reactor than the other was not determined. Although this background PM needs to be characterized before the chamber can be used for quantitative PM mechanism evaluations at very low PM levels, this background PM is low compared to the PM levels typically used in chamber experiments used to evaluate PM formation potentials. Such background PM formation probably occurs in other chambers, but to our knowledge has not been investigated or reported to the extent that it has been in this work.

The PM levels formed in the base case experiments were higher than the background experiments, but were still relatively low. The base case PM volume after 5 hours of irradiation varied somewhat from run to run, typically being ~1.5 - 3 $\mu g/m^3$ in the higher background reactor and ~0.5 - 1 $\mu g/m^3$ in the other. PM formation in the base case experiments is attributed to the aromatics in the base ROG surrogate, since only background PM levels were seen in the base case experiments in the ROG

surrogate with the aromatics removed. (By comparison, the current annual and 24-hour average PM 2.5 standards are 15 and 65 $\mu g/m^3$, respectively.) The PM levels in the added coatings VOC experiments varied considerably depending on the VOC tested, ranging from lower levels than in the base case to ~40 $\mu g/m^3$. Note that if a test VOC has no PM formation potential itself it could suppress PM in the experiments where it is added if its reactions suppress OH radical levels, because reaction with OH is the expected source of PM precursors from the aromatics in the base ROG.

Table E-1, above, includes a summary of the relative PM formation potentials for the various VOCs that were studied for this and the CARB architectural coatings reactivity projects. These are given as qualitative effects on PM for compounds or solvents with low or negative PM impacts and as estimated secondary organic aerosol (SOA) yields for those that measurably enhanced PM levels in the experiments. Note that the estimated SOA yields are approximate, since they are based on assumed SOA densities and molecular weights that may not be appropriate, and the estimated amounts of test compound reacted are highly approximate for the hydrocarbon mixtures. Note also that the SOA yields shown on the table do not take into account the effect of the added test compound on SOA formation from the VOCs in the base ROG mixture and the background PM source. Since most of these coatings VOCs tended to suppress OH radical levels, and thus decrease the amount of reaction of the base ROG constituents or background PM source, the effect of the added test VOC on SOA formation from the reactions of the base ROG constituents would tend to be negative. Therefore, the actual SOA yields of the test compounds under the conditions of these experiments would probably be somewhat higher than shown on the table, particularly for the compounds with the lowest SOA yields.

In addition to depending on the yields of condensable products, the SOA yields will also depend on the amount of condensable product that partitions into the gas phase. According to equilibrium partitioning theory (Pankow 1994a,b), this will depend on the amount of organic aerosol mass present, as well as the compound and the temperature. Therefore, the SOA yields shown in Table E-1 are strictly speaking applicable for the conditions of these experiments, which had relatively low background and base case organic aerosol (typically less than ~3 $\mu g/m^3$, depending on the reactor). Note that the highest PM experiments in this study correspond approximately to organic aerosol content of the 24-hour PM 2.5 standard, and that most of the chamber experiments for this project have organic PM levels and therefore potentially lower SOA yields than would occur in highly PM polluted atmospheres in California. To completely characterize the SOA formation potential it would be necessary to measure SOA yields at a variety of organic aerosol levels, and also at differing temperatures, humidities, and reactant concentrations.

In terms of relative PM impacts, Table 12 indicates that the ordering was found to be benzyl alcohol > DGBE >> petroleum distillate-derived hydrocarbon solvents > a synthetic hydrocarbon solvent consisting primarily of branched alkanes ≈ Texanol® ≥ ethylene and propylene glycols. In some respects these results are qualitatively as expected, but in others they are not. This is discussed further below.

Benzyl alcohol had the highest PM impact of the compounds studied, and it apparently it also has higher PM impacts than most other aromatics that have been studied. The reason for this is unknown, except that it is apparently not due to reactions of benzaldehyde, which was found not to have a large PM impact in separate reactivity experiments carried out for another project. It would be worthwhile to investigate the reasons for the relatively high PM impact of this compound.

The PM formation impact of DGBE in our experiments was also higher than those any of the other compounds or mixtures studied for this project other than benzyl alcohol. This is despite the fact that the molecular weight of Texanol®, which had no measurable PM impact, is 33% higher than that of

DGBE. The main difference between DGBE and the Texanol® isomers is that DGBE is a straight chain compound while the Texanol® isomers have a relatively high degree of branching. As a general rule, long chain compounds tend to react to a greater extent by increasing oxidation on the molecule, while branched compounds tend to have a greater tendency to fall apart as they react. However, more data are needed before generalizations of predictive utility can be derived, and probably the SOA formation potentials of these complex molecules will need to be looked at on a case-by case basis.

While it is not surprising that the petroleum distillate solvents used in architectural coatings have some PM impacts, it is surprising that the ordering of the PM impacts of these solvents was not predicted by their aromatic contents. In particular, the "ASTM-1A" and "ASTM-1B" solvents, which are respectively 20% and 6% aromatics and the rest C_9-C_{12} mixed alkanes, had approximately the same, and in some experiments even greater, PM impacts than the 100% aromatic Aromatic-100 solvent. The alkanes in these solvents appear to be contributing to the PM impacts of these solvents, and may be more important as SOA precursors relative to aromatics than previously realized. It is likely that the normal and cyclic alkanes are more important contributors than the branched alkanes, given the increased tendency for branched compounds to break apart when they react. This is consistent with the fact that the primarily branched alkane synthetic hydrocarbon solvent "ASTM-3C1" had the lowest PM impact of all the hydrocarbon solvents that were studied.

Texanol® was found to have essentially no measurable effect on the volume of PM formed in the chamber experiments. However, Texanol® is also a radical inhibitor, and the decreased OH radical levels in the experiments where Texanol® is added should cause decreased PM formation from the reactions of the aromatics in the base ROG surrogate. Indeed, the addition of ethylene or propylene glycol did decrease PM formation in the experiments, which can be attributed to this effect. The fact that Texanol® did not decrease PM formation suggests that it may have some small amount of SOA formation, that is counteracting its inhibition of SOA formation from the aromatics in the base mixture. However, improved characterization of background effects and the mechanism of SOA formation in the base case experiments is needed to quantitatively assess this.

Both ethylene and propylene glycols were found to reduce PM formation in the experiments where they were added, which can be attributed to their inhibiting radicals and SOA formation from the reactions of the base case VOCs. This is not surprising since they are not predicted to form high molecular weight condensable products, and the availability experiments, discussed below, do not indicate that the glycols themselves are interacting with or partitioning into the aerosol phase.

Utilization of Environmental Chamber to Investigate Glycol Availability

An additional objective of this project was to investigate the potential utility of the environmental chamber for testing models for availability of emitted VOCs to react in the atmosphere to form O_3 and secondary PM. After discussion with members of the atmospheric availability subgroup of the U.S. EPA's Reactivity Research Working Group (RRWG) it was decided to focus on conducting several experiments to assess the effects of humidity and seed aerosol on availability, decay rates and reactivities of ethylene and propylene glycol. The experiments consisted of determining whether the presence of humidity and ammonium sulfate or bisulfate seed aerosol affects the gas-phase loss rates of these glycols I the dark or when irradiated in the presence of the ROG surrogate and NO_x, and whether it affects their impact on the glycols on O_3 formation and other measures of gas-phase reactivity.

The results of these experiments did not indicate that there is any tendency for ethylene or propylene glycol to interact with or partition into ammonium sulfate or ammonium bisulphate seed

aerosol, at least for humidities up to ~30% and inorganic aerosol loadings up to ~10 μg/m^3. However, this does not rule out the possibility for interactions affecting glycol availability at higher humidities or aerosol loadings, or for different seed compositions (organic or acidic). Although the capacity of the humidification and aerosol generation system limited the scope of what could be carried out for this project, these systems are currently being enhanced under funding from an EPA earmark, so our chamber should be capable of carrying out more comprehensive studies of effects of aerosol and humidity on availability and reactivity in the future.

In order to more comprehensively determine whether interactions with PM in the atmosphere significantly affect atmospheric availability of VOCs, a potentially more sensitive approach that may be more useful for screening purposes would be to determine whether exposure to gas-phase coatings or other VOCs causes growth of aerosol particles under simulated atmospheric conditions. This would indicate partitioning of the VOC onto the particle, which may be occurring to a sufficient extent to affect ozone formation potential. Once an effect of the VOC exposure to the aerosol is observed, then chamber experiments such as described in this report (though probably with higher seed aerosol loadings) would be needed to investigate the system further, and to determine whether the effect the PM on reactivity is indeed significant.

Overall Conclusions and Recommendations

This project expanded the ozone mechanism evaluation database to several VOC compounds that are important in water-based coatings, which is important to reducing uncertainties in predictions of atmospheric impacts of these compounds. However, uncertainties exist in the mechanisms of aromatic hydrocarbons emitted from mobile and other sources that affect the results of the atmospheric simulation experiments with these compounds, and the atmosphere in which these VOCs react, that increase uncertainties in mechanism evaluation and atmospheric reactivity predictions for these and other compounds. Work is underway to improve the aromatics mechanisms, which should ultimately reduce these uncertainties. This is being covered by an ongoing CARB project, though additional work may be needed to resolve these problems. Once improved mechanisms for the compounds in the ambient VOC mixture, then the results of these experiments can then be used to more comprehensively evaluate the mechanisms for the compounds of specific interest in this project. Therefore, the mechanism evaluation discussed in this report should not be considered the final result for this project.

Despite the uncertainties in the current mechanism and mechanism evaluation, we believe that the mechanism and reactivity estimates for the compounds presented in this report represent the current best estimate, and are appropriate for ozone reactivity assessments for regulatory and research at the present time.

Impacts on ground level ozone formation are not the only potential areas of concern for architectural coatings VOCs. Exceedences of PM standards are becoming an increasing concern and focus of research because of the known or suspected health impacts of atmospheric PM. Although SOA formation from the reactions of VOCs is not the only source of PM, it is an important PM source that will need to be included in any PM attainment strategies, particular for the finer PM that is if particular concern. The data obtained in this project, as well as previous studies in other chambers, clearly indicate that VOCs can differ significantly in their impact on secondary PM, and these differences will eventually have to be taken into account in any PM control strategy.

The results of this study indicate the difficulties that will be encountered when attempting to predict, even qualitatively, the relative PM impacts of different types of VOCs, in the absence of

9

environmental chamber data. For example, the PM impacts of two different water-based coatings VOCs were found to be different than predicted by their relative molecular weights, the aromatic contents of petroleum distillate hydrocarbon solvents were found to be poor predictors of their relative PM impacts, and benzyl alcohol was found to have an unexpectedly high PM impact compared to other aromatic compounds. More well-characterized environmental chamber data such as obtained for this project will be needed to develop *predictive* models for the affects of VOCs on PM formation, and this includes not only the characterization of the PM but also characterization of the gas-phase processes that lead to SOA precursor formation. A necessary component of this is characterization of PM background effects in chamber experiments.

Environmental chambers can also play a role in assessing and testing models for the interactions of gas-phase VOCs with PM and other surfaces, and therefore the availability of VOCs to react in the gas phase and promote ozone and SOA formation. The work for this project represents only a beginning in this regard, and additional work is clearly needed.

INTRODUCTION

Introduction and Background

As a part of the 1999 amendments to Rule 1113 – Architectural Coatings, the California South Coast Air Quality Management District (SCAQMD) Board approved a resolution, directing the SCAQMD staff to assess the reactivity and availability of solvents typically used in the formulation of architectural coatings. In addition, the SCAQMD staff desires to further understand the interactions between various architectural coating emissions and mobile emission sources on ozone formation. Because of this, they initiated participation in the USEPA's Reactivity Research Working Group (RRWG) to conduct research on reactivity-based controls to determine whether it is feasible as an alternative compliance option. Previous research had found that different VOC species have varying reactive properties to form ozone under the same NO_x environment. However, the research also highlighted the need for additional effort needed to reduce the uncertainty associated with the reactivity values determined using an environmental chamber, especially for the most commonly used solvents in architectural coatings formulations, and their impacts relative to impacts of mobile source emissions. If feasible, this optional strategy could allow manufacturers to use greater quantities of less reactive solvents, and reduce the quantity of higher reactive solvents to achieve ozone reductions.

The environmental chambers previously used to develop the existing models have a number of limitations, particularly for evaluating effects of some VOC species, as well as effects on particulate matter (PM) formation under controlled temperature, humidity, and lighting conditions and for evaluating secondary pollutant formation under lower pollution conditions representing near-attainment scenarios. Because of this, the U.S. EPA provided $3 million funding to the College of Engineering Center for Environmental Research and Technology (CE-CERT) at the University of California at Riverside (UCR) for the design, construction and operation of a state-of-the-art, next-generation environmental chamber facility capable of obtaining the data needed for assessing the use of reactivity data as an alternative ozone control strategy to the established mass reduction method (Carter et al, 1999; Carter, 2002a). This chamber was completed in 2003 and successfully employed to evaluate mechanisms for photochemical O_3 formation under low NO_x conditions (Carter 2004) and for other projects, discussed below.

The California Air Resources Board (CARB), along with the SCAQMD, contracted CE-CERT to utilize the new chamber to improve reactivity assessments of some solvent species found in architectural coatings, with each group funding the evaluation of certain VOC species most commonly used in architectural coatings. Due to limited funding available to both agencies, CARB funded a subset of VOCs most commonly used in solvent-based coating formulations as well as Texanol®, whereas the SCAQMD funding was used exclusively for the most common VOC species used in waterborne formulations.

The types of coatings VOCs to study for the CARB and SCAQMD projects were determined in consultation with the CARB and SCAQMD staff and the CARB's Reactivity Research Advisory Committee (RRAC). The RRAC consists of representatives of industry and regulatory groups, including the SCAQMD. The compounds chosen for study for the CARB project included Texanol®[2], an important compound in water-based coatings, and six different types of petroleum distillates that are utilized in

---

[2] Texanol is a registered trademark of Eastman Chemical Company. It is used throughout this report rather than the generic chemical name for simplicity.

solvent-based and (to a lesser extent) water-based coatings. The compounds chosen for study in the SCAQMD project included ethylene and propylene glycols, 2-(2-butoxyethoxy) ethanol (DGBE), and benzyl alcohol. The SCAQMD study also included an objective to assess the PM formation potential of all the solvents studied for the CARB and SCAQMD projects.

Furthermore, as indicated in the 1999 resolution to the Governing Board by SCAQMD staff, the issue of availability of low volatility or highly hydrophilic solvents to react in the gas phase and promote ozone formation is another area of potential concern when assessing ozone impacts of VOCs. If these compounds tend to be absorbed to any significant extent on surfaces or PM before they have a chance to react in the gas phase, then their actual impact on ozone formation would be less than predicted using gas-phase mechanisms in current models. For this reason, conducting research to improve our understanding and ability to quantify availability of VOCs for gas-phase reaction is one of the priorities of the Reactivity Research Working Group (RRWG) (RRWG, 1999). Although the current research funded by the RRWG focuses on modeling availability, environmental chamber experiments were anticipated to be useful for assessing availability of the VOC species and evaluating model predictions of availability. Because of this, on April 4, 2003 the SCAQMD Board approved a proposal to authorize the SCAQMD Chairman to execute a contract to conduct Reactivity and Availability Studies for VOC Species used in Architectural Coatings and Mobile Source emissions. The specific objectives and work carried out for this project are described below.

A report on the CARB study has recently been completed (Carter and Malkina, 2005), and that report should be consulted for a detailed discussion of the methods and results obtained for that project. The results of the study yielded useful information concerning the atmospheric ozone impacts of these compounds and the ability of the current SAPRC-99 detailed chemical mechanism (Carter, 2000a) to accurately simulate these impacts (Carter and Malkina, 2005). This report documents the results of the SCAQMD study of coatings VOCs, and also includes a summary of the overall conclusions that can be drawn from both studies.

Objectives

The overall objectives of this project are to conduct environmental chamber studies of selected architectural coatings VOCs and mixtures representing current mobile-source-dominated emissions to assess their impacts on ground level ozone and PM formation. This project builds upon and supplements a previous EPA project to evaluate and utilize the new "next generation" environmental chamber system for chemical mechanism evaluation and a CARB project to conduct experiments in that chamber on selected architectural coatings VOCs. The specifics of the work carried out for this SCAQMD project were determined in discussions with SCAQMD staff and the CARB's RRAC and the members of the Availability group of the RRWG. The specific tasks that were carried out include the following:

- Conduct environmental chamber experiments for reactivity assessment and chemical mechanism evaluation for several types of coatings or solvent VOCs selected by the SCAQMD in conjunction with discussions with the CE-CERT investigators and RRAC. The compounds chosen for study were propylene and ethylene glycols, diethylene glycol n-butyl ether (2-(2-butoxyethoxy)-ethanol, or dipropylene glycol butyl ether, DGBE), and benzyl alcohol. The two glycols were considered not to have uncertain mechanisms but were studied because of their extreme importance in the emissions inventories. DGBE was studied because it is also important in the water-based coatings inventory and has not been experimentally studied previously. Benzyl alcohol was studied because it is also emitted to some extent and had extremely high chemical mechanism uncertainty.

- Conduct measurements of PM formation in reactivity assessment and mechanism evaluation experiments not only for this project but also for the experiments carried out for the CARB coatings reactivity project. The data obtained can then be used to evaluate, at least in a qualitative sense, the PM formation potentials of the types of VOCs studied, and be available for potentially developing and evaluating models for their impacts on PM formation in the atmosphere.

- Carry out a limited number of experiments to characterize background effects related to PM formation that can be used when interpreting or modeling the PM formation in the chamber experiments discussed above, and that can serve as a basis for designing future PM studies in this chamber.

- Evaluate the potential utility of the environmental chamber for testing models for availability of emitted VOCs to react in the atmosphere to form O_3 and secondary PM. After discussion with members of the atmospheric availability subgroup of the RRWG it was decided to focus on conducting several experiments to assess the effects of humidity and seed aerosol on availability, decay rates and reactivities of ethylene and propylene glycol.

An additional objective for this project was to conduct environmental chamber experiments with reactive organic gas (ROG) surrogates representing current ambient emissions and concentrations in order to determine the most appropriate set of "base case" experiments to use in incremental reactivity assessment experiments and in experiments and model calculations to evaluate atmospheric impacts of motor vehicle emissions. However, after discussions with the CARB and SCAQMD staff, we were unable to carry out experiments to address this objective because of insufficient time and resources to analyze the available data and derive an atmospheric composition to use as the basis for developing new atmospheric ROG surrogates during the time frame necessary for this project. The proposed statement of work and the results of the discussions concerning this task are given in Appendix A to this report. This work still needs to be carried out, but it would have to be part of a future project.

Overall Approach

The chamber experiments were carried out in the new UCR EPA chamber, which was developed under EPA funding for more precise mechanism evaluation at lower and more atmospherically representative pollutant levels than previously possible (Carter et al, 1999; Carter, 2002). Results of initial experiments carried out in this chamber, including characterization results that are applicable to this study, are given in a previous report to the CARB Carter (2004). The approach employed followed that used in the CARB study of architectural coating VOC reactivity, which is described by Carter and Malkina (2005), and many of the experiments discussed there are also described in that report.

The major effort of this project consisted of conducting environmental chamber experiments, using the state-of-the-art UCR EPA chamber (Carter et al 2002; Carter, 2004), to assess their ozone and secondary PM formation potentials of selected compounds. As discussed in more detail previously (Carter and Malkina, 2005), the primary objective of these experiments with respect to ozone formation is not to directly measure atmospheric ozone reactivity, but to provide data to test the ability of chemical mechanisms used in models to predict their ozone impacts in the atmosphere. This is because atmospheric conditions that affect VOC reactivity are highly variable, and it is not practical to duplicate in an environmental chamber all of the physical conditions that will affect quantitative measures of atmospheric reactivity. Even if it were, the results would only be representative of the conditions of the particular experiments that were carried out. Instead the objective of the experiments is simulate, under well characterized conditions, representative *chemical* environments in which the VOCs react, and use the results to test the abilities of the chemical mechanisms used in models to predict the impacts of the VOCs

on ozone formation and other measures of reactivity in these environments. If the mechanism can be shown to adequately simulate the relevant impacts of the VOC in a range of chemical conditions representative of the atmosphere, one has increased confidence in the predictive capabilities of the model when applied to atmospheric scenarios. If the mechanism performance in simulating well-characterized experiments is less than satisfactory, then the need to improve the mechanism is indicated, and one has decreased confidence in its predictions of atmospheric reactivity.

On the other hand, the ability of current mechanisms to predict secondary PM formation in chamber experiments has not yet advanced to the point where chamber experiments can be used to test mechanisms for PM formation in the same way as they are used for testing ozone mechanisms. Therefore, at least for this initial study, the objective is to use the chamber data simply to assess qualitative impacts on PM formation, i.e., which compounds have measurable affects on PM and which are particularly reactive in this regard. The data obtained in these experiments may eventually be useful for this purpose, provided that background and chamber effects are adequately characterized. In any case, for this purpose it is important that the experiments reflect a chemical environment that is as representative of the atmosphere as possible, so that the empirical results may be reasonably indicative of trends in PM reactivity in the atmosphere.

The most realistic chemical environment in this regard is one where the test compounds or mixtures react in the presence of the other pollutants present in the atmosphere. Therefore, most of the environmental chamber experiments for this and the CARB program consisted of measurements of "incremental reactivity" of the subject compounds or solvents under various conditions. These involve two types of irradiations of model photochemical smog mixtures. The first is a "base case" experiment where a mixture of reactive organic gases (ROGs) representing those present in polluted atmospheres (the "ROG surrogate") is irradiated in the presence of oxides of nitrogen (NO_x) in air. The second is the "test" experiment that consists of duplicating the base case irradiation except that the VOC whose reactivity is being assessed is added. The differences between the results of these experiments provide a measure of the atmospheric impact of the test compound, and can be used as a basis to test a chemical mechanism's to predict these atmospheric impacts under the chemical conditions of the experiment.

Base case experiments to simulate ambient chemical environments require choice of an appropriate reactive organic gas (ROG) surrogate mixture to represent the reactive organics that are important in affecting ozone formation in the urban atmospheres. For this and the CARB project, we continued to use the 8-component "full surrogate" that was employed in our previous reactivity studies for the initial reactivity studies for this project. This is because as discussed previously (Carter et al, 1995a) use of this surrogate gives a reasonably good representation of ambient anthropogenic VOC emissions as represented in current models, and use of more detailed mixtures would not give significantly different reactivity results. However, because of experimental problems, for some experiments for this project the formaldehyde was removed from the surrogate and the initial concentrations of the other ROG components were increased by 10% to make up for the reactivity. Model calculations indicate that this surrogate modification should not have significant effects on experimental incremental reactivity results (Carter and Malkina, 2005). The surrogate without formaldehyde was used for all the experiments carried out for this program, but the surrogate with formaldehyde was used in the earlier experiments for the CARB project whose PM data are discussed in this report. Target and average measured compositions of the ROG surrogates for the reactivity experiments for these projects are given by Carter and Malkina (2005).

In order to provide data to test mechanism impacts of the test compounds or mixtures under differing atmospheric conditions, the incremental reactivity experiments for this and the CARB projects

were carried out using two different standard conditions of NO_x availability relevant to VOC reactivity assessment. Probably the most relevant for California regulatory applications is "maximum incremental reactivity" (MIR) conditions, which are relatively high NO_x conditions where ozone formation is most sensitive to VOC emissions. However, it is also necessary to provide data to test mechanism predictions under lower NO_x conditions, since different aspects of the mechanisms are important when NO_x is limited. The NO_x levels that define the boundary line between VOC-sensitive, MIR-like conditions and NO_x-limited (and therefore NO_x-sensitive) conditions is that which yields the maximum ozone concentrations for the given level of ROGs, or the conditions of the "maximum ozone incremental reactivity" (MOIR) scale. Therefore, experiments with NO_x levels that are approximately half that for MOIR conditions might provide an appropriate test of the mechanism under NO_x-limited conditions. This is referred to as "MOIR/2" conditions in the subsequent discussion. If NO_x levels are reduced significantly below this, the experiment becomes less sensitive to VOC levels and thus less relevant to VOC reactivity assessment.

The conditions of NO_x availability are determined by the ROG/NO_x ratios in the base case incremental reactivity experiments. In order to completely fix the conditions of these experiments, it is also necessary to specify a desired absolute NO_x level. In order to determine this, we sought input from the CARB staff concerning the NO_x levels they would consider to be appropriate to use for reactivity studies in the new chamber (Carter and Malkina, 2005). Based on their input, and model simulations of reactivity characteristics in our chamber, it was determined that the nominal initial concentrations of the MIR base case experiment would consist of ~30 ppb NO_x and ~0.5 ppmC ROG surrogate, and the MOIR/2 experiment would consist of ~25 ppb NO_x and ~1 ppmC ROG surrogate (Carter and Malkina, 2005). These were therefore the two standard base cases for all the incremental reactivity experiments discussed in this report.

In order to investigate the extent to which uncertainties in the aromatics mechanisms may be affecting model simulations of the reactivity experiments with ethylene and propylene glycol, one reactivity experiment each for these two compounds were carried out using a non-aromatic base ROG surrogate. These experiments were based on the base case for the MIR reactivity experiments, except that the toluene and m-xylene were removed from the surrogate, and the initial concentrations of the other base ROG components were increased to yield approximately the same total base ROG concentration. These are designated "MIR-NA" in the tabulations (since they are still considered to represent relatively high NO_x MIR-like conditions that sensitive to VOCs) and are also referred to as the "non-aromatic surrogate" experiments in the discussions of the results.

In order to provide additional mechanism evaluation data for the benzyl alcohol, we also carried out an experiment where this mixture was irradiated in the presence of NO_x without any added base ROGs. Such experiments are not useful for alkanes or alkane-like materials such as glycols or glycol ethers that do not have large internal radical sources because the results are too sensitive to chamber effects to be useful for mechanism evaluation (Carter et al, 1982, Carter and Lurmann, 1991). However, for highly reactive materials such as aromatics and olefins such experiments are very useful because they are more sensitive to some aspects of the mechanism, and are not affected by uncertainties in mechanisms for other VOCs. An additional experiment was carried out where CO was added to the benzyl alcohol - NO_x irradiation, since experiments with other aromatics indicated problems with model predictions of the effects of CO on aromatic - NO_x irradiations (Carter, 2004a).

A number of other control and characterization experiments were also carried out in order to adequately characterize the conditions of the chamber for mechanism evaluation and background PM. These experiments are discussed where applicable in the results and modeling methods sections.

METHODS

Experimental Methods

Chamber Description

All of the environmental chamber experiments for this project were carried out using the UCR EPA chamber. This chamber was constructed under EPA funding to address the needs for an improved environmental chamber database for mechanism evaluation (Carter, 2002). The objectives, design, construction, and results of the initial evaluation of this chamber facility are described in more detail elsewhere (Carter, 2002; Carter, 2004). A description of the chamber is also given below.

The UCR EPA chamber consists of two ~85,000-liter Teflon® reactors located inside a 16,000 cubic ft temperature-controlled "clean room" that is continuously flushed with purified air. The clean room design is employed in order to minimize background contaminants into the reactor due to permeation or leaks. The primary light source consists of a 200 KW argon arc lamp with specially designed UV filters that give a UV and visible spectrum similar to sunlight. This light source was used for almost all of the experiments discussed in this report. Banks of blacklights are also present to serve as a backup light source for experiments where blacklight irradiation is sufficient. The interior of the enclosure is covered with reflective aluminum panels in order to maximize the available light intensity and to attain sufficient light uniformity, which is estimated to be ±10% or better in the portion of the enclosure where the reactors are located (Carter, 2002). A diagram of the enclosure and reactors is shown in Figure 1, and the spectrum of the light source is shown in Figure 2.

The dual reactors are constructed of flexible 2 mil Teflon® film, which is the same material used in the other UCR Teflon chambers used for mechanism evaluation (e.g., Carter et al, 1995b; Carter, 2000a, and references therein). A semi-flexible framework design was developed to minimize leakage and simplify the management of large volume reactors. The Teflon film is heat-sealed into separate sheets for the top, bottom, and sides (the latter sealed into a cylindrical shape) that are held together and in place using bottom frames attached to the floor and moveable top frames. The moveable top frame is held to the ceiling by cables that are controlled by motors that raise the top to allow the reactors to expand when filled or lower the top to allow the volume to contract when the reactors are being emptied or flushed. These motors are in turn controlled by pressure sensors that raise or lower the reactors as needed to maintain slight positive pressure. During experiments the top frames are slowly lowered to maintain continuous positive pressure as the reactor volumes decrease due to sampling or leaks. The experiment is terminated once the volume of one of the reactor reaches about 1/3 the maximum value, where the time this took varied depending on the amount of leaks in the reactor, but was greater than the duration of most of the experiments discussed in this report. Since at least some leaks are unavoidable in large Teflon film reactors, the constant positive pressure is important to minimize the introduction of enclosure air into the reactor that may otherwise result.

As indicated in Figure 1, the floor of the reactors has openings for a high volume mixing system for mixing reactants within a reactor and also for exchanging reactants between the reactors to achieve equal concentrations in each. This utilizes four 10" Teflon pipes with Teflon-coated blowers and flanges to either blow air from one side of a reactor to the other, or to move air between each of the two reactors. Teflon-coated air-driven metal valves are used to close off the openings to the mixing system when not in use, and during the irradiation experiments.

16
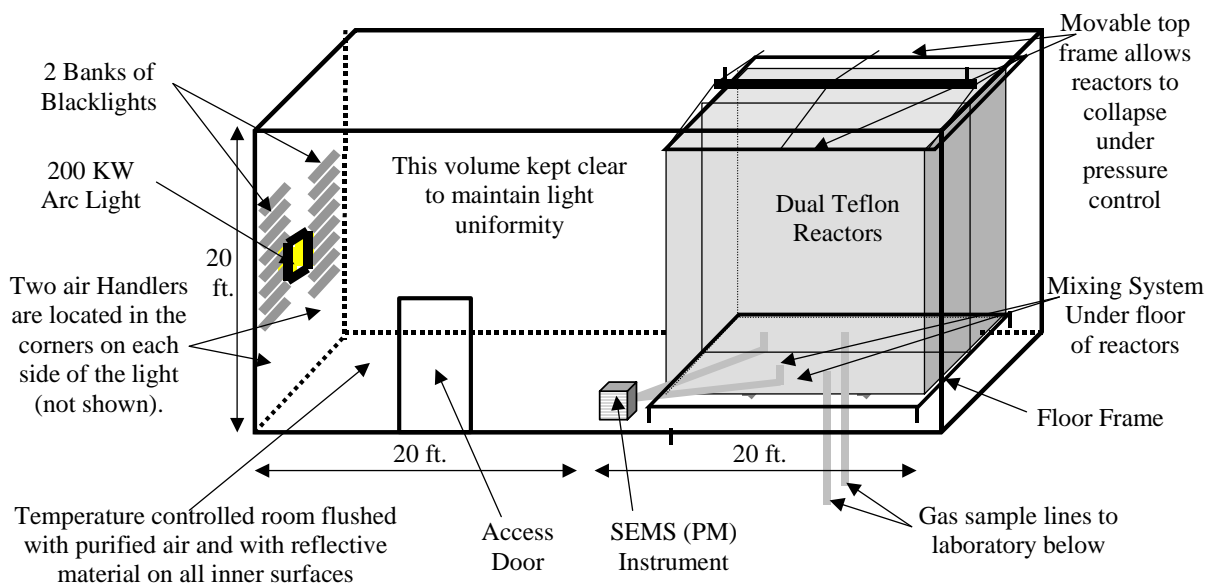
Figure 1.   Schematic of the UCR EPA environmental chamber reactors and enclosure.
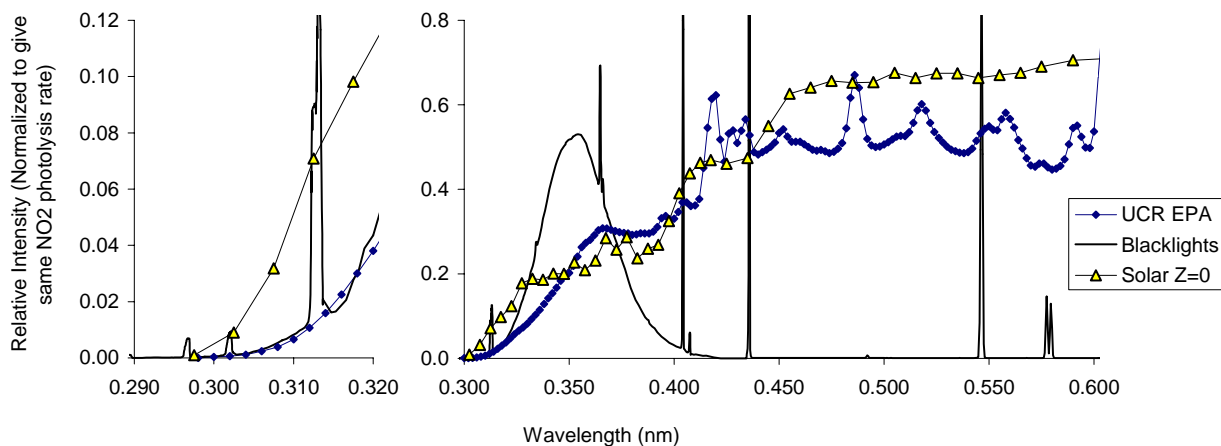
Figure 2.   Spectrum of the argon arc light source used in the UCR EPA chamber. Blacklight and representative solar spectra, with relative intensities normalized to give the same NO_2 photolysis rate as that for the UCR EPA spectrum, are also shown.

An AADCO air purification system that provides dry purified air at flow rates up to 1500 liters min^{-1} is used to supply the air to flush the enclosure and to flush and fill the reactors between experiments. The air is further purified by passing it through cartridges filled with Purafil® and heated Carulite 300® which is a Hopcalite® type catalyst and also through a filter to remove particulate matter. The measured NO_x, CO, and non-methane organic concentrations in the purified air were found to be less than the detection limits of the instrumentation employed (see Analytical Equipment, below).

The chamber enclosure is located on the second floor of a two-floor laboratory building that was designed and constructed specifically to house this facility (Carter et al, 2002). Most of the analytical instrumentation is located on the ground floor beneath the chamber, with sampling lines leading down as indicated in Figure 1.

Analytical Instrumentation

Table 1 gives a listing of the analytical and characterization instrumentation whose data were utilized for this project. Other instrumentation was available and used for some of these experiments, as discussed by Carter 2002a, but the data obtained were not characterized for modeling and thus not used in the mechanism evaluations for this project. The table includes a brief description of the equipment, species monitored, and their approximate sensitivities, where applicable. These are discussed further in the following sections.

Ozone, CO, NO, and NO_y were monitored using commercially available instruments as indicated in Table 1. A second ozone analyzer, based on the chemiluminescence method, was utilized in some experiments, and its data were consistent with the UV absorption instrument listed in Table 1. The instruments were spanned for NO, NO_2, and CO and zeroed prior to most experiments using the gas calibration system indicated in Table 1, and a prepared calibration gas cylinder with known amounts of NO and CO. O_3 and NO_2 spans were conducted by gas phase titration using the calibrator during this period. Span and zero corrections were made to the NO, NO_2, and CO data as appropriate based on the results of these span measurements, and the O_3 spans indicated that the UV absorption instrument was performing within its specifications.

As discussed by Carter (2002), two Tunable Diode Laser Absorption Spectroscopy (TDLAS) are available at our laboratories, with the potential for monitoring up to four different species, though only data for NO_2 and (for some earlier experiments) formaldehyde were used in this project. TDLAS analysis is described in detail elsewhere (Hastie et al., 1983; Schiff et al., 1994) and is based on measuring single rotational - vibrational lines of the target molecules in the near to mid infrared using laser diodes with very narrow line widths and tunability. The sample for analysis is flushed through closed absorption cells with multi-pass optics held at low pressure (~25 Torr) to minimize spectral broadening. Because of the narrow bandwidth of the diode lasers required to get the highly species-specific measurement, usually separate diode lasers are required for each compound being monitored. Both TDLAS systems have two lasers and detection systems, permitting analysis of up to four different species using this method. However, for most experiments discussed in this report, only one detector was operational for each instrument, one for monitoring NO_2 and the other for monitoring formaldehyde.

The TDLAS NO_2 measurements were calibrated as using the NO_2 span measurements made by gas phase titration with the gas calibrator at the same time the NO-NO_y analyzer was calibrated. Span data were taken in conjunction with most experiments, and these data were used to derive span factors for the entire data set. The TDLAS formaldehyde measurements were calibrated using a formaldehyde

Table 1.   List of analytical and characterization instrumentation for the UCR EPA chamber.

Type	Model or Description	Species	Sensitivity	Comments
Ozone Analyzer	Dasibi Model 1003-AH. UV absorption analysis. Also, a Monitor Labs Chemiluminescence Ozone Analyzer Model 8410 was used as a backup.	O_3	2 ppb	Standard monitoring instrument.
NO - NO_y Analyzer	Teco Model 42 C with external converter. Chemiluminescent analysis for NO, NOy by catalytic conversion.	NO NO_y	1 ppb 1 ppb	Useful for NO and initial NO_2 monitoring. Converter close-coupled to the reactors so the "NO_y" channel should include HNO_3 as well as NO_2, PANs, organic nitrates, and other species converted to NO by the catalyst.
CO Analyzer	Dasibi Model 48C. Gas correlation IR analysis.	CO	50 ppb	Standard monitoring instrument
TDLAS #1	Purchased from Unisearch Inc. in 1995, but upgraded for this chamber. See Carter (2002). Data transmitted to DAC system using RS-232.	NO_2 HNO_3	0.5 ppb ~ 1 ppb	NO_2 data from this instrument are considered to be interference-free. HNO_3 data are not available for most of the experiments modeled in this report and were not used for this project.
TDLAS #2	Purchased from Unisearch Inc. for this chamber. See Carter (2002). Data transmitted to DAC system using RS-232.	HCHO H_2O_2	~ 1 ppb ~2 ppb	Formaldehyde data from this instrument are considered to be interference-free. This instrument was not operational for many of the experiments discussed in this report. H_2O_2 data were not taken during the experiments discussed in this report
GC-FID #1	HP 5890 Series II GC with dual columns, loop injectors and FID detectors. Controlled by computer interfaced to network.	VOCs	~10 ppbC	30 m x 0.53 mm GS-Alumina column used for the analysis of light hydrocarbons such as ethylene, propylene, n-butane and trans-2-butene and 30 m x 0.53 mm DB-5 column used for the analysis of C_{5+} alkanes and aromatics, such as toluene and m-xylene. Loop injection suitable for low to medium volatility VOCs that are not too "sticky" to pass through valves.
GC-FID #2	HP 5890 Series II GC with dual columns and FID detectors, one with loop sampling and one set up for Tenax cartridge sampling. (Only the Tenax cartridge system used for this project.) Controlled by computer interfaced to network.	VOCs	1 ppbC	Tenax cartridge sampling used for low volatility or moderately "sticky" VOCs that cannot go through GC valves but can go through GC columns. Initially, a 30 m x 0.53 mm DB-1701 column was used to monitor ethylene glycol and propylene glycol. However, the peak shapes and the quality of the analysis was not satisfactory, and on June 7, 2004 this column was replaced with 30m x 0.53 mm DB-5 column which improved the

Table 1 (continued)

Type	Model or Description	Species	Sensitivity	Comments
				analyses for these glycols. This column was also used for the analysis of 2-(2-butoxyethoxy)-ethanol (DGBE) and benzyl alcohol.
Total Hydrocarbon analyzer, FID	Ratfisch Instruments, Model RS 55CA	VOCs	50 ppb	Standard commercial instrument. Used for injection tests only.
Gas Calibrator	Model 146C Thermo Environmental Dynamic Gas Calibrator	N/A	N/A	Used for calibration of NO_x and other analyzers. Instrument acquired early in project and under continuous use.
Data Acquisition Sytem	Windows PC with custom LabView software, 16 analog input, 40 I/O, 16 thermo-couple, and 8 RS-232 channels.	N/A	N/A	Used to collect data from most monitoring instruments and control sampling solenoids. In-house LabView software was developed using software developed by Sonoma Technology for ARB for the Central California Air Quality Study as the starting point.
Temperature sensors	Various thermocouples, radiation shielded thermocouple housing	Tempera-ture	~0.1 ^{o}C	Primary measurement is thermocouples inside reactor. However, comparison with temperature measurements in the sample line suggest that irradiative heating may bias these data high by ~2.5^{o}C. See text.
Humidity Monitor	General Eastern HYGRO-M1 Dew Point Monitor	Humid-ity	Dew point range: -40 - 50°C	Instrument performs as expected, but dew point below the performance range for most of the experiments discussed in this report, except for those with added humidity.
Spectro-radiometer	LiCor LI-1800 Spectroradiometer	300-850 nm Light Spect-rum	Adequate	Resolution relatively low but adequate for this project. Used to obtain relative spectrum. Also gives an absolute intensity measurement on surface useful for assessing relative trends.
QSL Spherical Irradiance Sensor	Biospherical QSL-2100 PAR Irradiance Sensor. Responds to 400-700 nm light.	Spherical Broad-band Light Intensity	Adequate	Provides a measure of absolute intensity and light uniformity that is more directly related to photolysis rates than light intensity on surface. Gives more precise measurement of light intensity trends than NO_2 actinometry, but is relatively sensitive to small changes in position.
Scanning Electrical Mobility Spectrometer (SEMS)	TSI 3080L column, TSI 3077 [85]Kr neutralizer, and TSI 3760A CPC. Instrument design, control, and operation Similar to that described in Cocker et al. (2001)	Aerosol number and size distribut-ions	Adequate	Provides information on size distribution of aerosols in the 28-730 nm size range, which accounts for most of the aerosol mass formed in our experiments. Data can be used to assess effects of VOCs on secondary PM formation.

permeation source that in turn was calibrated based on Wet chemical calibration procedure using Purpald reagent (Jacobsen and Dickinson, 1974; Quesenberry and Lee, 1996; NIOSH, 1994)

Organic reactants other than formaldehyde were measured by gas chromatography with FID detection as described elsewhere (Carter et al, 1993, 1995b); see also Table 1. The surrogate gaseous compounds ethylene, propylene, n-butane and trans-2-butene were monitored by using 30 m megabore GS-Alumina column and the loop sampling system. The second signal of the same GC outfitted with FID, loop sampling system and 30 m megabore DB-5 column was used to analyze surrogate liquid components toluene, n-octane and m-xylene.

Low volatility, more "sticky" test compounds such as the glycols were monitored on a second GC-FID using the Tenax cartridge sampling system. During the initial experiments discussed in this report this GC was outfitted with a 30 m DB-1701 megabore column. Although this gave good results in the analysis of the Texanol® isomers (Carter and Malkina, 2005), the column did not perform satisfactorily for analysis of the glycols. The GC peaks seen when using this column for glycol analysis were very broad and asymmetrical, and irreproducible results were frequently obtained. Efforts were made to improve the analysis using this column, but improvements were not obtained until the column was replaced by a the 30 m megabore DB-5 column, the same length and type that we used when we were conducting previous experiments with propylene glycol (Carter et al, 1997). This column resulted in a significantly improved glycol analyses and was used in few experiments with glycols starting with run EPA315. It was also used in all the experiments with 2-(2-butoxyethoxy)-ethanol (DGBE) and Benzyl Alcohol to monitor those test compounds.

The Tenax GC system was calibrated by preparing methanol solutions of the analyzed compound and placing measured amounts of the solution directly on the Tenax® cartridge for subsequent desorption onto the column. This gave results in good agreement with calculated amounts injected in the Texanol® experiments carried out previously (Carter and Malkina, 2005), and also with most of the experiments with benzyl alcohol carried out for this project. However, for the glycols and DGBE the measurements calibrated in this way were consistently lower, by as much as a factor of 2, than the calculated amounts injected into the reactor. Because separate injection experiments, discussed below, indicated that all of these compounds should be injected into the chamber with the procedures employed, for experiments for those compounds the initial concentrations were assumed to be those derived calculated from the amounts of material injected and the volume of the reactors. The reasons for the inconsistency between the methanol solution analysis and the gas-phase analyses for these compounds are unknown.

Both the GC instruments were controlled and their data were analyzed using HPChem software installed on a dedicated PC. The GC's were spanned using the prepared calibration cylinder with known amounts of ethylene, propane, propylene, n-butane, n-hexane, toluene, n-octane and m-xylene in ultrapure nitrogen. Analyses of the span mixture were conducted approximately every day an experiment was run, and the results were tracked for consistency.

As indicated in Table 1, aerosol number and size distributions were also measured in conjunction with our experiments. The instrumentation employed is similar to that described by Cocker et al. (2001). Particle size distributions are obtained using a scanning electrical mobility spectrometer (SEMS) (Wang and Flagan, 1990) equipped with a 3077 [85]Kr charger, a 3081L cylindrical long column, and a 3760A condensation particle counter (CPC). Flow rates of 2.5 LPM and 0.25 LPM for sheath and aerosol flow, respectively, are maintained using Labview 6.0-assisted PID control of MKS proportional solenoid control valves. Both the sheath and aerosol flow are obtained from the reactor enclosure. The data inversion algorithm described by Collins et al (2002) converts CPC counts versus time to particle size distribution.

Most of the instruments other than the GCs and aerosol instrument were interfaced to a PC-based computer data acquisition system under the control of a LabView program written for this purpose. The TDLAS instruments were controlled by their own computers, but the data obtained were sent to the LabView data acquisition system during the course of the experiments using RS-232 connections. These data, and the GC data from the HP ChemStation computer, were collected over the CE-CERT computer network and merged into Excel files that are used for applying span, zero, and other corrections, and preparation of the data for modeling.

Sampling methods

Samples for analysis by the continuous monitoring instrument were withdrawn alternately from the two reactors, zero air, under the control of solenoid valves that were in turn controlled by the data acquisition system discussed above. For most experiments the sampling cycle was 5 minutes for each reactor, the zero air, or (for control purpose) the chamber enclosure. The program controlling the sampling sent data to the data acquisition program to indicate which state was being sampled, so the data could be appropriately apportioned when being processed. Data taken less than 3-4 minutes after the sample switched were not used for subsequent data processing. The sampling system employed is described in more detail by Carter (2002).

Samples for GC analysis of surrogate compounds were taken at approximately 20-minute intervals directly from each of the reactors through the separate sample lines attached to the bottom of the reactors. The GC sample loops were flushed for a desired time with the air from reactors using pump. In the analyses using the Tenax system the 100 ml sample was collected directly from the reactors onto Tenax-GC solid adsorbent cartridge and then placed in series with the GC column, thermally desorbed at 300 C and cryofocused on the column. 100 ml gas-tight, all-glass syringe was used to collect Tenax sample. Additional sampling lines were attached to the bottom of each reactor for the Tenax sample collection, and their length was minimized to avoid possible losses.

Characterization Methods

Use of chamber data for mechanism evaluation requires that the conditions of the experiments be adequately characterized. This includes measurements of temperature, humidity, light and wall effects characterization. Wall effects characterization is discussed in detail by Carter (2004) and updated by Carter and Malkina (2005) and most of that discussion is applicable to the experiments for this project. The instrumentation used for the other characterization measurements is summarized in Table 1, above, and these measurements are discussed further below.

Temperature was monitored during chamber experiments using calibrated thermocouples attached to thermocouple boards on our computer data acquisition system. The temperature in each of the reactors was continuously measured using relatively fine gauge thermocouples that were located ~1' above the floor of the reactors. These thermocouples were not shielded from the light, though it was hoped that irradiative heating would be minimized because of their small size. In order to obtain information about possible radiative heating effects, for a number of experiments (carried out prior to those for this project) the thermocouple for one of the reactors was relocated to inside the sample line. The results indicated that radiative heating is probably non-negligible, and that a correction needs to be made for this by subtracting ~2.5°C from the readings of the thermocouples in the reactors. This is discussed by Carter (2004).

Light Spectrum and Intensity. The spectrum of the light source in the 300-850 nm region was measured using a LiCor LI-1800 spectroradiometer, which is periodically calibrated at the factory. Spectroradiometer readings were taken several times during a typical experiment, though the relative

spectra were found to have very little variation during the course of these experiments. Changes in light intensity over time were measured using a PAR spherical irradiance sensor that was located immediately in front of the reactors. In addition, NO_2 actinometry experiments were carried out periodically using the quartz tube method of Zafonte et al (1977) modified as discussed by Carter et al (1995b). In most cases the quartz tube was located in front of the reactors near where the PAR sensor was located. Since this location is closer to the light than the centers of the reactors, the measurement at this location is expected to be biased high, so the primary utility of these data are to assess potential variation of intensity over time. However, several special actinometry experiments were conducted where the quartz tube was located inside the reactors, to provide a direct measurement of the NO_2 photolysis rates inside the reactors. The actinometry results obtained for the experiments of interest are discussed later in this report.

Humidity. Humidity was measured using an EG&G model Hygro M1 chilled mirror dew point sensor. Its lower limit of -40^oC is above the expected dew point of the purified air used in most of the experiments described in this report, but adequate for the few humidified experiments carried out for this project.

Experimental Procedures

The reaction bags were collapsed to the minimum volume by lowering the top frames, and then emptying and refilling them at least six times after each experiment, and then filling them with dry purified air on the nights before experiments. Span measurements were generally made on the continuous instruments prior to injecting the reactants for the experiments. The reactants were then injected through Teflon injection lines (that are separate from the sampling lines) leading from the laboratory below to the reactors. The common reactants were injected in both reactors simultaneously, and were mixed by using the reactor-to-reactor exchange blowers and pipes for 10 minutes. The valves to the exchange system were then closed and the other reactants were injected to their respective sides and mixed using the in-reactor mixing blowers and pipes for 1 minute. The contents of the chamber were then monitored for at least 30 minutes prior to irradiation, and samples were taken from each reactor for GC analysis.

Once the initial reactants are injected, stabilized, and sampled, the light or lights employed (argon arc or blacklights) are turned on to begin the irradiation. During the irradiation the contents of the reactors are kept at a constant positive pressure by lowering the top frames as needed, under positive pressure control. The reactor volumes therefore decrease during the course of the experiments, in part due to sample withdrawal and in part due to small leaks in the reactor. A typical irradiation experiment ended after about 6 hours, by which time the reactors are typically down to about half their fully filled volume. Larger leaks are manifested by more rapid decline of reactor volumes, and the run is aborted early if the volume declines to about 1/3 the maximum. This was not the case for the experiments discussed in this report. After the irradiation the reactors were emptied and filled six times as indicated above.

The procedures for injecting the various types of reactants were as follows. The NO and NO_2 were prepared for injection using a vacuum rack. Known pressures of NO, measured with MKS Baratron capacitance manometers, were expanded into Pyrex bulbs with known volumes, which were then filled with nitrogen (for NO) or oxygen (for NO_2). In order to maintain constant NO/NO_2 ratios the same two bulbs of specified volume were utilized in most of experiments. The contents of the bulbs were then flushed into the reactor(s) with nitrogen. Some of the gaseous reactants such as propylene and n-butane (other than for surrogate experiments) were prepared for injection using a high vacuum rack as well. For experiments with added CO, the CO was purified by passing it through an in-line activated charcoal trap and flushing it into the reactor at a known rate for the amount of time required to obtain the desired concentration. Measured volumes of volatile liquid reactants were injected, using a micro syringe, into a 2 ft long Pyrex injection tube surrounded with heat tape and equipped with one port for the injection of the liquid and other ports to attach bulbs with gas reactants. Then one end of the injection tube was attached

to the "Y"-shape glass tube (equipped with stopcocks) that was connected to reactors and the other end of injection tube was connected to a nitrogen source. The test compound was injected, using a microsyringe, into a glass injection tube leading into the reactor to be employed for the compound. The optimal temperature of the glass injection tube and optimal duration of the injection were determined in preliminary tests as described below. The injection lines into the reactors were wrapped in heat tape and heated as well.

The procedures for injection of the hydrocarbon surrogate components were as follows. A cylinder containing n-butane, trans-2-butene, propylene and ethylene in nitrogen, was used for injecting the gaseous components of the surrogate. The cylinder was attached to the injection system and a gas stream was introduced into reactors at controlled flow for certain time to obtain desired concentrations. A prepared mixture with the appropriate ratios of toluene, n-octane and m-xylene was utilized for injection of these surrogate components, using the procedures as discussed above for pure liquid reactants. All the gas and liquid reactants intended to be the same in both reactors were injected at the same time. The injection consisted of opening the stopcocks and flushing the contents of the bulbs and the liquid reactants with nitrogen, with the liquid reactants being heated slightly using heat that surrounded the injection tube. The flushing continued for approximately 10 minutes.

Special Procedures for Availability Experiments

As indicated in Table B-1, below, as part of our study of effects of humidity and added aerosol on glycol availability, runs EPA308, 309, 310 were carried out with added seed aerosol and runs EPA 313-316, and 324 were carried out with humidified air and added seed aerosol. In case of experiments 313-316 and 324 the initial aerosol was added into reactor A only, and only that reactor had humidified air. This is because of the limited capacity of the humidification and aerosol generation system used for these experiments. The initial relative humidity in all the humidified experiments was about 30%.

The humidification procedure was as follows. Approximately 1.2 liters of distilled water was placed in a 4-liter round-bottom flask that was maintained at $21^{\circ}C$ using a heating mantle. Purified air was flushed through the flask at 100 liters/minute for 2 hours prior seed aerosol injection and then for another 3 hours after aerosol injection started. The outlet of flask was connected to a condensation trap and then to the reactor.

For the experiments with seed aerosol, the initial seed aerosol was generated from 0.005M solution of $(NH_4)_2SO_4$ or NH_4HSO_4 using a stainless steel atomizer based on the original design of Liu and Lee (1975). Compressed air expands through the diameter orifice to form a high-velocity jet. Atomization of the salt solution occurs as it is aspirated into the high-velocity jet. Large droplets are removed by impaction on the wall opposite the jet and excess liquid is returned to the salt solution reservoir. The fine spray is then passed through a heated copper line followed by a diffusion dryer. Approximately 1.5 - 3 $\mu g/m^3$ of 125 – 130 nm mean diameter seed aerosol was added to the chamber (particle number concentration about 1600 - 3000 cm^{-3}) for dual bag injection. For single bag injection, the seed aerosol volume and number concentration were 7.5 – 9.0 $\mu g/m^3$ and 7000 – 9000 cm^{-3}, respectively.

Modeling methods

Standard Chemical Mechanism

The chemical mechanism evaluated in this work is the SAPRC-99 mechanism as documented by Carter (2000a). A complete listing of this mechanism is given by Carter (2000a) and in subsequent reports

from our laboratory where this mechanism was used, all of which are available on our web site[3]. Files and software implementing this chemical mechanism are also available at our web site[4], with the chemical mechanism simulation computer programs available there being essentially the same as those employed in this work. Changes have been made to the mechanisms of some individual VOCs due to subsequent experimental studies and reactivity assessment projects (Carter, 2003a), including the addition of a mechanism for 2-(2-butoxyethoxy)-ethanol (DGBE), one of the compounds studied for this project. The mechanisms used for DGBE and the other test compounds studied for this project are discussed later in this section.

As discussed previously (Carter, 2000a,b), the SAPRC-99 mechanism consists of a "base mechanism" that represents the reactions of the inorganic species and common organic products and lumped organic radical model species and "operators", and separate mechanisms for the initial reactions of the many types other organic compounds that are not in the base mechanism. The compounds, or groups of compounds, that are not included in the base mechanism but for which mechanism assignments have been made, are referred to as detailed model species. The latter include all the base ROG surrogate constituents and compounds whose reactivities were evaluated in this work. These compounds can either be represented explicitly, with separate model species with individual reactions or sets of reactions for each, or using lumped model species similar to those employed in the "fixed parameter" version of SAPRC-99 (Carter, 2000b). The latter approach is useful when modeling complex mixtures in ambient simulations or simulations of experiments with complex mixtures, but the other approach, representing each compound explicitly, is more appropriate when evaluating mechanisms for individual compounds or simple mixtures. This is because the purpose of mechanism evaluations against chamber data is to assess the performance of the mechanism itself, not to assess the performance lumping approaches. The latter is most appropriately assessed by comparing simulations of explicit and condensed versions of the same mechanism in ambient simulations.

In view of this, all of the organic constituents of the base ROG surrogate were represented explicitly using separate model species for each compound. In addition, the individual test compounds were also represented explicitly when simulating experiments with those compounds. This gives the least approximate representation of the atmospheric reactions of these compounds within the framework of the SAPRC-99 mechanism. The mechanisms for the individual test compounds are discussed separately later in this section.

Adjusted Base Mechanism

As discussed by Carter (2004) and Carter and Malkina (2005), the standard SAPRC-99 mechanism has a consistent bias to underpredict O_3 formation in the surrogate - NO_x irradiations at the lower ROG/NO_x ratios. This bias showed up in a consistent underprediction of O_3 in the base case of the standard MIR incremental reactivity experiment for this project. This bias should to some extent cancel out when modeling incremental reactivities because incremental reactivities are differences, and a similar bias would also occur to some extent in the added VOC test experiment. However, the addition of the test compound would change the effective ROG/NO_x ratio, and therefore the magnitude of the underprediction bias may be different than in the base case. Also, the bias means that the model is not correctly simulating the chemical environment in which the VOC is reacting, and could result in inaccurate predictions of the impacts of the reactions of the test compounds, even if their mechanisms are correct. Worse, the possibility of errors in the base case simulation compensating for errors in the mechanism of the test compounds can not necessarily be ruled out.

---

[3] These reports can be downloaded from http://www.cert.ucr.edu/~carter/bycarter.htm.
[4] Files and software implementing the SAPRC-99 mechanism are available at http://www.cert.ucr.edu/~carter/SAPRC99.htm.

To assess this, it is useful to provide an alternative approach for evaluating the model performance for the test compounds where the biases in the simulations of the base case is removed or at least modified. Therefore, for this purpose we developed an adjusted version of the base mechanism where the bias is removed, and show the results of the model simulations of the incremental reactivity experiments using this mechanism as well as the standard base mechanism (Carter and Malkina, 2005). This adjustment involved increasing the yields of the aromatic fragmentation products AFG2 and AFG3 for toluene and m-xylene by a factor of 1.75, and increasing the rate constant for the reaction of the aromatic fragmentation product AFG1 by a factor of 10. These adjustments remove the underprediction bias in the model simulations of NO oxidation and O_3 formation in the MIR experiments without significantly impacting the ability of the model to simulate the MOIR/2 and other low NO_x experiments, as shown by Carter and Malkina (2005), and also in the Results section, below.

Although this adjustment to the mechanism for toluene and m-xylene mechanisms in the base ROG improved the simulations of the base case experiments used in this and the CARB project (Carter and Malkina, 2005), it also resulted in significant overpredictions of O_3 formation rates in many of the aromatics - NO_x experiments that were well simulated by the standard SAPRC-99 mechanism. This is shown on Figure 3, which shows experimental and calculated concentration-time plots of O_3 formed and NO oxidized, $\Delta([O_3]-[NO])$, in representative surrogate - NO_x and m-xylene - NO_x experiments with both versions of the mechanism. Therefore, this adjusted base aromatics mechanism is not a "better"
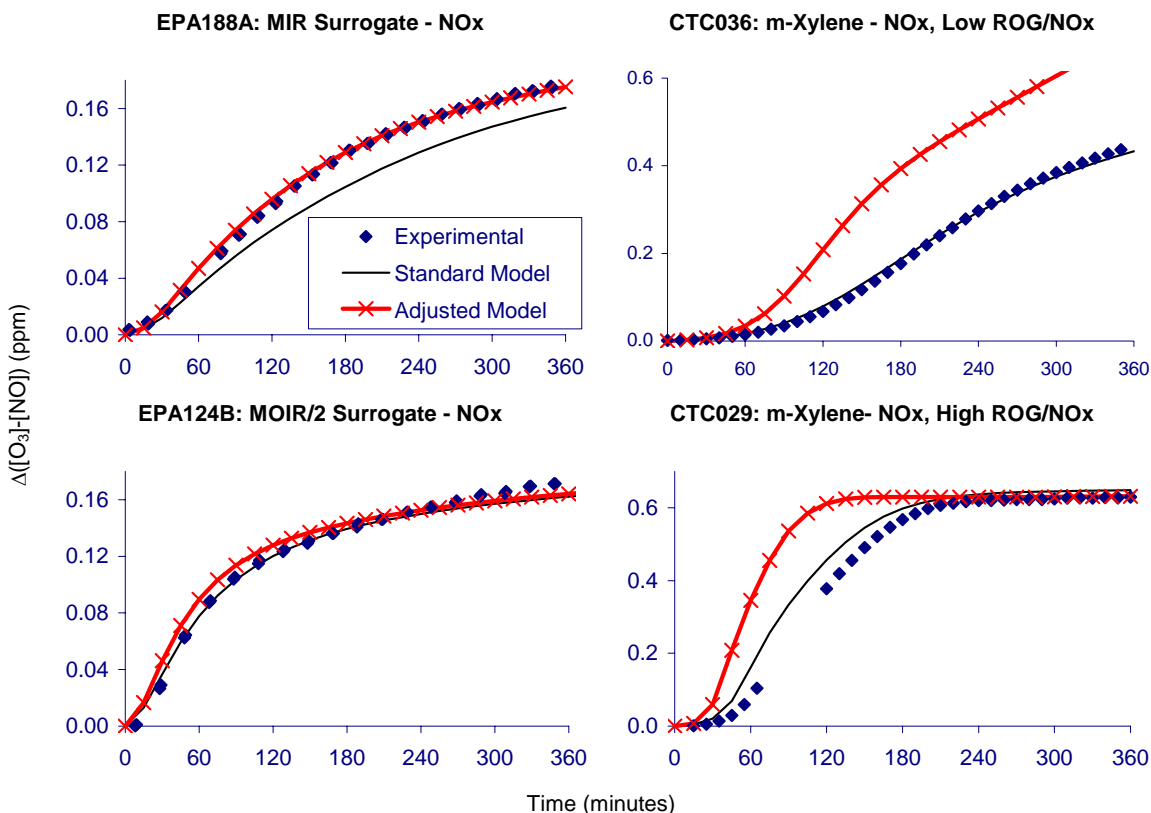
Figure 3.   Experimental and calculated $\Delta([O_3]-[NO])$ for representative surrogate - NO_x and m-xylene - NO_x experiments, with calculations using the standard and adjusted base aromatics version of the SAPRC-99 mechanism.

mechanism for these aromatics, it just has biases and problems that are different from the standard version. For that reason, as with Carter and Malkina (2005) the mechanisms for the test compounds are evaluated using model simulations of the chamber experiments with both versions of the base mechanism, to provide useful information on effects of the base mechanism biases on results of incremental reactivity simulations for the test compounds of interest.

Representation of Chamber Conditions

The procedures used in the model simulations of the environmental chamber experiments for this project were the based on those discussed in detail by Carter (2004) and were employed in the study of Carter and Malkina (2005), except as indicated below. Carter (2004) should be consulted for details of the characterization model and chamber effects parameters employed. The temperatures used when modeling were the averages of the temperatures measured in the reactors, corrected as discussed by Carter (2004). The light intensity and spectrum for the arc light experiments was assumed to be constant, and a constant NO_2 photolysis rate of 0.260 min^{-1} was used, as indicated by the results of the actinometry measurements discussed in the "Characterization Results" section, below. The arc light spectral distribution used by Carter (2004) was also used in this work because the spectral distribution measurements made during the experiments indicated no significant changes with time. The light intensity for the black light experiments varied with time, and the NO_2 photolysis rate for those experiments was derived as discussed in the "Characterization Results" section, below. The blacklight spectral distribution given by Carter et al (1995b) was found to be appropriate for the blacklights in this chamber and was therefore used when modeling the blacklight runs discussed in this report.

The chamber effects parameters used when modeling the experiments in this chamber were the same as those given by Carter (2004) except for the HONO offgasing parameters, which were derived based on results of characterization runs carried out in conjunction with these experiments. As discussed by Carter (2004), the chamber effects model currently used for this chamber represents both the chamber radical source and background NO_x offgasing by HONO offgasing, whose magnitude is determined by the chamber effects parameter RN-I, which is the ratio of the HONO offgasing rate to the NO_2 photolysis rate. The RN-I parameter that best fits the characterization data tends to vary over time depending on the conditions of the chamber, and the results of the characterization experiments applicable to modeling the experiments discussed in this report, and the assignment of the RN-I values used, are given in the Characterization Results section, below.

The initial reactant concentrations used in the model simulations were based on the measured values except for ethylene and propylene glycol and DGBE, whose initial concentrations used for modeling were calculated based on the volume of liquid injected and the calculated or estimated volume of the reactors. As discussed in the "Results of Injection Tests" section, below, variability in and inconsistencies GC analyses indicated that GC analysis was a less reliable way to determine the initial concentrations of these compounds than the calculated amounts injected. The assumption of complete injection was supported by results of injection tests carried out with these compounds, as discussed below. The volumes of the reactors were determined in separate experiments where known amounts of materials were injected and analyzed in the gas-phase. Although the reactors are flexible, their initial volumes were very consistent from run to run because of the use of the pressure control system when filling the reactor to its maximum volume prior to the reactant injections (see Chamber Description section, above, and Carter, 2004).

Atmospheric Reactivity Simulations

Conducting atmospheric reactivity model simulations was not a major component of this project, but such calculations needed to be carried out to derive MIR and other atmospheric reactivity values for

compounds whose mechanisms were developed or modified for this project. These included benzyl alcohol, whose mechanism was developed for this project, and ethylene glycol, where the representation of its major oxidation product was made more explicit. The scenarios and methods used were the same as those used when calculating the MIR and other atmospheric ozone reactivity scales, and were described previously (Carter, 1994a,b 2000a). The base ROG constituents were represented using the lumping procedures incorporated in the condensed version of the SAPRC-99 mechanism (Carter, 2000b), and individual compounds whose reactivities were being assessed were represented explicitly.

Mechanisms for Test Compounds

The mechanisms used for the four test compounds studied for this project are given in Table 2. Ethylene glycol, propylene glycol, and DGBE are already represented in the current SAPRC-99 detailed mechanism, and except as indicated these mechanism were not modified as a result of this study. The only exception is that slightly better fits to the data were obtained if the glycolaldehyde that is predicted as the major product from ethylene glycol is represented explicitly, rather than using the acetaldehyde model species as used in the previous mechanism. Therefore, the reactions of glycolaldehyde have been added to the mechanism, and its reactions are included in Table 2 as part of the ethylene glycol mechanism. Footnotes to the table indicate the sources of the rate constants and mechanisms used.

As indicated in Table 2, the more reactive products from propylene glycol and DGBE are represented using the SAPRC-99 "adjusted product" representation, whereby the mechanisms for the model species used to represent these products are derived from the estimated mechanisms of the specific products predicted to be formed, weighed by the predicted yields of these products (Carter, 2000a). This was the method used for calculating the reactivities of these compounds in the existing SAPRC-99 reactivity scales (Carter, 2000a, 2003), and therefore is the appropriate method to use when evaluating these mechanisms against the chamber data obtained in this project. The mechanisms derived for these adjusted products are included in Table 2 as part of the mechanism given for those compounds. Note that this adjusted product representation was not previously used for ethylene glycol, so the explicit representation of its major product is new to this work.

There was no representation for benzyl alcohol in the SAPRC-99 mechanism prior to this work, so its mechanism had to be derived as part of the work for this project. As with other aromatics, it is expected that its major atmospheric reaction would be with the OH radical, and as indicated in Table 2 a measurement exists for this rate constant. However, we are not aware of any data concerning its subsequent reactions, and presently there exist no reliable methods to estimate aromatic photooxidation mechanisms a-priori. Therefore, for this project the benzyl alcohol mechanism was estimated based on that for toluene, which is very similar except for the lack of an OH on the methyl group, and other considerations as discussed below.

As with toluene, part of the reaction is expected to involve abstraction of an H atom from the side group, ultimately forming benzaldehyde and HO_2. The difference is that in this case the process does not involve an NO to NO_2 conversion, since O_2 will directly react with the α-hydroxy radical formed in the abstraction to form benzaldehyde + HO_2, without the intermediacy of a benzyl peroxy radical such as that formed in the case of toluene. It is also expected that the rate constant for this reaction would be faster than that for the corresponding reaction in toluene, because α-OH substitution tends to increase rates of OH radical abstraction reactions. Therefore, the benzaldehyde yield in the reaction of OH with benzyl alcohol is expected to be higher than that from toluene, and using the yield from toluene would probably be an underestimate.

Fortunately, we were able to derive the branching ratio for benzaldehyde formation in the OH + benzyl alcohol reaction by modeling the benzaldehyde formation observed in the benzyl alcohol - NO_x

Table 2.   Mechanisms used for test compounds studied for this project.

Compound	Rate Constant [a]	Reactions and Products [b]	Notes [c]
Ethylene Glycol	1.47×10^{-11}	ET-GLYCL + HO. = HO2. + 0.067 HCHO + 0.966 HOCCHO	1, 2, 3
	1.3×10^{-11}	HOCCHO + HO. = 0.8 {CCO-O2. + H2O} + 0.2 {GLY + HO2.}	3, 4, 5
	See note	HOCCHO + HV = CO + HCHO + 2 HO2.	3, 6
	1.4×10^{-12}	HOCCHO + NO3 = HNO3 + CCO-O2.	3, 5, 7
Propylene Glycol	2.15×10^{-11}	PR-GLYCL + HO. = 0.987 HO2. + 0.013 RO2-R. + 0.039 HCHO + 0.039 CCHO + 0.315 PG-RCHO + 0.646 MEK	1, 2, 8
	2.46×10^{-11}	PG-RCHO + HO. = 0.209 HO2. + 0.791 RCO-O2. + 0.209 MGLY	9
	Same as RCHO	PG-RCHO + HV = 2 HO2. + CO + CCHO	9
	3.8×10^{-15}	PG-RCHO + NO3 = HNO3 + CCO-O2.	9
2-(2-butoxy-ethoxy) ethanol	7.44×10^{-11}	DGBE + HO. = 0.820 RO2-R. + 0.180 RO2-N. + 0.530 R2O2. + 0.198 HCHO + 0.010 CCHO + 0.345 DG-RCHO + 0.317 MEK + 0.708 DG-PROD2	2, 10, 11
	5.46×10^{-11}	DG-RCHO + HO. = 0.236 HO2. + 0.329 RO2-R. + 0.072 RO2-N. + 0.278 R2O2. + 0.363 RCO-O2. + 0.101 CO + 0.01 HCHO + 0.004 CCHO + 0.549 RCHO + 0.188 MEK + 0.065 PROD2	9
	Same as RCHO	DG-RCHO + HV = 0.456 HO2. + 01.427 RO2-R. + 0.118 RO2-N. + 0.064 R2O2. + 01.0 CO + 0.04 HCHO + 0.006 RCHO + 0.971 MEK + 0.152 PROD2 + 0.033 HCOOH	9
	3.8×10^{-15}	DG-RCHO + NO3 = HNO3 + RCO-O2.	9
	1.5×10^{-11}	DG-PROD2 + HO. = 0.35 HO2. + 0.542 RO2-R. + 0.054 RO2-N. + 0.297 R2O2. + 0.054 RCO-O2. + 0.129 CO + 0.011 CO2 + 0.163 HCHO + 0.011 CCHO + 0.487 RCHO + 0.321 MEK + 0.126 PROD2 + 0.165 HCOOH	9
Benzyl Alcohol	2.29×10^{-11}	BZ-CH2OH + HO. = 0.482 RO2-R. + 0.050 RO2-NP. + 0.468 HO2. + 0.300 BALD + 0.168 CRES + 0.083 GLY + 0.097 MGLY + 0.330 DCB1 + 0.112 DCB2 + 0.041 DCB3	12, 13

[a] Rate constant in units of cm^3 $molec^{-1}$ s^{-1}. Assumed to be independent of temperature.

[b] See Carter (2000a) for discussion of the SAPRC-99 model species.

[c] Notes on reactions and rate constants are as follows:

1. OH Radical rate constant from Aschmann and Atkinson (1998)
2. Mechanism derived using SAPRC-99 estimated mechanism generation system (Carter, 2000a).
3. HOCCHO is glycolaldehyde ($HOCH_2CHO$), which is added to the mechanism because explicit representation of this product gives slightly better fits to the chamber data. Its reactions have been added to the mechanism and are included on this table. In the standard mechanism (Carter, 2000a), this is represented by the Acetaldehyde model species, CCHO.
4. Rate constant and mechanism based on IUPAC (2002a) recommendation.
5. The acetyl peroxy model species (CCO-O2.) is used to represent $HOCH_2C(O)OO\cdot$.

Table 2 (continued)

6. The absorption cross sections used for glycolaldehyde are given by IUPAC (2000b). An overall, wavelength-independent quantum yield of 0.75 is assumed, based on the IUPAC (2000b) recommendation.

7. The rate constant and mechanism is assumed to be the same as used for acetaldehyde

8. The MEK model species used to represent hydroxy acetone. The PG-RCHO model species is used to represent products normally represented by RCHO, which in this case is primarily (but not entirely) α-hydroxy propionaldehyde. These are represented using the SAPRC-99 "adjustable product" representation as discussed by Carter (2000a).

9. The mechanisms for these lumped product model species are derived based on mechanisms for the distributions of products they are used to represent, which in turn are derived using the SAPRC-99 mechanism estimation and generation system (Carter, 2000a).

10. OH rate constant derived using the SAPRC-99 mechanism estimation system based on structure-reactivity relationships (Carter, 2000a, and references therein).

11. A variety of products are predicted to be formed, with no single compound dominating. The products that are normally lumped with RCHO and PROD2 are represented by model species with mechanisms derived based on the compounds they represent using the SAPRC-99 "adjustable product" representation (Carter, 2000a). RO2-N. represents nitrate formation in the organic peroxy + NO reactions.

12. OH radical rate constant based on an unpublished measurement by Notling et al (1988) as cited by Atkinson (1989).

13. The benzyl alcohol mechanism is derived as discussed in the text. RO2-NP. represents organic nitrate formation from the peroxy + NO reaction, with the aromatic nitrate formed being represented by the nitrophenol (NPHE) model species.

experiments carried out for this project, as discussed in the "Incremental Reactivity and Mechanism Evaluation Results" section, below. The benzaldehyde data were best fit by assuming that the H-abstraction process forming benzaldehyde occurs 30% of the time. Note that, as expected, this is higher than the ~9% benzaldehyde yield in the toluene mechanism.

The addition of OH radicals to the aromatic ring is assumed to occur the remainder of the time, giving rise to a complex distribution of ring-opening products through a mechanism that is not adequately understood. For this work, we assume that the mechanism and products for the ring-opening processes are the same as used for toluene. However, in order to improve fits to final ozone yields, we assume a somewhat higher overall yield of organic nitrates from the peroxy + NO reactions involved, with the data being best fit by assuming a 5% overall nitrate yield, compared to the 0.8% that is used in the current toluene mechanism.

RESULTS AND DISCUSSION

A chronological listing of the environmental chamber experiments carried out for this project is given in Table B-1 in Appendix B. These included experiments with the test compounds of interest for this study and appropriate characterization and control experiments needed for the data to be useful for mechanism evaluation. However, these do not include experiments carried out for the CARB coatings project, which are listed in Table A-4 in Appendix A in the report for that project (Carter and Malkina, 2005). The relevant results of the characterization experiments are discussed first, followed by a summary of the results of the experiments with the test compounds, and then a discussion of the results of the PM measurements and the availability experiments. Relevant results of experiments for the CARB coatings project, listed in Table A-4 of Carter and Malkina (2005) are also discussed where applicable.

Characterization Results

The results of the individual characterization experiments that are relevant to the experiments for this project are summarized in the "Results" column of Table B-1. The initial characterization experiments relevant to the characterization of this chamber for are described in detail by Carter (2004a) or by Carter and Malkina (2005), and thus need not be discussed further here. Characterization results specific to this project are discussed below.

Arc Light Characterization

The arc light source was used for most of the experiments discussed in this report. The characterization results for this light source, applicable for runs through ~EPA245, and the assignments of NO_2 photolysis rates and spectrum used for modeling based on these results, were discussed previously by Carter (2004a), but Table B-1 indicates that several actinometry experiments were carried out subsequently. Figure 4 shows a plot of various measures of light intensity against run number for arc light experiments discussed by Carter (2004a) and for subsequent experiments applicable to the runs discussed in this report. These include the following:

- NO_2 actinometry measurements were made using the quartz tube method of Zafonte et al (1977), modified as discussed by Carter et al (1995b), either inside one of the reactors or in a standardized location in front of the reactors between the reactors and the light.

- Most chamber experiments had PAR light intensity measurements made by the QSL PAR spherical radiometer instrument during the course of the experiments. Figure 4 shows the average values of the PAR measurements made during the arc light experiments, data placed on the same basis as the out-of-reactor NO_2 actinometry measurements by normalizing them so that they give the same average value.

Figure 4 shows that the PAR data and the results of most of the out-of-reactor NO_2 actinometry experiments indicated that the light intensity with this light source did not change during the period of these experiments. The data through ~EPA245 were used as the basis for the NO_2 photolysis rate assignments used for modeling by Carter (2004a) and in our modeling of the CARB coatings reactivity experiments reported by Carter and Malkina (2005). However, the results of the in-chamber actinometry experiments EPA331 and EPA333 indicated higher in-reactor NO_2 photolysis rates than the results of the previous runs, while the PAR data after ~EPA360 suggest a decline in the light intensity, and the out-of-reactor NO_2 actinometry results suggest no change in light intensity. In view of the apparent constant light intensity up to EPA240 and the fact that there is no known change in operating procedure or equipment
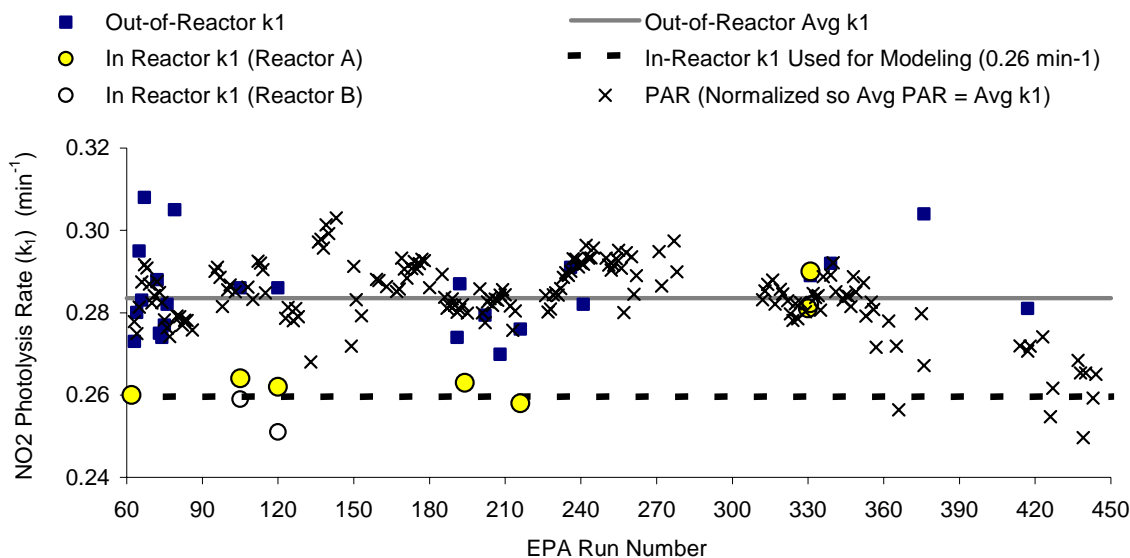
Figure 4.   Plots of various measures of light intensity for EPA chamber experiments using the arc light source vs. EPA run number.

that would lead us to expect this to change after that run, we assume that the out-of-reactor light intensity has not changed during the period of the experiments carried out for this project. We also assume that there is no change in the ratio between the out-of-reactor and in-reactor light intensities, which means that the in-reactor light intensity should also be constant. Therefore, we continue to use an NO_2 photolysis rate or 0.26 min^{-1} for modeling purposes, as used in the previous studies of Carter (2004a) and Carter and Malkina (2005).

The spectrum of the light source was measured periodically using our LI-1800 spectroradiometer, and the results indicated that the spectrum did not change significantly with time, and that the spectrum given by Carter (2004a) is applicable for all arc light experiments carried out for this project.

Blacklight Characterization

Several experiments carried out or modeled for this project were conducted using blacklight irradiation. Since the characterization of the intensity and assignments of photolysis rates for modeling runs with this light source have not been discussed previously, this is discussed in this section. Blacklights tend to decrease in intensity in time as they are used (Carter et al, 1995b), and this needs to be taken into account when assigning photolysis rates when modeling blacklight experiments. Relevant information concerning the intensity of this light source comes from the following sources:

- A few NO_2 actinometry measurements were made using the quartz tube method of Zafonte et al (1977), modified as discussed by Carter et al (1995b) with the quartz tube inside the reactors. These were used as the standard to derive absolute photolysis rates within the chamber, but were insufficient in number to verify trends in light intensity with time.

- NO_2 actinometry measurements were also made with the quartz tube located in the "standard" position in front of the reactors and between the reactors and the light source. Since the tube is closer to the light than the reactors, these measurements are expected to be higher than the in-
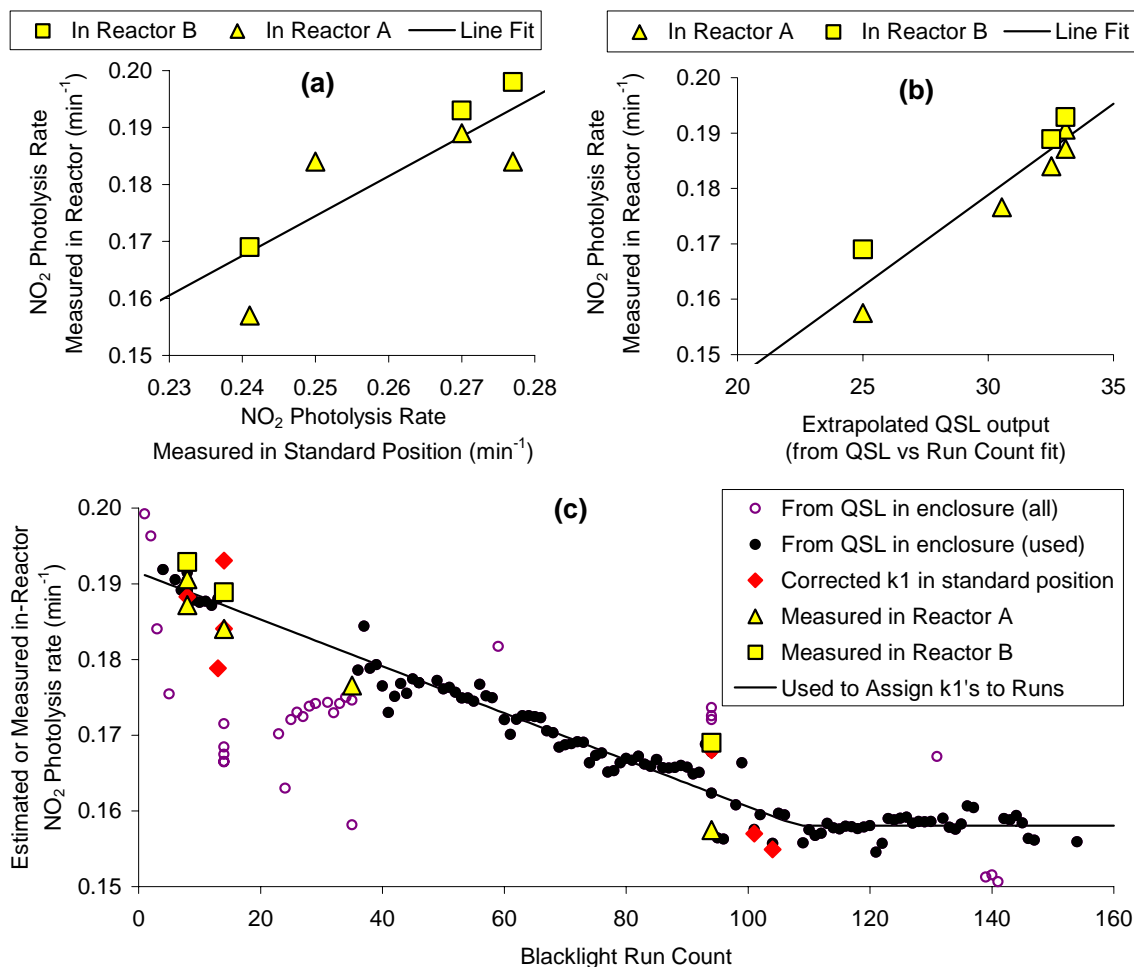
Figure 5. Plots of light intensity data used to assign NO$_2$ photolysis rates for the blacklight light source.

chamber photolysis rates. Figure 5a shows plots of in-reactor NO2 photolysis rates against measurements in the standard location made on the same day. The data are fit by a line through zero with a slope of 0.698, which is also shown on Figure 5a. This correction factor was used to derive in-chamber NO$_2$ photolysis rates from measurements in the standard position.

- The most useful dataset for determining how light intensity varied with time came from the QSL Spherical irradiance sensor located in front of the reactors near the NO$_2$ actinometry tube in the "standard" location. Data from this sensor are available for almost all experiments, and averages during the experiments are used as the relative measure of light intensity during the run. These data are calibrated by comparing results of in-chamber NO$_2$ actinometry measurements and standard QSL measurements appropriate for the time of the actinometry measurements (derived as discussed below), and the results are shown on Figure 5b. The line shows the least squares line fit through the data, which can be used to derive in-chamber NO$_2$ photolysis rates from averages of the QSL measurements made during the experiments.

Since blacklight experiments were conducted only intermittently and the blacklights were not used during the arc light experiments, the EPA run number did not provide a useful measurement of the aging of the light source for estimating the trends in light intensity with time. Instead, the "blacklight run count", which is the number of experiments carried out using blacklights up to the time of the experiment being considered, is used for this purpose. Plots against blacklight run count of in-chamber NO_2 photolysis rates derived by direct measurement or from the actinometry measurements in the "standard" location or from the QSL data from the fits shown on Figure 5a and Figure 5b are shown on Figure 5c. It can be seen that up to blacklight run count 110 (around run EPA384) the actinometry results and most of the QSL data are well fit by a straight line, which can be used as a basis for assigning NO_2 photolysis rates for individual experiments. After around the time of EPA384 the QSL data indicate that the light intensity no longer declines significantly.

Figure 5 shows that not all the QSL measurements were well fit by the trend line. In general, the outliers tended to be QSL measurements from experiments where the QSL was not in the standard location, or where there were indications that QSL measurements were being affected by structures within the enclosure. These data were not used in determining the trend line. Note that a similar trend line was used to derive the QSL values for the times of the in-chamber NO_2 actinometry measurements for the purpose of relating the QSL data to the in-chamber NO_2 photolysis rates as shown on Figure 5b. This permitted the use of the QSL data to derive the trend line shown on Figure 5c used for estimating NO_2 photolysis rates for individual experiments.

The results of this analysis indicates that the NO_2 photolysis rate for blacklight experiments declines from about 0.191 min^{-1} when the lights were first installed to about 0.158 at the time of blacklight run count 110 (EPA384), and then levels off at that value. This was used when deriving photolysis rates for experiments using this light source. The reason why the decline in intensity apparently ends around the time of run EPA384 is unknown.

The spectrum of the blacklights in this chamber were measured periodically and found to be essentially the same as the spectrum recommended by Carter et al (1995b) for modeling blacklight chamber runs.

Chamber Effects Characterization

The results of the individual characterization experiments that are relevant to the CARB experiments discussed in this report are summarized in the "Results" column of Table A-4 of Carter and Malkina (2005), and the results of the more recent characterization runs relevant to the experiments for this project are listed in Table B-1 in Appendix B of this report. The results that were used to derive characterization parameters used when modeling experiments for this project are discussed below.

Except as discussed below, the characterization results for the more recent experiments for this project are consistent with those discussed by Carter and Malkina (2005), and the same characterization parameters were used for modeling. The most important chamber effect, and the only chamber effect where some change may have occurred during the experiments discussed in this report, concerns the apparent HONO offgasing, which is believed to be responsible for both the chamber radical source and NO_x offgasing effects (Carter, 2004a). This is represented in the chamber effects model by the parameter RN-I, which is the HONO offgasing rate used in the simulations divided by the light intensity as measured by the NO_2 photolysis rate. Figure 6 shows the HONO offgasing parameters that best fit the radical or NO_x - sensitive characterization experiments carried out in the UCR EPA chamber in its current configuration, plotted against the EPA run number. Note that the discussion of Carter and Malkina (2005) cover runs through EPA250, so the runs with higher numbers have not been discussed previously.
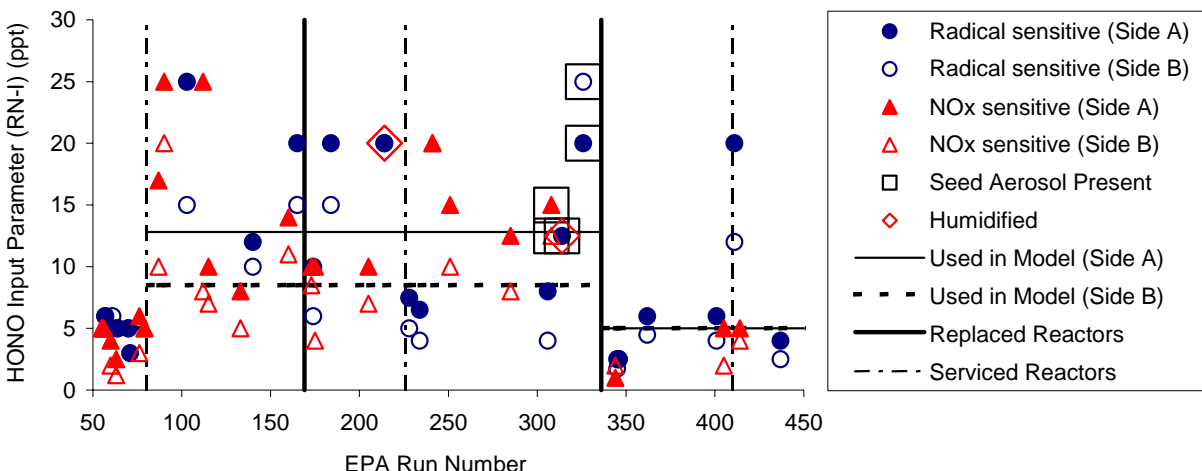
Figure 6. Plots of best fit HONO offgasing parameters against UCR EPA run number. (Data from Carter (2004a), with results of newer experiments for this project added.)

As indicated in Table B-1, some runs were humidified and/or had seed aerosol present, and such runs are indicated by special symbols on Figure 6. Although some such runs has somewhat higher apparent HONO offgasing rates than indicated by the chamber model, the result is not significantly outside the range of variability and other such runs have apparent HONO offgasing rates within thenormal range. Therefore, for the purpose of modeling we assume that the humidification or presence of seed aerosol, at least at the levels employed in these experiments, does not significantly affect the HONO offgasing rates.

After run EPA336 both of the reactors were replaced, and the results of most of the radical source and NOx offgasing characterization experiments indicated significantly lower apparent HONO offgasing rates than in the previous reactor. The results were within the range of the first reactors in the chamber in its present configuration, as discussed by Carter (2004a). The only exception was a radical-source sensitive experiment carried out right after maintenance was done in the chamber, but the results of subsequent runs indicated that this may be anomalous. A more recent NOx-sensitive experiment (EPA440) also indicated a somewhat higher apparent HONO offgasing (RN-I of 12 ppt for Side A), but that run was carried out subsequently to the period of this report and its results are assumed not to be applicable.

For modeling purposes, we use the same chamber effects parameters as used by Carter (2004a) and Carter and Malkina (2005) for runs through EPA336, which are given by Carter (2004a). For the more recent runs in the reactor installed after EPA336, an RN-I value of 5 ppt is used for modeling experiments in both reactors, but the other chamber effects parameters are the same as given by Carter (2004a) for the previous runs. The RN-I values assigned for modeling the runs in the two reactors are indicated on Figure 6.

The results of the side equivalency test experiments are shown on Table 7, below, where they can be compared with the results of the incremental reactivity experiments with added test compounds. These are discussed below in conjunction with the discussion of the incremental reactivity experiments with the added test compounds.

35

Results of Injection Tests and Test VOC Analyses

Preliminary tests were performed also to assure that all of the reactant VOCs used as test compounds for this projects (the glycols, DGBE and benzyl alcohol) were completely injected into the gas phase in experiments for this project. It is important that all of the reactant be injected because of uncertainties in the GC analyses and calibrations of these compounds, and this is a concern because of the injection system location on the first floor of laboratory building and long length of injection lines leading into the reactors on the second floor. In these test injections, a total carbon analyzer was used to determine the total amounts of gas-phase carbon after the test compounds has been injected until it was all gone and returned back to purified air reading and to track any changes occurred during injection. These tests were used to determine the necessary injection times and injection system temperatures to assure complete injection of the compounds being evaluated. Different parts of injection system were evaluated using total hydrocarbon analyzer to avoid any hang up of test compound or test mixture while it was injected. In most of experiments with glycols glass injection tube was maintained at 150°C while injection lines into reactors were heated up to 100°C. Slightly lower temperatures were used for injection of DGBE (140°C for the injection tube and 100°C for the injection lines) and Benzyl Alcohol (130°C and 80°C, respectively).

The results indicated that with these procedures that it is reasonable to assume that complete injection of the glycols, DGBE, and benzyl alcohol is occurring during our experiments. Because of this, and because of inconsistent results in the calibrations of these compounds using methanol solutions as discussed above, we used the calculated amounts injected for determining the initial concentrations of the glycols and DGBE when modeling experiments with these compounds. (Test calculations were carried out using measured amounts injected for selected glycol experiments, but the results did not give better fits of model to chamber data.) In the case of benzyl alcohol, the GC measurements, calibrated using methanol solutions discussed above, were reasonably consistent with the calculated amounts injected for most experiments, so the measured concentrations were used for determining initial benzyl alcohol concentrations when modeling experiments with this reactant.

One complication observed in the glycol analysis was that we observed an unexpected peaks in our GC loop analysis of surrogate mixture in experiments with ethylene glycol and propylene glycol, with one unexpected peak being seen in experiments with ethylene glycol injected, and a different unexpected peek being seen in the propylene glycol experiments. The peaks had good shape but were not consistent in area from analysis to analysis. Since we did not expect the glycols to make it through the valve in the loop analysis, and no GC peaks were observed in our previous experiments with propylene glycol using the same columns and sampling methods (Carter et al, 1997), we were concerned that this might be a contaminant or a glycol decomposition product forming during the injection process. Therefore, a number of tests were carried out to investigate this problem, with no evidence for decomposition or contaminates being observed. Eventually, we concluded that the peaks were the glycols themselves, though the reason they were observed in the loop analysis now and not in our previous study (Carter et al, 1997) is not known. However, the net effect of this was that we conducted more tests to assure satisfactory injection procedures for the glycols than otherwise would have been the case.

OH Radical Rate Constant Determinations

All four of the compounds studied for this project are consumed in the atmosphere primarily by reactions with the OH radical. Although measuring OH radical rate constants was not in the scope of this project, we found that for many of the experiments the GC analysis employed in our laboratory using the Tenax cartridge method gave sufficiently precise measurements of these compounds in the gas phase to make a relative rate constant determination feasible. The m-xylene present in the MIR or MOIR/2 surrogate experiments provided a suitable reference compound that is needed for this purpose. As with

Texanol® (Carter and Malkina, 2005) the measurements made during the reactivity experiments were sufficient for this purpose, and separate experiments for rate constant determination purposes were not necessary.

If it is assumed that the test compounds react in our experiments only with OH radicals, then the ratio of OH radical rate constants with other compounds present that also only react with OH can be determined from their relative rates of decay. In this case, the kinetic differential equations for the organics can be solved and rearranged to yield

$$\ln(\frac{[\text{Organic}]_{t0}}{[\text{Organic}]_t}) - D_t = \frac{k_{\text{Organic}}}{k_{\text{Reference}}} \ln\left[(\frac{[\text{Reference}]_{t0}}{[\text{Reference}]_t}) - D_t \right] \tag{I}$$

where $[\text{Organic}]_{t0}$ and $[\text{Organic}]_t$, $[\text{Reference}]_{t0}$, and $[\text{Reference}]_t$ are the initial and time=t concentrations of the test and reference compounds, respectively, k_{Organic} and $k_{\text{Reference}}$ are the test and reference compound's OH rate constant, and D_t is a factor added to account for dilution, which is assumed to be zero in our experiments. Therefore plots of $\ln([\text{Organic}]_{t0}/[\text{Organic}]_t)$ against $\ln([\text{Reference}]_{t0}/[\text{Reference}]_t)$ should yield a straight line with intercept of approximately zero and a slope that is the ratio of rate constants. Given the known value of $k_{\text{Reference}}$, then k_{Organic} can then be derived. m-Xylene is chosen as the reference compound because it is the most rapidly reacting compound in our reactivity experiments that reacts significantly only with OH radicals, and its OH radical rate constant is well known.

The test and reference compound measurement data taken during the incremental reactivity experiments with data suitable for OH radical rate constant determinations given in Table 3 for DGBE and benzyl alcohol, Table 4 for ethylene glycol and Table 5 for propylene glycol. The slopes of these plots (taken as the rate constant ratios, as indicated in Equation I, above) for the individual experiments, and those derived from fits to all the data (excluding rejected data and data from experiments with added seed aerosol, where applicable) are also given on the tables. Figure 7 and Figure 8 shows plots of Equation (I) derived from these data for the various compounds. (Plots of data for the glycol experiments with the wet seed aerosol are given later in this report, in the context of the discussion of those experiments.) The solid line shows the fits of these data to Equation (I), whose slope is taken as the measured rate constant ratio, and the dotted lines show the predictions of Equation (I) using the rate constant in the current SAPRC-99 mechanism. The rate constant results, and the derivations of the rate constants used in the current SAPRC-99 mechanism, are summarized in Table 6.

As indicated on Table 6 and Figure 7, the DGBE rate constants derived from the reactivity experiments with this compound was only 17% higher than the estimated value used in the current mechanism. This good agreement between chamber experiment-derived and estimated OH rate constant is similar to the result observed with the Texanol® isomers (Carter and Malkina, 2005), where equally good agreement between experimental and estimated values were obtained. Because the estimated value used in the current mechanism was essentially within the uncertainty of the experimental measurement, the rate constant used in the mechanism for this compound was not changed.

Table 6 and Figure 7 also shows that the rate constant derived for benzyl alcohol from the chamber experiments is in excellent agreement with the experimental value reported by Atkinson (1989), which is used as the basis for the rate constant in the current mechanism.

Figure 8 shows that there is somewhat more scatter in the data for ethylene and propylene glycol than was the case for the other two compounds, reflecting the greater difficulty in obtaining quantitative GC measurements for these glycols. However, if the obvious outliers are excluded, then the OH radical rate constant ratio derived from these data are the same, within the experimental uncertainty, as the measured values reported by Aschmann and Atkinson (1998).

Table 3.   Data used for OH radical rate constant determinations for 2-(2-butoxyethoxy)-ethanol (DGBE) and benzyl alcohol.

DGBE Experiments			Benzyl Alcohol Experiments		
Irrad. Time	m-Xylene (ppm)	DGBE (ppm)	Irrad. Time	m-Xylene (ppm)	Benzyl Alc. (ppm)
Run EPA353, Ratio = 2.26			EPA319, Ratio = 1.06		
Init [a]	0.026	0.019	Init	0.013	0.106
8	0.026	0.019	-6	0.013	0.104
38	0.025	0.018	22	0.012	0.101
66	0.022	0.013	97	0.008	0.060
106	0.020	0.010	133	0.007	0.055
126	0.019	0.010	165	0.006	0.048
163	0.018	0.008	194	0.006	0.047
193	0.017	0.007	222	0.006	0.046
229	0.017	0.007	252	0.005	0.042
267	0.016	0.007	279	0.005	0.042
303	0.016	0.006	307	0.005	0.039
337	0.015	0.005	337	0.005	0.037
368	0.015	0.005	363	0.005	0.036
Run EPA335, Ratio = 1.98			EPA323, Ratio = 1.19		
Init	0.027	0.037	Init	0.013	0.068
75	0.023	0.024	-9	0.013	0.066
102	0.019	0.020	18	0.013	0.062
134	0.017	0.017	93	0.007	0.038
161	0.015	0.013	122	0.006	0.025
186	0.016	0.012	148	0.005	0.022
221	0.015	0.011	175	0.005	0.022
248	0.014	0.009	200	0.005	0.020
			225	0.004	0.019
			256	0.004	0.018
			281	0.004	0.017
			366	0.004	0.014
Run EPA352, Ratio = 2.31			EPA320, Ratio = 1.00		
Init.	0.014	0.016	Init	0.027	0.115
-3	0.014	0.015	-59	0.028	0.116
28	0.013	0.015	-30	0.027	0.112
61	0.013	0.014	-5	0.026	0.116
126	0.011	0.010	85	0.018	0.078
196	0.010	0.008	155	0.016	0.072
231	0.009	0.006	185	0.015	0.066
260	0.009	0.006	214	0.016	0.068
324	0.008	0.004	274	0.015	0.063
354	0.008	0.004	305	0.015	0.063
Fits to all Data: Ratio = 2.14			Fits to all Data: Ratio = 1.08		

[a] The initial concentrations for each experiment were set to force a zero intercept for plots of Equation (I) for the experiment.

Table 4.   Data used for OH radical rate constant determinations for ethylene glycol.

Irrad. Time	m-Xylene (ppm)	Ethylen. Glycol (ppm)	Irrad. Time	m-Xylene (ppm)	Prop. Glycol (ppm)
EPA258, Ratio=0.46			EPA 253, Ratio=0.47		
Init [a]	0.021	0.107	Init.	0.029	0.157
-7	0.021	0.096	-10	0.029	0.158
33	0.018	0.104	29	0.025	0.144
185	0.010	0.066	65	0.021	0.134
240	0.009	0.079	164	0.015	0.121
295	0.009	0.076	303	0.014	0.147 [b]
			350	0.013	0.143 [b]
			367	0.013	0.104
			EPA 325, Ratio=0.50 (wet seed aerosol) [c]		
EPA 250, Ratio=0.58					
Init.	0.027	0.200	Init.	0.010	0.174
0	0.027	0.190	-1	0.010	0.172
85	0.019	0.169	30	0.008	0.160
120	0.017	0.176	57	0.007	0.147
160	0.016	0.144	84	0.006	0.140
205	0.015	0.137	110	0.006	0.131
265	0.014	0.123	137	0.005	0.124
360	0.013	0.135	164	0.005	0.110
			224	0.004	0.098
			261	0.004	0.095
			289	0.004	0.088
			320	0.004	0.083
			350	0.003	0.083
			Fits to all Data: Ratio [c] = 0.49		

[a] The initial concentrations for each experiment were set to force a zero intercept for plots of Equation (I) for the experiment.

[b] Data considered to be anomalous and not used for determining the rate constant ratio.

[c] Data from the wet seed aerosol experiment not used to determine the "best fit" rate constant ratio shown on Figure 8.

Table 5.   Data used for OH radical rate constant determinations for propylene glycol.

Irrad. Time	m-Xylene (ppm)	Prop. Glycol (ppm)	Irrad. Time	m-Xylene (ppm)	Prop. Glycol (ppm)
EPA257, Ratio=0.73			EPA245, Ratio=1.11		
Init [a]	0.014	0.213	Init	0.027	0.276
0	0.014	0.201	0	0.027	0.297
33	0.013	0.214	45	0.021	0.180
72	0.011	0.159	137	0.018	0.100 [b]
152	0.008	0.154	167	0.017	0.078 [b]
198	0.008	0.145	286	0.016	0.157
251	0.007	0.123			
295	0.007	0.121			
337	0.007	0.122			
377	0.007	0.116			
EPA273, Ratio=1.13			EPA252, Ratio=1.23		
Init	0.014	0.179	Init	0.027	0.334
0	0.014	0.153	-4	0.027	0.353
102	0.010	0.136	30	0.024	0.259
148	0.009	0.125	70	0.021	0.240
188	0.008	0.113	106	0.019	0.203
275	0.004	0.051	177	0.017	0.199
321	0.006	0.053	209	0.017	0.193
357	0.005	0.059	245	0.015	0.167
			284	0.015	0.146
			EPA316, Ratio= 0.80 (wet seed aerosol) [c]		
EPA277, Ratio=0.85					
Init	0.014	0.140	Init	0.026	0.287
-6	0.014	0.140	-54	0.027	0.314
29	0.013	0.145	-27	0.026	0.286
75	0.010	0.112	-4	0.026	0.283
141	0.007	0.085	26	0.025	0.271
181	0.006	0.088	57	0.021	0.257
217	0.006	0.067	90	0.018	0.200
256	0.005	0.074	181	0.015	0.168
341	0.004	0.045	211	0.014	0.153

Fits to all Data: Ratio [c] = 0.90

[a] The initial concentrations for each experiment were set to force a zero intercept for plots of Equation (I) for the experiment.

[b] Data considered to be anomalous and not used for determining the rate constant ratio.

[c] Data from the wet seed aerosol experiment not used to determine the "best fit" rate constant ratio.
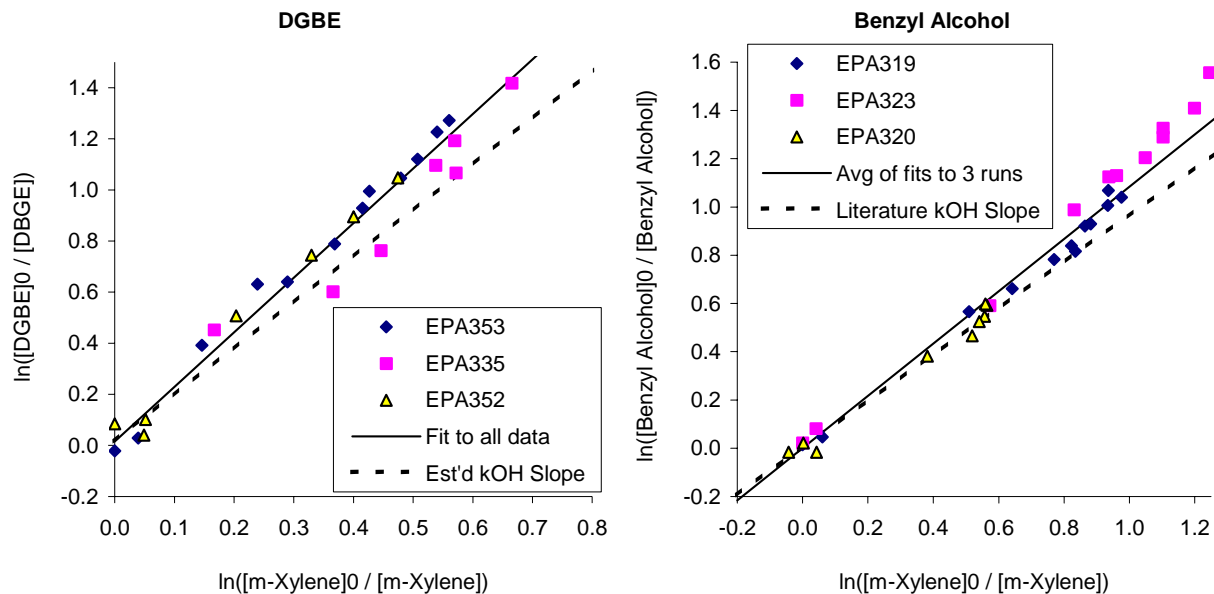
Figure 7.   Plots of Equation (I) for the data from the 2-(2-Butoxyethoxy)-ethanol (DGBE) and benzyl alcohol reactivity experiments.
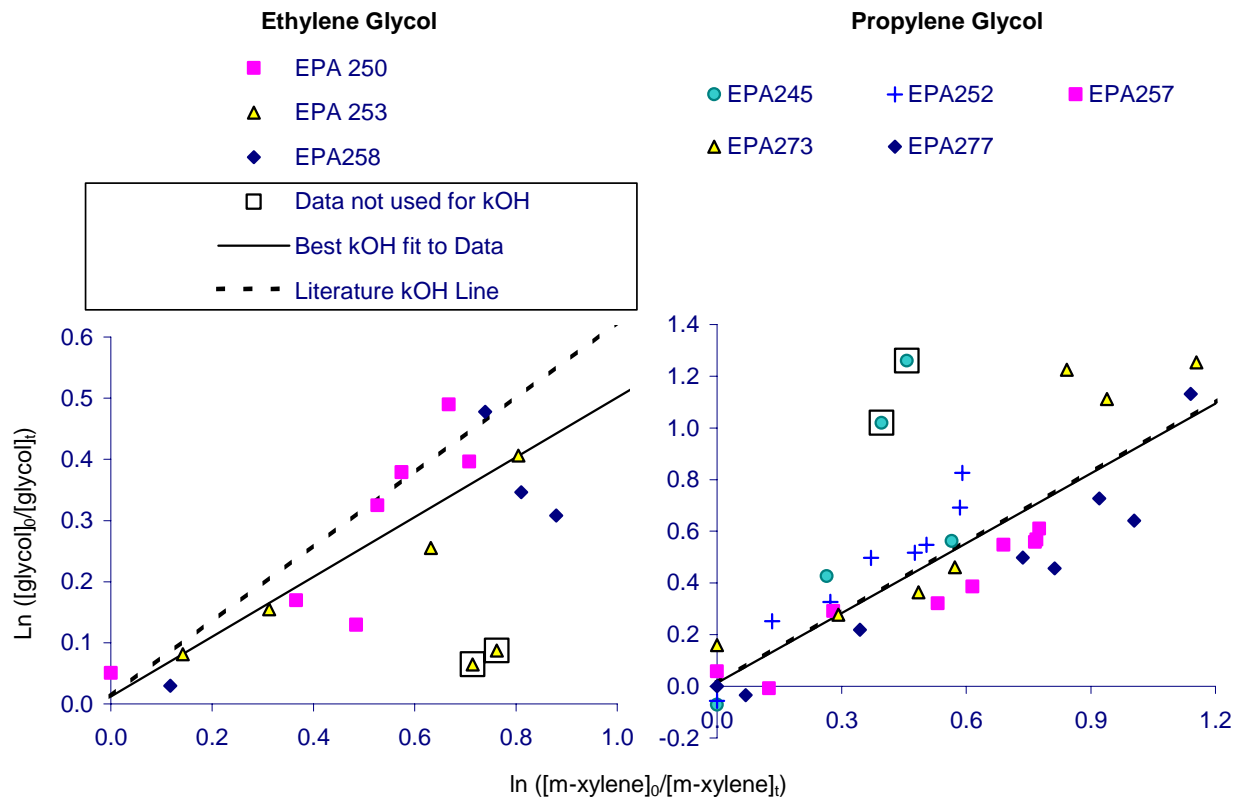
Figure 8.   Plots of Equation (I) for the data from the ethylene and propylene glycol experiments.

Table 6.   Summary of results of relative OH radical rate constant measurements for DGBE, benzyl alcohol, and the glycols, and comparison with the OH rate constants used in the SAPRC-99 mechanism

Compound	kOH relative to m-xylene	Absolute kOH [a] (cm^3 $molec^{-1}$ s^{-1})	SAPRC-99 kOH (cm^3 $molec^{-1}$ s^{-1})	SAPRC-99 kOH derivation
2-(2-Butoxyethoxy)-ethanol (DGBE)	2.14	5.04×10^{-11}	4.29×10^{-11}	Structure-reactivity estimate (Carter, 2000a)
Benzyl Alcohol	1.08	2.56×10^{-11}	2.29×10^{-11}	Single unpublished measurement cited by Atkinson (1989)
Ethylene Glycol	0.49 [b]	1.15×10^{-11}	1.47×10^{-11}	Aschmann and Atkinson (1998).
Propylene Glycol	0.90 [b]	2.13×10^{-11}	2.15×10^{-11}	Aschmann and Atkinson (1998).

[a] Based on m-xylene rate constant of 2.36×10^{-11} and cm^3 $molec^{-1}$ s^{-1} (Atkinson, 1989).

[b] Results of added seed aerosol experiments not included in the average. See Table 4 or Table 5.

Table 4 and Table 5 indicate that relative OH radical rate constant measurements were derived from the wet seed aerosol experiments as well. The results were not used to derive the overall rate constants for these compounds because the purpose of the wet seed aerosol experiments were to investigate the possibility of heterogeneous interactions between the glycols and the aerosols that were present, which would affect the apparent relative rate constant results if the interactions were significant. These results, and plots of these data, are discussed below in the context of the discussion of these seed aerosol and "availability" investigation experiments.

Incremental Reactivity and Mechanism Evaluation Results

Table 7 lists the initial concentrations and selected results for the incremental reactivity and other ozone mechanism evaluation experiments with the coatings solvents carried out for this project. The measures of gas-phase reactivity used to evaluate the mechanisms in the incremental reactivity experiments are the effects of the test compound or solvent on $\Delta([O_3]-[NO])$, or $([O_3]_t-[NO]_t)-([O_3]_0-[NO]_0)$, and IntOH, the integrated OH radical levels. As discussed elsewhere (e.g., Johnson, 1983; Carter and Atkinson, 1987; Carter and Lurmann, 1991, Carter et al, 1993), $\Delta([O_3]-[NO])$ gives a direct measure of the amount of conversion of NO to NO_2 by peroxy radicals formed in the photooxidation reactions, which is the process that is directly responsible for ozone formation in the atmosphere. This gives a useful measure of factors affecting O_3 reactivity even early in the experiments where O_3 formation is suppressed by the unreacted NO. Although this is the primary measure of the effect of the VOC on O_3 formation, the effect on radical levels is also a useful measure for mechanism evaluation, because radical levels affect how rapidly all VOCs present, including the base ROG components, react to form ozone.

The integrated OH radical levels are not measured directly, but can be derived from the amounts of consumption of reactive VOCs that react only with OH radical levels. In particular,

$$\text{IntOH}_t = \frac{\ln([\text{tracer}]_0/[\text{tracer}]_t) - \text{Dt}}{\text{kOH}^{\text{tracer}}} \tag{II}$$

Table 7.   Summary of initial concentrations and selected gas-phase results of the incremental reactivity and solvent - NO$_x$ experiments.

Run	Test Side	Type [a]	Added	Base Run Initial Concentrations		Hours	Final O$_3$ (ppb)		Δ([O$_3$]-[NO]) Change (ppb)		IntOH Change
				NOx (ppb)	ROG (ppmC)		Test	Base	2 Hr	Final	(ppt-min)
				Side Equivalency Tests							
235	B	MIR		32	0.55	5	164	160	4	4	3
233	B	MOIR/2		27	1.11	6	175	175	2	0	0
334	B	MOIR/2		28	1.28	5	179	178	0	-1	2
				Propylene glycol (calculated ppm added)							
257	B	MIR	0.40	33	0.63	6	246	167	95	81	-31
273	A	MIR [b]	0.20	32	0.60	5	162	94	60	69	-15
277	A	MIR	0.20	32	0.59	6	229	182	58	42	-34
245	B	MOIR/2	0.40	27	1.17	5	213	159	52	53	-17
252	A	MOIR/2	0.40	27	1.23	6	216	174	46	41	-18
404	B	MIR-NA [b]	0.20	27	0.59	5	130	55	25	76	-1
				Ethylene glycol (calculated ppm added)							
278	B	MIR	0.30	33	0.62	5	232	161	55	70	-15
250	B	MOIR/2	0.40	27	1.21	5	212	165	36	45	-13
253	A	MOIR/2	0.40	27	1.16	5	202	157	35	44	-12
415	B	MIR-NA [b]	0.20	27	0.59	6	132	72	34	61	0
				2-(2-Butoxyethoxy)-ethanol (DGBE) (measured ppm added)							
352	B	MIR	0.050	31	0.58	5	147	152	-18	-5	-32
335	A	MOIR/2	0.050	28	1.24	4	147	149	0	0	-15
353	B	MOIR/2	0.050	26	1.18	6	173	171	3	1	-16
				Benzyl alcohol (measured ppm added)							
319	A	MIR	0.088	31	0.56	5	139	153	58	-15	-28
323	B	MIR	0.059	27	0.53	5	134	140	39	-4	-20
320	B	MOIR/2	0.102	21	1.09	3	115	119	7	-2	-10
321	A	Compound - NO$_x$ [b,c]	0.32	25		6	126				
321	B		0.32	50		6	97				
322	A	Compound - NO$_x$ [c]	0.37	26		5	159				
322	B		0.37	51		5	126				
325	A		0.24	55		5	159				
325	B	Compound - NO$_x$ + CO	0.21	59	26 ppm CO	6	200				

[a] Codes for types of base case experiments for the incremental reactivity experiments are as follows: "MIR": ~30 ppb NO$_x$ and ~0.55 ppmC 7-component ROG surrogate without formaldehyde; "MOIR/2": ~25 ppb NO$_x$ and ~1.1 ppmC 7-component surrogate without formaldehyde; "MIR-NA": ~30 ppb NO$_x$ and ~0.6 ppmC non-aromatic surrogate with blacklight irradiation.

[b] Blacklights used

[c] No base case ROG surrogate added; not an incremental reactivity experiment. Equal benzyl alcohol injections in both sides, with NO$_x$ varied or CO added.

where [tracer]$_0$ and [tracer]$_t$ are the initial and time t concentrations of the compound used as the OH tracer, kOH^{tracer} its OH rate constant, and D is the dilution rate in the experiments. The latter is small in our chamber and is neglected in our analysis. For most experiments, the base ROG surrogate component m-xylene is the most reactive compound in the experiment that reacts only with OH radicals, and was therefore used as the OH tracer to derive the IntOH data. However, for the non-aromatic surrogate experiments the base ROG component n-octane was used for the OH radical tracer. The m-xylene and n-octane OH radical rate constant used in this analysis were 2.36×10^{-11} and cm^3 molec^{-1} s^{-1} (Atkinson, 1989) and 8.76×10^{-12} and cm^3 molec^{-1} s^{-1} (Atkinson, 1997), respectively.

The side equivalency tests, where equal base ROG - NO$_x$ mixtures are simultaneously irradiated without added test compounds, provide a measure of the sensitivity of the experiments to distinguish the effects of the added VOCs. In most cases, the side equivalency for the gas-phase measurements was excellent, with the O$_3$ and $\Delta([O_3]-[NO])$ differences being no greater than ~5 ppb and the IntOH differences being less than 5 ppt-min. The results of these tests are summarized on Table 7.

The results for the individual test compounds are discussed in the following sections. However, before discussing the results of the incremental reactivity experiments, it is important to emphasize again that incremental reactivities in the chamber are not necessarily those in the atmosphere. The purpose of the experiments is to test the predictive capabilities of the mechanisms, as discussed in the following section of this report. Although the experiments are designed to represent a range of *chemical* conditions applicable to the atmosphere, it is not practical to duplicate atmospheric conditions exactly, and different aspects of the mechanism have somewhat different relative importances in affecting the results of chamber experiments than in model simulations of the atmosphere. This was discussed in more detail by Carter and Malkina (2005), where specific examples of the differences are given.

Measurements were also made of PM formation during these reactivity experiments, allowing effects of these compounds on PM formation to be assessed. These and other PM results are discussed later in this report.

Propylene Glycol

Three MIR (one with blacklights), two MIOR/2 and one non-aromatic surrogate MIR (with blacklights) reactivity experiments were carried out for propylene glycol for evaluating its gas-phase mechanism. As indicated on Table 7, the addition of the glycol caused a significant increase in the amount of ozone formed and NO oxidized in all the reactivity experiments with this compound. The addition of the glycol caused a decrease in the integrated OH radicals in the experiments with the standard ROG surrogate but had no significant effect on the integrated OH in the experiments with the non-aromatic surrogate. The IntOH results with the non-aromatic surrogate suggest that this compound does not have large inhibiting effects on radicals. The negative effect on IntOH in the experiments with the full surrogate cam be attributed, at least in part, to the reactions of OH radicals with the glycols reducing the availability of OH to react with the aromatics, whose photooxidation products are strong radical initiators. These IntOH results also indicate that this compound and its major products do not have large radical initiating properties. The relatively large positive effect on ozone is attributed to the direct reactivities of the compound and the fact that this direct reactivity is not being countered by radical inhibiting effects, as is observed for higher glycols such as DGBE (discussed below) or the non-aromatic solvents studied for the CARB coatings project (Carter and Malkina, 2005).

Concentration-time plots of $\Delta([O_3]-[NO])$ and IntOH, and changes in these quantities caused by the addition of propylene glycol are shown on Figure 9 for the MIR and the non-aromatic MIR (MIR-NA) experiments, and on Figure 10 for the MOIR/2 reactivity experiments. Results of SAPRC-99 model calculations of these quantities are also shown. As indicated above, the calculations were carried out both

44

Figure 9.   Experimental and calculated concentration-time plots of selected measurements for the MIR and the non-aromatic MIR incremental reactivity experiments with propylene glycol.

45

Figure 10.   Experimental and calculated concentration-time plots of selected measurements for the MOIR/2 incremental reactivity experiments with propylene glycol.

using the standard SAPRC-99 mechanism (shown as the darker, thinner solid and dashed lines on the figures) and the version where the mechanisms for the aromatics in the base ROG surrogate were adjusted to give improved simulations of the base case MIR experiments. (If only the adjusted model line is shown, it is because it gives essentially the same result as the standard model calculation.) Adjusted base aromatics model calculations are not shown for the MIR-NA experiment because the aromatics are not present in that run, so the adjustment has no effect on the simulations.

Incremental reactivity experiments with propylene glycol were also carried out previously under funding from the Philip Morris company, though with much higher base case ROG and NO_x levels and using only blacklight irradiation (Carter et al, 1997). Concentration-time plots of $\Delta([O3]-[NO])$ and IntOH, and changes in these quantities caused by the addition of propylene glycol for those experiments are shown on Figure 11. The codes for the base ROG surrogates used are as follows:

Code	Type	NO_x (ppb)	ROG (ppmC)	Surrogate
MR3	MIR	380	5.3	3-Component mini- surrogate
MR8	MIR	280	3.8	8-Component full surrogate
R8	Low NO_x	110	3.7	8-Component full surrogate

Results of model calculations with the standard SAPRC-99 mechanism are also shown. Calculations with the adjusted aromatic model calculations are now shown for these higher concentration surrogate
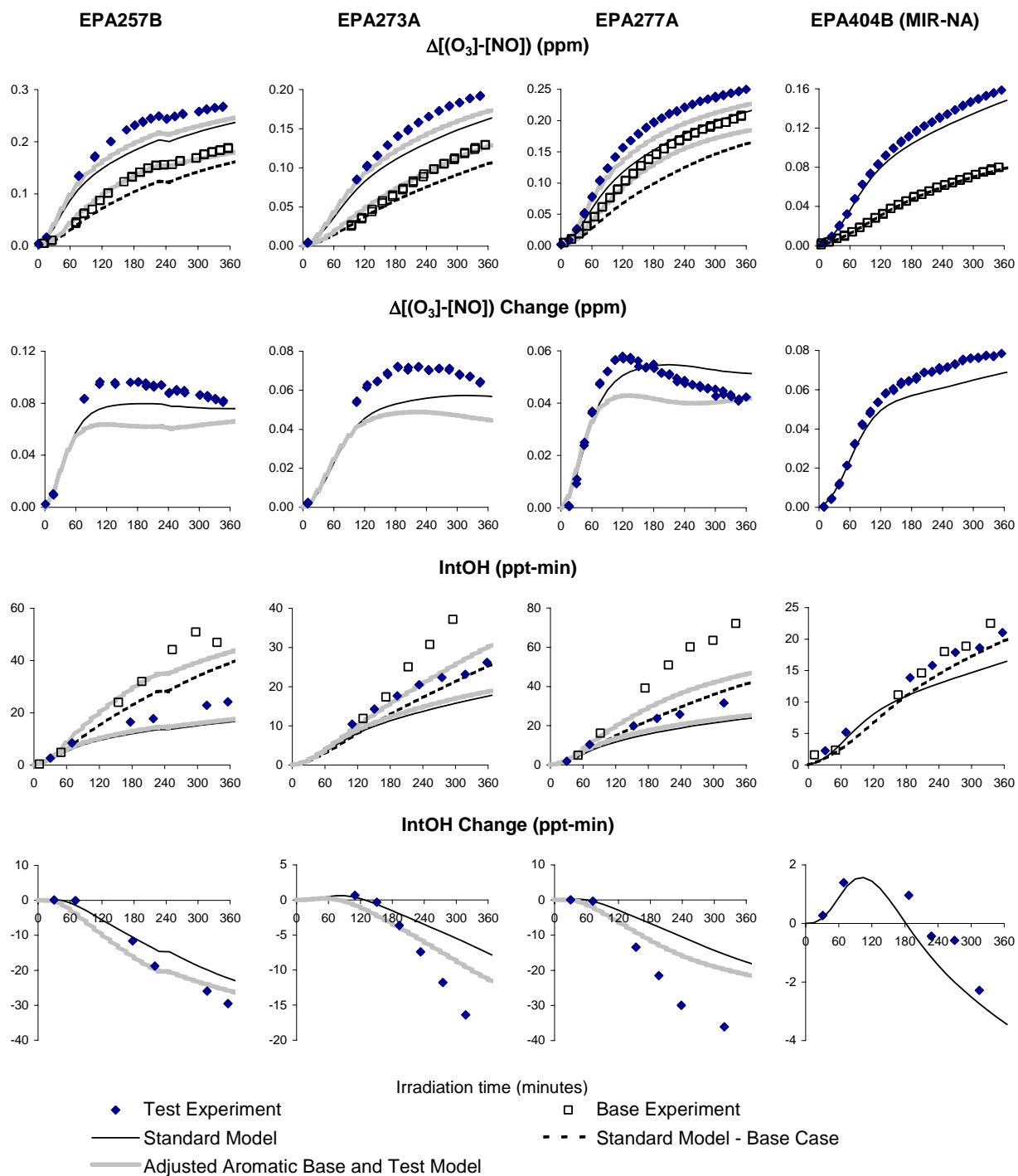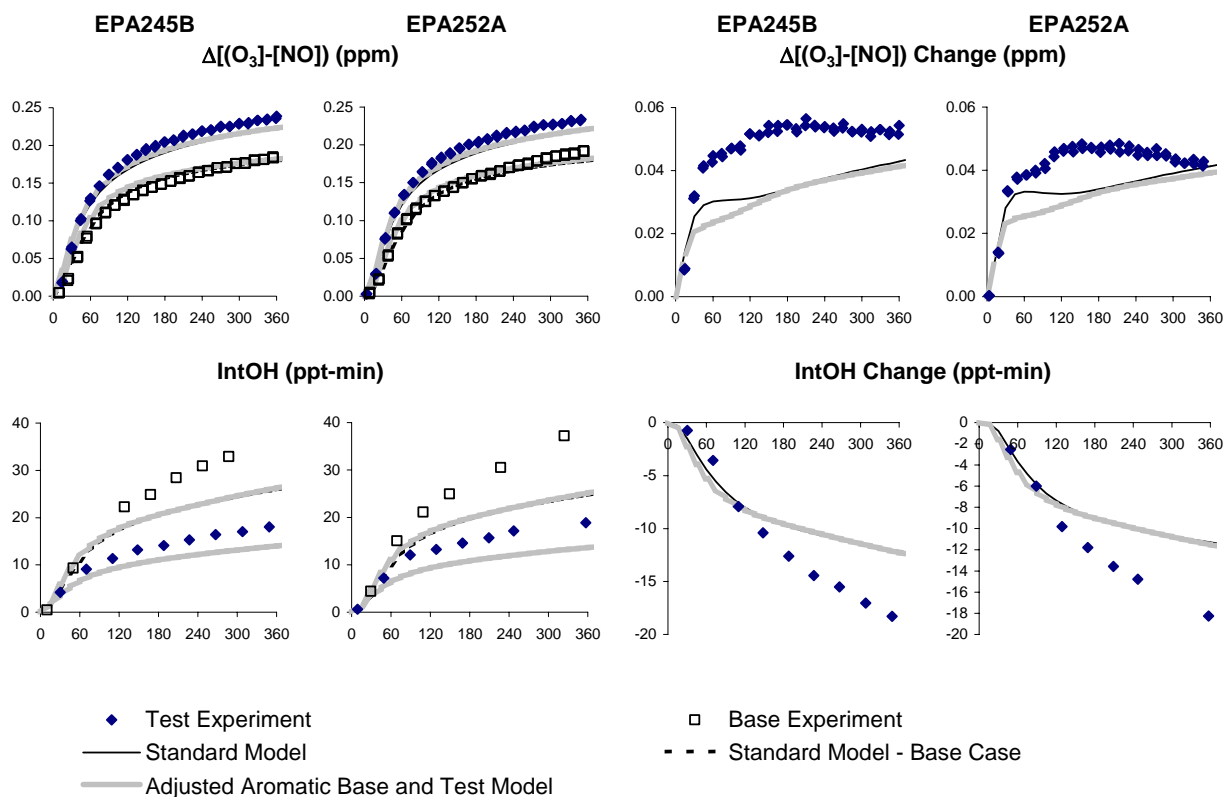
Figure 11.   Experimental and calculated concentration-time plots of selected measurements for the incremental reactivity experiments with propylene glycol carried out previously for Philip Morris (Carter et al, 1997).

47

experiments because the standard mechanism yields acceptable fits to the results of the base case experiments.

It can be seen that the mechanism gives moderately good fits to the data, though there is a tendency to underpredict, by up to ~20%, the O_3 impact of the added propylene glycol in most of the full surrogate reactivity experiments carried out for this project. This tendency to underpredict is not seen or is smaller in most of the Philip Morris experiments and for the experiment for this project with the non-aromatic surrogate. The model has a tendency to underpredict IntOH in the base case and the IntOH impacts for the test compounds, but this tendency is seen for many other compounds (e.g., see Carter and Malkina, 2005), and may reflect problems with the base mechanism. The IntOH underprediction tendency is less with the non-aromatic surrogate experiments and also with the higher concentration experiments carried out previously. The model correctly predicts that although propylene glycol suppresses IntOH in the experiments with the full (aromatic-containing) surrogates, it does not suppress IntOH in the experiment where the aromatics have been removed.

There is some uncertainty in the initial propylene glycol reactant concentrations in these experiments because the measured initial concentrations of these reactants (calibrated using methanol solutions) are consistently lower than the calculated amount injected. As discussed above, we use the calculated amounts injected in the model simulations because of inconsistencies with the GC calibration and because injection tests indicate that we should be injecting all of the glycols in the gas phase. In addition, using the lower measured amounts of glycol injected in the model simulations does not improve the fits of the model calculations to the experimental data. Note that this is also applicable to the ethylene glycol experiments, discussed in the following subsection.

In general, use of the adjusted mechanisms for the aromatics in the base ROG mixture causes slight improvements in model predictions of IntOH or and IntOH reactivity in the MIR experiments for this project, but tends to make the underprediction bias in the simulations of the O_3 impacts in those experiments somewhat worse. The adjustment has only small effects on the simulations of the MOIR/2 experiments, consistent with its smaller effects on the base case simulations. The sensitivity of the simulations of the O_3 impacts on the mechanism for the aromatics in the base ROG, and the fact that better simulations of the O_3 impacts are seen in the non-aromatic surrogate, suggests the possibility that this ~20% underprediction bias may have as much or more to do with problems with the aromatics mechanism as it has with the mechanism for this compound.

In any case, it is not clear what aspect of the propylene glycol mechanism would be appropriate for adjustment to remove this possible underprediction bias in some of the experiments. For a compound such as this, which has moderate or small effects on radical initiation and termination processes, the most important factor affecting reactivity in these experiments would be its direct reactivity, which is affected by its rate of reaction and number of NO to NO_2 conversions involved when it is oxidized. As discussed in the previous section, the measured rates of propylene glycol decay are consistent with the OH radical rate constant used in the mechanism, so the underprediction bias is unlikely to be due to the rate constant used. The oxidation mechanism is relatively straightforward, and is unlikely to be in error sufficiently to materially affect model predictions. The model simulations of propylene glycol reactivity were also found not to be insensitive to how the reactions of the major products were represented when reasonable alternatives were examined.

Based on these results and the factors discussed above, we do not believe that it is appropriate to modify the SAPRC-99 propylene glycol mechanism at the present time. The existing mechanism and reactivity calculation methodology and scenarios (Carter, 2000, 2003), give the following incremental reactivity values for propylene glycol in the MIR, MOIR, and EBIR scales.

Scale	Incremental Reactivity (gm O_3 / gm VOC)
MIR	2.74
MOIR	1.23
EBIR	0.83

These remain our recommended values for the incremental reactivities of propylene glycol in these scales.

Ethylene Glycol

One MIR, two MIOR/2 and one non-aromatic surrogate MIR (with blacklights) reactivity experiments were carried out for ethylene glycol for this project. As indicated on Table 7, the results for this compound were qualitatively similar to those with propylene glycol as discussed above. The addition of the glycol caused a significant increase in the amount of ozone formed and NO oxidized in all the reactivity experiments with this compound, but also caused a decrease in the integrated OH radicals in the experiments with the standard ROG surrogate, and had no significant effect on the integrated OH in the experiments with the non-aromatic surrogate. The IntOH results with the non-aromatic surrogate suggest that this compound, like propylene glycol, does not have large inhibiting or initiating effects on radicals.

Concentration-time plots of $\Delta([O_3]-[NO])$ and IntOH, and changes in these quantities caused by the addition of ethylene glycol are shown on Figure 12 for the experiments with the full surrogate and on Figure 13 for the experiments with the surrogate with the aromatics removed. Results of model calculations, using the both the standard and adjusted-aromatics mechanism for the base ROG are also shown. As before, the adjusted aromatics calculations are not shown on Figure 13 because the adjustments are not applicable to the non-aromatic surrogate.

As with propylene glycol, the model was shown to have a tendency to underpredict the impact of the glycol in the experiments with the full surrogate (with the underprediction being somewhat worse when the adjusted aromatics base mechanisms is used), but to give good fits to the O_3 impact in the non-aromatic surrogate experiment. However, in this case the O_3 impact underprediction tendency in the full surrogate experiments is somewhat greater, being on the order of 25-30%. As with propylene glycol, the model gives reasonably good predictions of the IntOH impact predictions for this compounds (considering the general tendency to underpredict impacts for most compounds), and correctly predicts the much smaller IntOH impact in the non-aromatic surrogate experiment.

As with propylene glycol, it is unclear what reasonable changes can be made to the ethylene glycol mechanism to improve the fits of the model simulations to the full surrogate experiments. The OH radical rate constant used in the model is unlikely to be the problem, since, as discussed in the previous section, the experimental measurements of the relative glycol decay rates in these experiments were in reasonably good agreement with the OH rate constant used in the model. There is relatively little uncertainty in the photooxidation mechanism for this compound, since the major reaction pathway is expected to be OH radical abstraction from the -CH_2, forming HO_2 and glycolaldehyde ($HOCH_2CHO$). A minor (~5% or less) reaction pathway would form two formaldehydes and a HO_2, but this does not affect the total number of NO to NO_2 conversions in the product formation process.

The most likely source of uncertainty in the ethylene glycol mechanism is the representation of glycolaldehyde, the major reaction product. The current version of the SAPRC-99 mechanism represents glycolaldehyde with the acetaldehyde model species, but in order to improve the representation of ethylene glycol an explicit representation of glycolaldehyde was added to the model for this work (see Table 2, above. This explicit representation did result in somewhat improved fits of model simulations to the glycol reactivity data, as is shown on Figure 14 and Figure 15, which show of the glycol
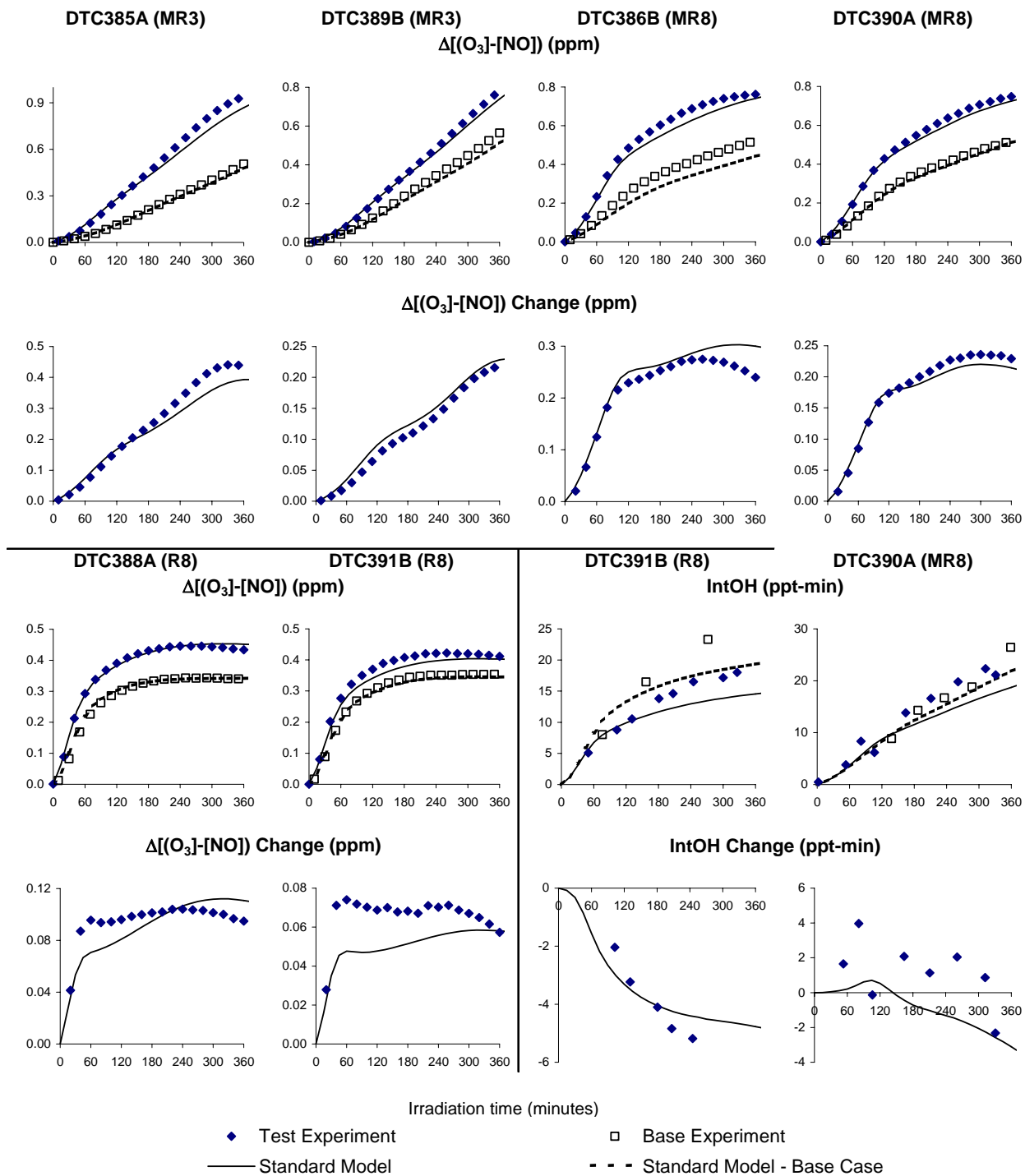
Figure 12. Experimental and calculated concentration-time plots of selected measurements for the full surrogate incremental reactivity experiments with ethylene glycol.

50

EPA415B (MIR-NA)

Δ[(O₃)-[NO]) (ppm)   Δ[(O₃)-[NO]) Change (ppm)   IntOH (ppt-min)   IntOH Change (ppt-min)

Irradiation time (minutes)

◆ Test Experiment   □ Base Experiment
── Standard Model   - - - Standard Model - Base Case

Figure 13.   Experimental and calculated concentration-time plots of selected measurements for the non-aromatic surrogate incremental reactivity experiment with ethylene glycol.

EPA278B (MIRa)   **EPA250B (MOIR/2a)**   **EPA253A (MOIR/2a)**   **EPA258B (MOIR/2a)**

Δ[(O₃)-[NO]) Change (ppm)

IntOH Change (ppt-min)

Irradiation time (minutes)

◆ Test Experiment   □ Base Experiment
── Explicit glycolaldehyde mechanism   ── Glycolahdehyde represented by acetaldehyde
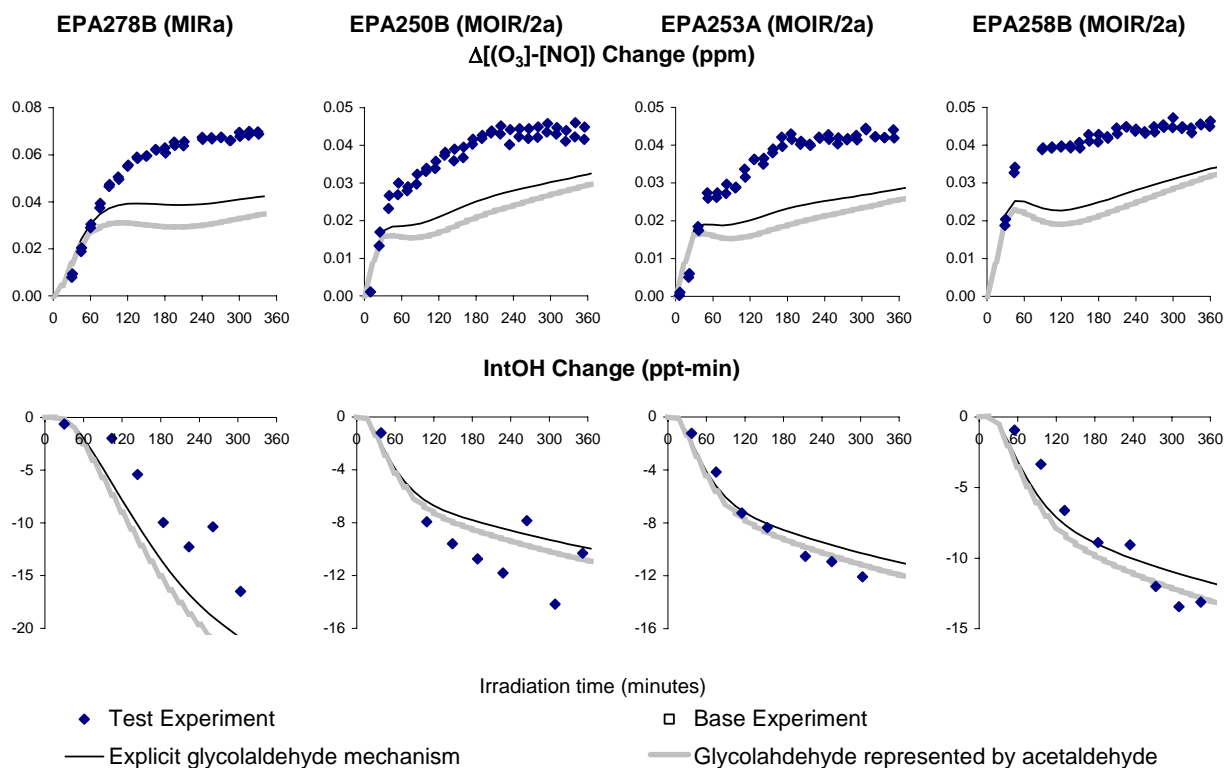
Figure 14.   Effects of changing the glycolaldehyde representation on the results of the model simulations of effects of added ethylene glycol on the incremental reactivity experiments. Model calculations used the adjusted aromatics base mechanism.

EPA415B (MIR-NA)
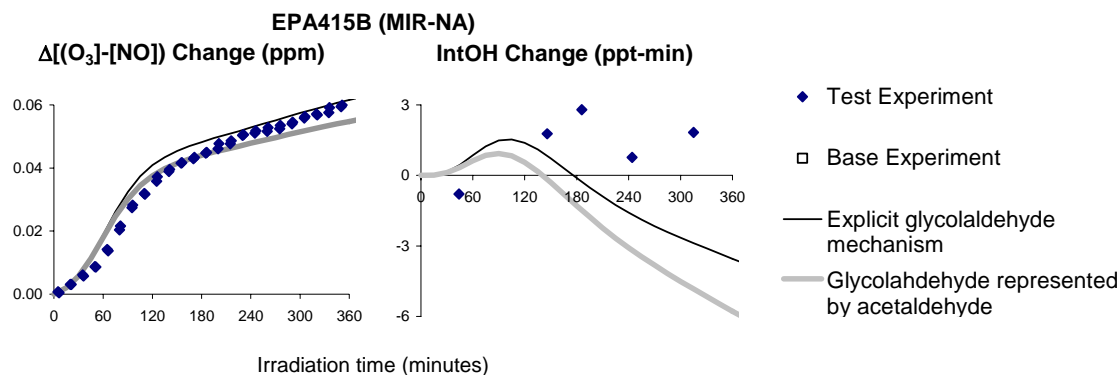
Figure 15.   Effects of changing the glycolaldehyde representation on the results of the model simulations of effects of added ethylene glycol on the non-aromatic surrogate incremental reactivity experiments.

representation on the model predictions of the change in $\Delta([O_3]-[NO])$ and IntOH observed in the ethylene glycol reactivity experiments. (The calculations on Figure 14 all use the adjusted aromatics base mechanism to give the best fits to the base case data.) It can be seen that changing the glycolaldehyde representation has a small but not totally negligible effect on the $\Delta([O_3]-[NO])$ and IntOH reactivity predictions, and that the underprediction bias is somewhat greater if the more approximate representation, used in the previous ethylene glycol mechanism (Carter, 2000a; Carter et al, 1997) is used. For that reason, the propylene mechanism used in this work (and to produce the model simulations shown on Figure 12 and Figure 13) employed the explicit glycolaldehyde representation. However, the effect of changing the glycol representation was relatively small and insufficient to eliminate the tendency of the model to underpredict the O_3 impacts of ethylene glycol in the full surrogate experiments.

Since there are data available concerning the major reactions of glycolaldehyde (IUPAC, 2002a,b). it is unlikely that the mechanism we use for glycolaldehyde is sufficiently in error to be the cause of the ethylene glycol model underprediction bias seen in these experiments. It is interesting to note, however, when we accidentally ran simulations with a mechanism where the rate constants for the non-photolysis reactions of glycolaldehyde were essentially zero, making photodecomposition the only significant loss process for this compound, then the fits of the model simulations were significantly improved. However, since the photolysis reactions of glycolaldehyde have been studied (IUPAC, 2002b), it is unlikely that the photolysis of this compound would be so rapid to dominate over the competing processes under the conditions of these experiments, and this mechanism is not chemically reasonable.

Since the ethylene glycol mechanism was modified for this work to represent glycolaldehyde explicitly instead of using the acetaldehyde model species, it was necessary to recalculate its atmospheric reactivities. Except for the representation the glycolaldehyde formed from ethylene glycol, the procedures used were the same as in the previous calculations of the SAPRC-99 reactivity scales (Carter, 2000a, 2003), as used to calculate the propylene glycol incremental reactivities given above. The reactivities, in units of grams O_3 per gram VOC is as follows:

Scale	Previous	Revised	Change
MIR	3.36	3.63	8%
MOIR	1.57	1.59	1%
EBIR	1.10	1.06	-3%

52

It can be seen that the greatest change caused by representing glycolaldehyde explicitly was in the MIR scale, where the reactivity is increased by 8%. The effect of the change declines as the NO_x levels are reduced, and it eventually causes a slight reduction of reactivity in low NO_x scenarios.

2-(2-butoxyethoxy) ethanol (DGBE)

One MIR and two MOIR/2 reactivity experiments were carried out with 2-(2-Butoxyethoxy)-ethanol (DGBE). As shown on Table 7, the reactivity results for this compound were very similar to those observed previously for Texanol® (Carter and Malkina, 2005) in that the addition of the compound had only small effects on O_3 formation and NO oxidation, but consistently inhibited integrated OH radical levels. This observation of small, variable, or negative effects on O_3 combined with negative effects on OH radicals is consistent with what is observed in chamber experiments with other higher molecular weight glycol ethers or esters (Carter, 2000a, and references therein). The relatively small or variable effects on O_3 are attributed to the positive effects on O_3 caused by the direct reactions of the compounds or their products being counteracted by the reduced O_3 from the reactions of the other VOCs due to their negative effects on OH radical levels.

Concentration-time plots of $\Delta([O_3]-[NO])$ and IntOH, and changes in these quantities caused by the addition of DGBE are shown on Figure 16 for all the experiments with this compound. Results of model calculations, using both the standard and adjusted aromatics base mechanism, are also shown. In this case, the model gives reasonably good simulations of the effects of DGBE on the results of these reactivity experiments. The model correctly predicts that while the addition of DGBE has only very small effects on O_3 formation and NO oxidation, it significantly reduces overall OH radical levels in the experiments. The model slightly underpredicts the magnitude of the IntOH inhibition, but the extent of underprediction is consistent with the IntOH reactivity prediction observed for many other compounds (e.g., see Carter and Malkina, 2005), and may be related to the consistent underprediction of IntOH levels in the base case experiments.

It should be noted that the mechanism for DGBE and its major photooxidation products used in the model simulations shown on Figure 16 are the same as used in the previous reactivity calculation for this compound (Carter, 2003), without any adjustments being made to the uncertain portions of the mechanism to obtain these fits. The mechanism employed is based entirely on the estimates and mechanism generation procedures incorporated in the SAPRC-99 mechanism, as documented by Carter (2000a). The estimated DGBE + OH radical rate constant incorporated in this mechanism is also in good agreement with the relative decay rates for DGBE observed in these experiments, as discussed above in the "OH Radical Rate Constant Determinations" results, discussed above. This good performance of the SAPRC-99 estimated mechanism is is similar to the results observed previously with the Texanol® isomers in the CARB coatings reactivity study (Carter and Malkina, 2005).

The previously calculated reactivity values for DGBE (Carter, 2003), using the scales, scenarios, and methodology of Carter (2000), are as follows:

Scale	Incremental Reactivity (gm O_3 / gm VOC)
MIR	2.87
MOIR	1.32
EBIR	0.89

As indicated above, the experiments for this project tended to validate the mechanism used to calculate these previous values, so the recommended reactivities for this compound do not change.
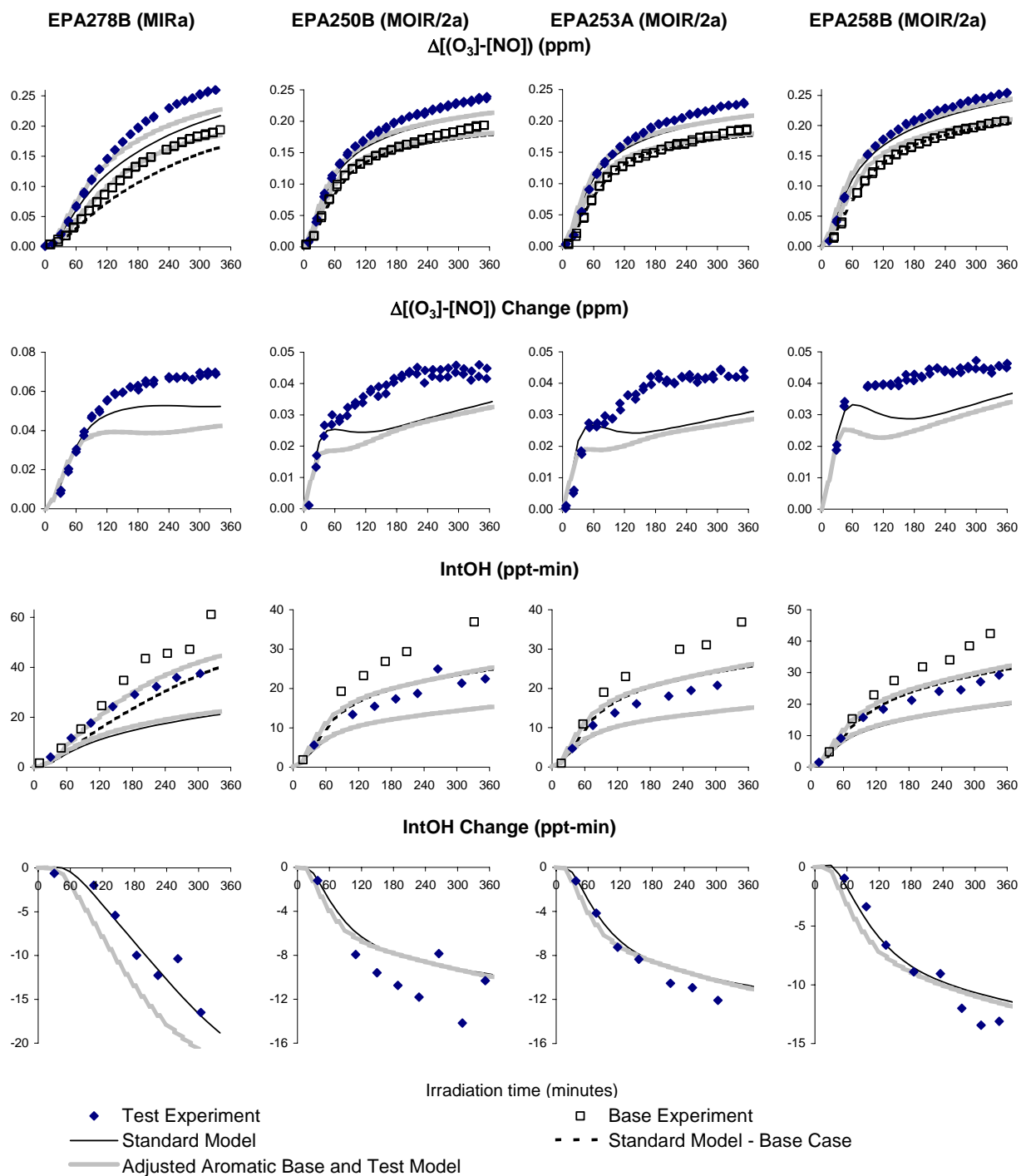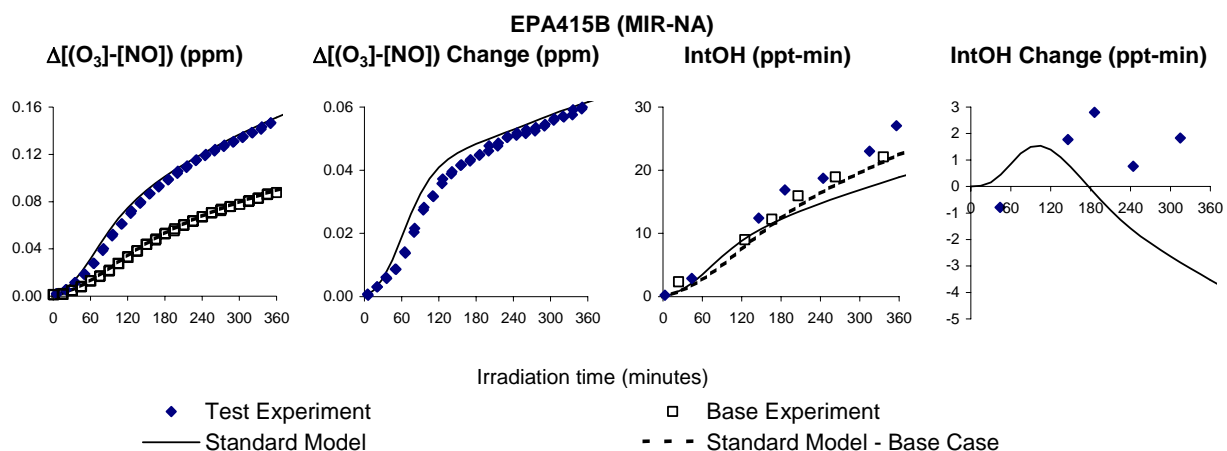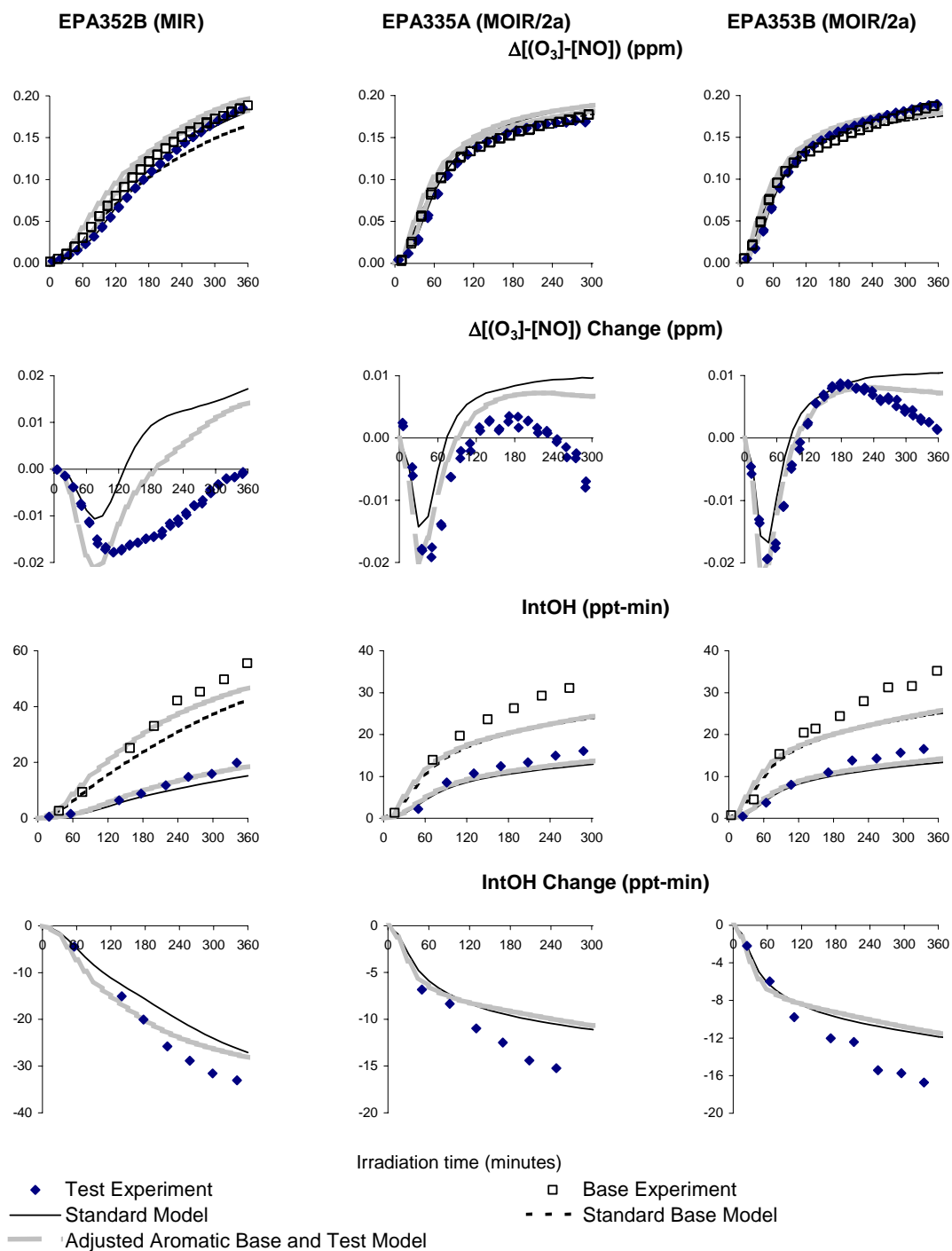
Figure 16.   Experimental and calculated concentration-time plots of selected measurements for the incremental reactivity experiments with 2-(2-Butoxyethoxy)-Ethanol (DGBE).

Benzyl Alcohol

Two MIR, one MOIR/2 and three compound - NO_x or compound - NO_x + CO experiments were carried out for benzyl alcohol. In all experiments the addition of benzyl alcohol enhanced the initial rates of NO oxidation and O_3 formation, but the O_3 formation leveled off earlier in the added benzyl alcohol side than in the base case experiment, resulting in a small net negative effect on O_3 by the time the experiments ended. The benzyl alcohol addition also inhibited integrated OH radical levels. The results are qualitatively similar to those observed for Aromatics 100 as discussed in our previous report (Carter and Malkina, 2005), and are consistent with what we would expect given the aromatic nature of this compound. As with other aromatics, available mechanistic information is insufficient to derive a complete mechanism for benzyl alcohol *a-priori*, and it is necessary to derive simplified mechanisms with parameter adjusted to fit chamber data. The derivation of the benzyl alcohol mechanism used for this project is discussed in the "Modeling Methods" section, above. Compound - NO_x experiments are useful for evaluating mechanisms for aromatics because their results are highly sensitive to portions of the mechanisms involving internal radical sources, which are among the most important factors affecting aromatics reactivity. (Such experiments are much less useful for glycols, glycol ethers, alkanes, etc., that have no significant internal radical sources or are radical inhibitors because their results are highly sensitive to chamber effects; see, for example, Carter et al, 1982). Aromatic - NO_x experiments with added CO are also useful for testing aspects of aromatics mechanisms, since the added CO enhances the effects of the aromatics' internal radical source on O_3 formation, and the current mechanisms for aromatics have a tendency to underpredict this effect (Carter, 2004).

Because of this, and because the reactivity experiments indicated that the reactivity characteristics of benzyl alcohol should be similar to those for other aromatics, benzyl alcohol - NO_x irradiations were carried out at various benzyl alcohol and NO_x levels, and benzyl alcohol - NO_x experiments with added CO were also carried out. Benzaldehyde was observed as a photooxidation product in those experiments, which could be used as a basis for determining the branching ratio for reactions forming benzaldehyde in its mechanism. Complete O_3 formation potentials were observed in all these experiments, to serve as a basis for testing model predictions of final O_3 yields.

Experimental and calculated concentration-time plots for selected species in the benzyl alcohol - NO_x and benzyl alcohol - CO - NO_x experiments are shown on Figure 17 and Figure 18, respectively, and experimental and calculated results of the incremental reactivity experiments with this compound are shown on Figure 19. As with the other compounds, the Figure 19 shows simulations with the reactivity experiments with both the standard and the adjusted mechanism for the aromatics in the base ROG surrogate.

The results shown on these figures indicate that the model is able to simulate the benzyl alcohol - NO_x, benzyl alcohol - NO_x + CO, and benzyl alcohol reactivity experiments about as well as the model performs in simulating comparable experiments with other aromatic compounds. Note that these fits are in part due to adjustments in the mechanism, with the portions of the mechanism affecting benzaldehyde yields adjusted to fit the benzaldehyde data shown on Figure 17 and Figure 18, and the overall nitrate yield adjusted to improve the fits to the $\Delta([O_3]-[NO])$ reactivity data shown on Figure 19. We consider the model performance as good as can reasonably be expected given the uncertainties and the current formulation of the aromatics mechanisms, but problems exist that eventually need to be resolved. As with the other aromatics, the model tends to underpredict the OH levels in the aromatics - NO_x experiments, as indicated by the underprediction of the rate of consumption of benzyl alcohol shown on Figure 17 and Figure 18. This is despite the fact that the benzyl alcohol + OH radical rate constant used in the model is consistent with the relative rates of benzyl alcohol decay in the reactivity experiments, as discussed in the "OH Radical Rate Constant Determinations" section, above. In addition, the model underpredicts the increase in $\Delta([O_3]-[NO])$ caused by the addition of CO in the benzaldehyde - NO_x experiments, as shown
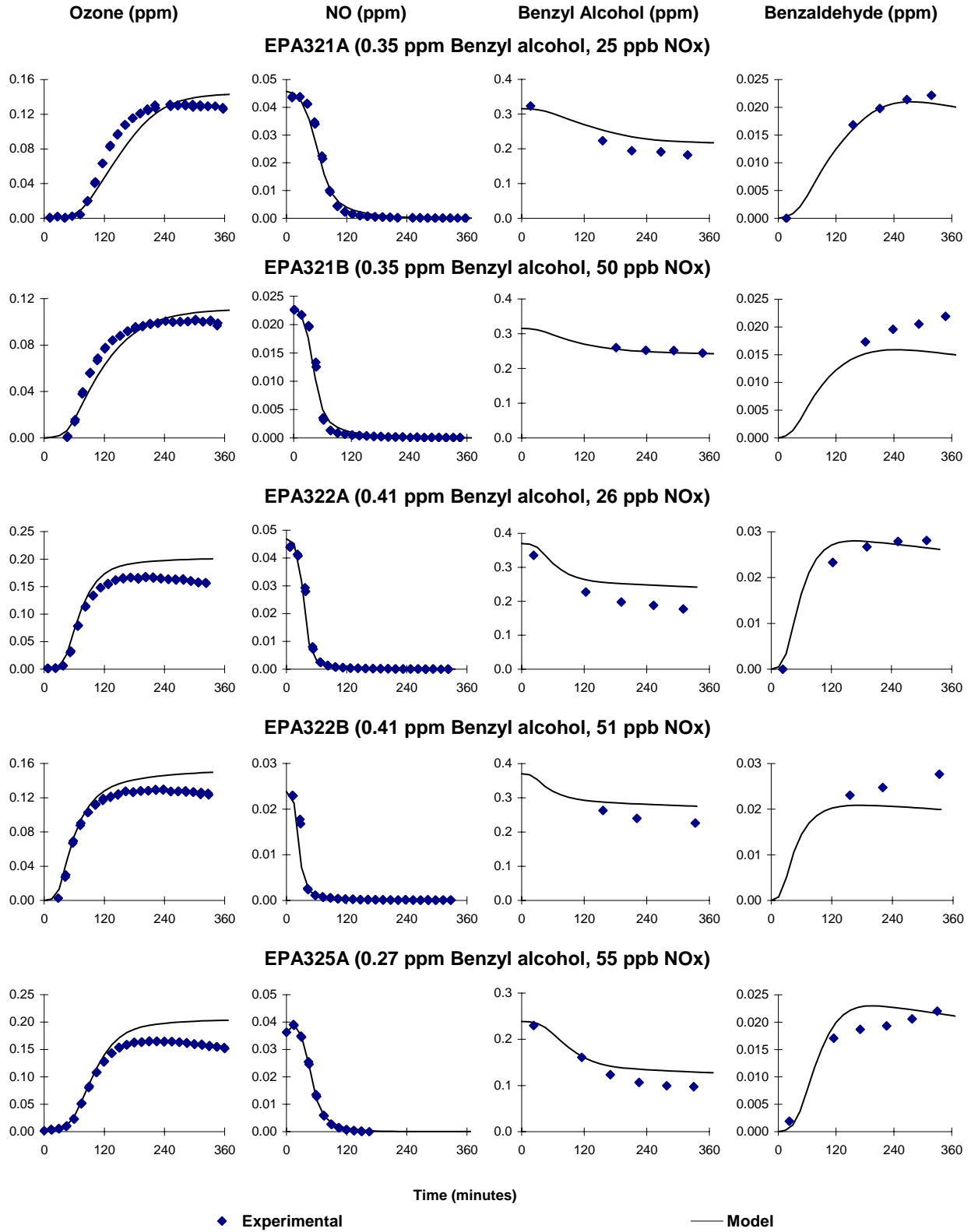
Figure 17. Experimental and calculated concentration-time plots of selected measurements for the benzyl alcohol - NOx irradiations.

56

EPA325B (0.23 ppm Benzyl alcohol, 59 ppb NOx, 26 ppm CO)
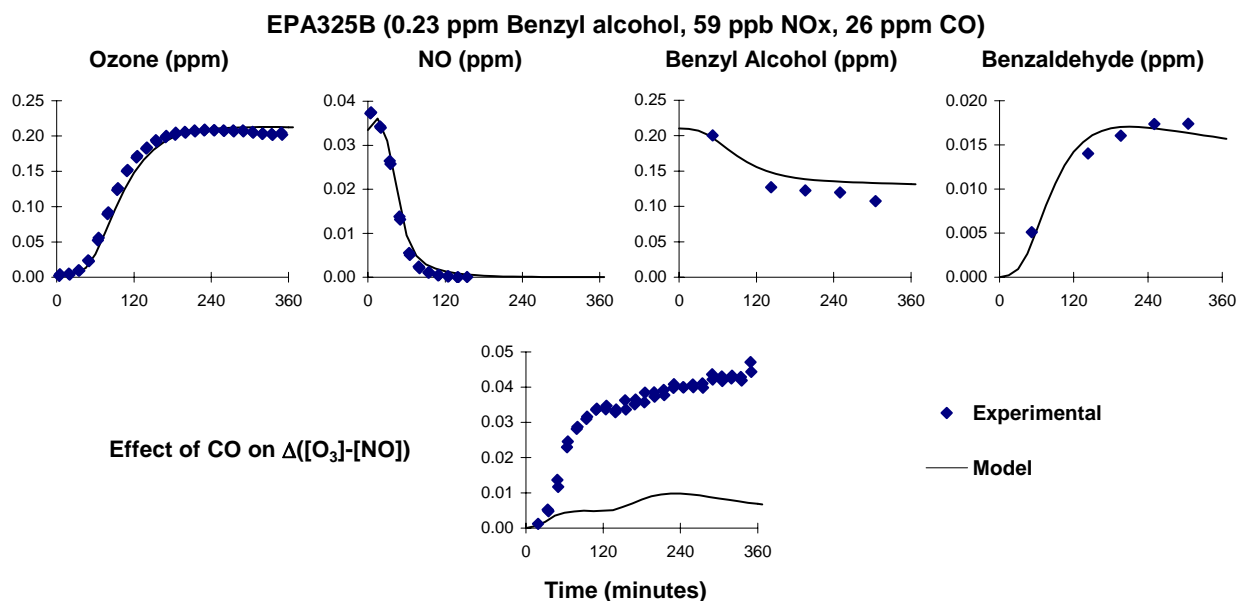
Figure 18.   Experimental and calculated concentration-time plots of selected measurements for the benzyl alcohol - CO - NO_x irradiation.

on Figure 18. In this case, this is manifested by the mechanism, which is adjusted to fit the reactivity experiments shown on Figure 19, tending to somewhat overpredict O_3 in the benzyl alcohol - NO_x experiments, while giving good simulations of O_3 in the benzyl alcohol - NO_x experiment with added CO.

Because there were no previous mechanism and reactivity estimates for benzyl alcohol, it was necessary to calculate its atmospheric reactivity for this project. The procedures and the base mechanism employed was the same as used when calculating the previous SAPRC-99 reactivity scales (Carter, 2000a, 2003). The calculated reactivities, in units of grams O_3 per gram of VOC, are as follows, with the reactivities of toluene also shown for comparison:

Scale	Benzyl Alcohol	Toluene	Difference
MIR	4.89	3.97	23%
MOIR	1.08	1.17	-8%
EBIR	0.01	0.35	-97%

It can be seen that benzyl alcohol is predicted to be slightly more reactive than toluene in the MIR scale, but its reactivity relative to toluene declines rapidly as relative NO_x levels are reduced. The higher MIR is attributed largely to its higher OH radical rate constant, and its reduced reactivity under low NO_x conditions is probably due to the NO_x-removal effects of the benzaldehyde formation reaction, which is more important for benzyl alcohol than is the case for toluene, whose mechanism is otherwise similar.

PM Measurement Results

One of the tasks in this project was to carry out measurements of secondary particulate matter (PM) formation during the experiments carried out for this and the CARB coatings projects. As discussed above in the "Experimental Methods" section, the PM size distributions were obtained using a Scanning

EPA319A (MIRa) EPA323B (MIRa) EPA320B (MOIR/2a)

$\Delta[(O_3)-[NO])$ (ppm)

$\Delta[(O_3)-[NO])$ Change (ppm)

IntOH (ppt-min)

IntOH Change (ppt-min)

Irradiation time (minutes)

♦ Test Experiment   □ Base Experiment
— Standard Model   - - Standard Base Model
▬ Adjusted Aromatic Base and Test Model
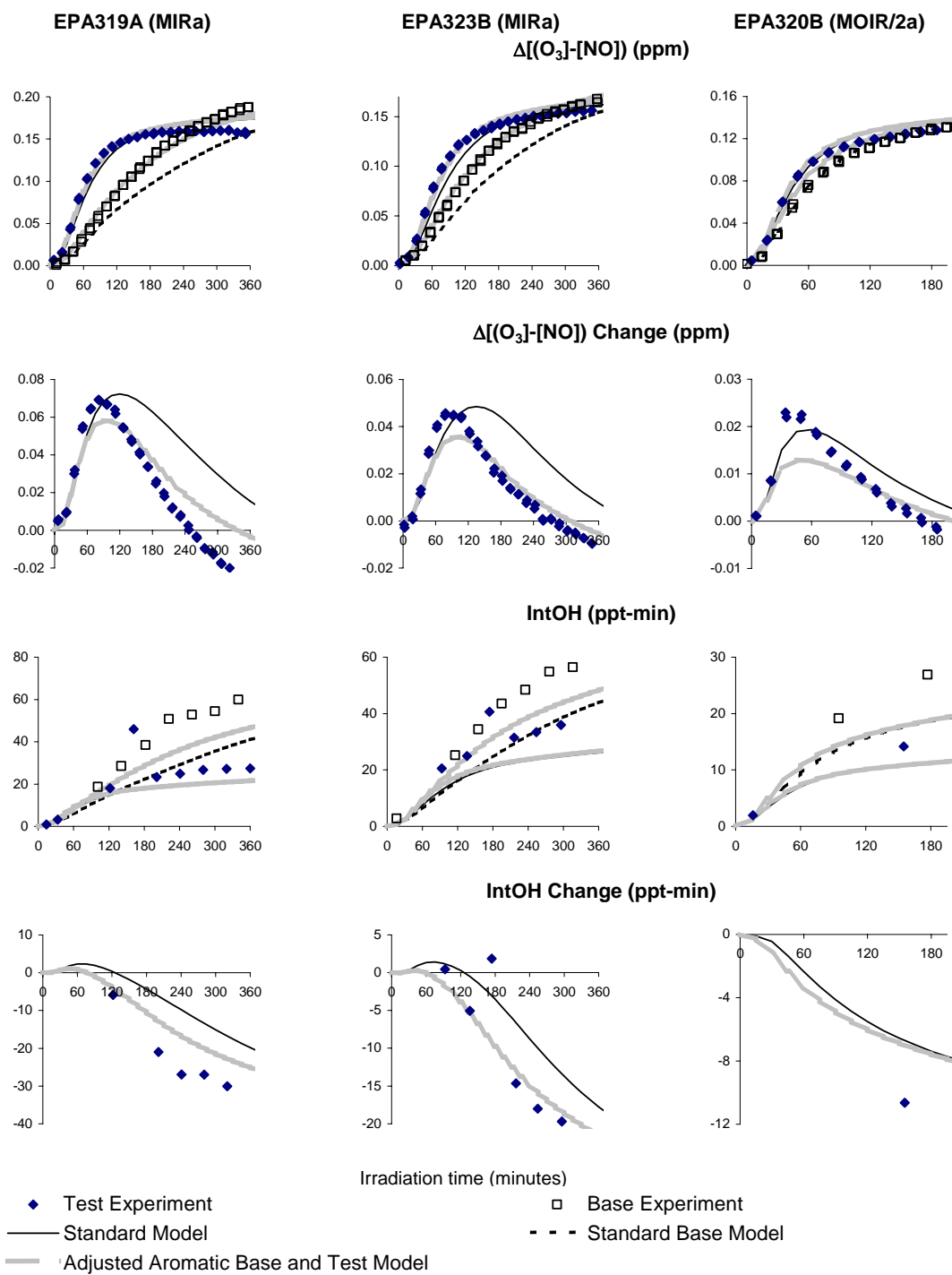
Figure 19.   Experimental and calculated concentration-time plots of selected measurements for the incremental reactivity experiments with benzyl alcohol

58

Electrical Mobility Spectrometer (SEMS), as described by Cocker et al (2001). The size distribution is used to calculate a particle number density and total aerosol volume concentration. The volume concentration is converted to mass units (e.g., µg/m^3) by assuming that the particles have the same density as water (specific gravity of 1). Although the particles formed in our experiments probably don't have exactly the same density of water, the results are given in water-equivalent mass units because this is the usual means of quantifying particle loadings in the atmosphere. Most of the results of the PM measurements will be given in terms of computed particle volume expressed in water-equivalent mass units because this provides a measure of the total amount of material that is condensed into the aerosol phase.

Representative examples of PM data taken for various types of experiments are shown in Figure 20 and Figure 21. Figure 20 shows plots of the total particle number and volume as a function of time measured simultaneously in the dual reactor experiment, where "A" and "B" refer to the reactor where the measurement was made. The high degree of scatter in the CO-air experiment is due to instrument noise for the extremely low aerosol concentrations. Easily measurable PM is formed in all the other experiments shown. The implications of the results for the different types of experiments are discussed in the following sections, but the features common to most experiments are discussed here. In general it was observed that higher levels of PM formation tended to occur in Side A, all else being equal; this is discussed further in the PM Background Experiments section, below. In general, if measurable PM formation occurred, and if the onset of PM formation occurred sufficiently early in the experiment, the PM number reached a maximum and began to decline, while the PM volume continued to increase, and either reached a maximum later in the experiment or continued to increase until the irradiation was ended. The decay in PM number is attributed to loss of PM on the walls, and the rate of decay, after the decay is established and is approximately exponential, can be used to provide an estimate of the PM wall loss rate (Cocker et al, 2001).

Figure 21 shows plots of the particle size distributions measured at four selected times in selected experiments. The four selected times include (1) the time halfway between the start of nucleation and the time of the maximum particle number; (2) the time of the maximum particle number; (3) the time halfway between the time of the maximum particle number and the end of the experiment; and (4) the last measurement before the light is turned off. It can be seen that in all cases the size distribution gets narrower and tends to increase in diameter as the experiment progresses, and the sizes are usually less than 200 nm in most experiments except those with added test compounds with the most particle formation. In the tabulations of the results of the various types of experiments, the characteristic particle size is given as the average particle size at hour 5 of the irradiation, which is usually about one hour before the end of the irradiation and almost well after the time of the maximum particle number (e.g., see Figure 20).

For the purpose of this discussion of PM results, three types of experiments were carried out: PM background experiments, base case reactivity experiments, and added test compound reactivity experiments. The results of these three types of experiments are discussed in the following sections, following a discussion of information obtained about PM wall losses that are applicable to all the experiments.

Characterization of PM Wall Loss Rates

The fact that the particle numbers peak relatively early in the experiments and then decline can be taken as evidence for loss of particles to the walls. The wall loss rates are estimated by assuming that no significant new particle formation occurs after the total particle number concentration has peaked (with additional PM formation being characterized by growth of the existing particles), and that coagulation is a less important factor in the decline in particle numbers in the latter part of the experiments than wall

59
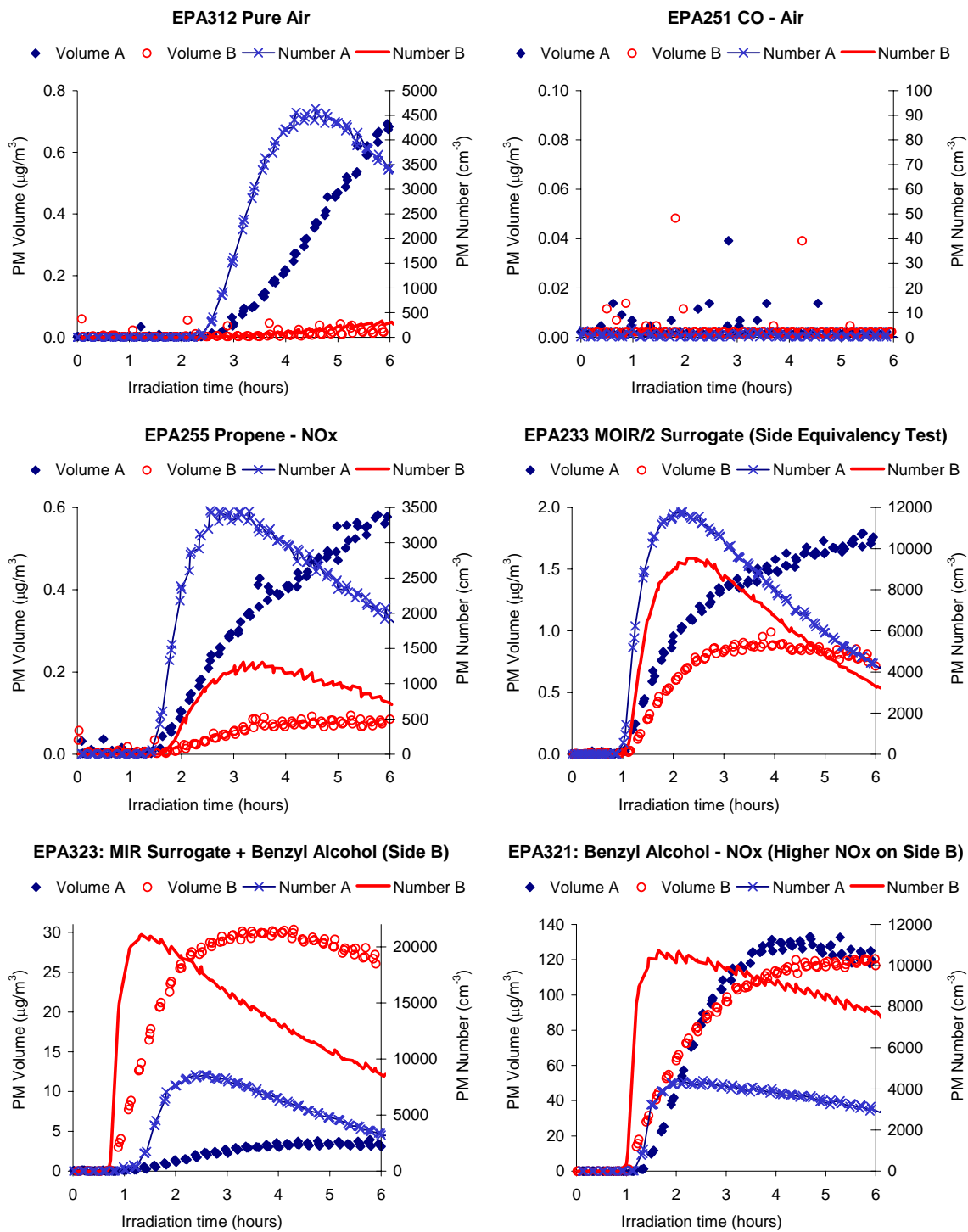
Figure 20.   Examples of PM number and PM volume data for representative chamber experiments.
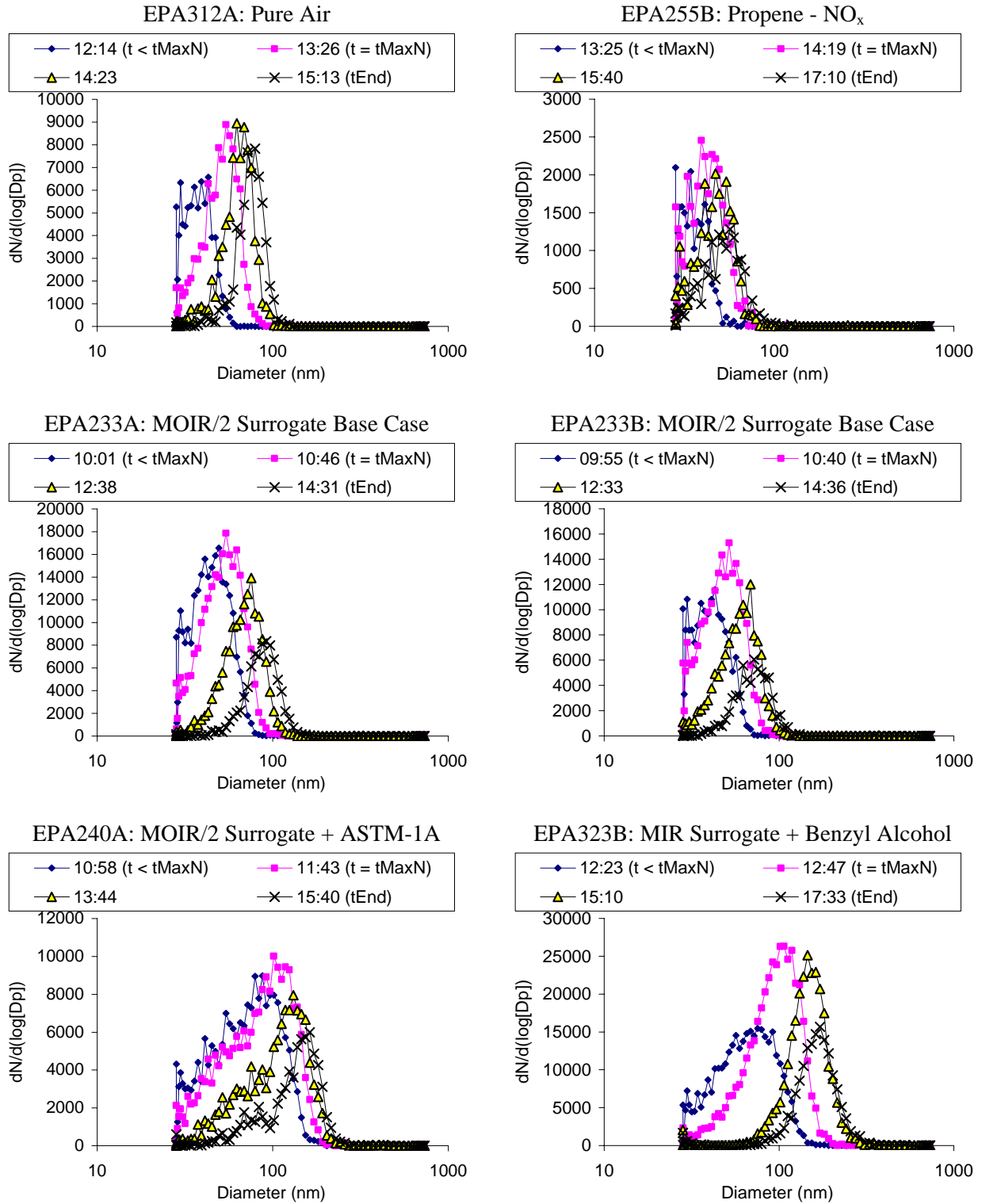
Time designations: tMaxN = time of maximum PM number; tEND = end of experiment.

Figure 21.   Examples of plots of size distributions of PM measurements at selected times in selected experiments.

losses. These assumptions predict an approximately exponential decline in particle number after the PM number maximum, reflecting a first-order wall loss rate. Dependences of particle size on wall loss rates are ignored in this analysis. For most, though not all, experiments the decline in the PM numbers during the latter parts of the experiments are indeed approximately exponential, allowing wall loss rates to be derived from time profile of the PM number data.

Plots of wall loss rates against EPA run number and against maximum PM diameter derived from the PM volume relative to the PM number, are shown in Figure 22. Note that the data shown include experiments carried out for other projects, including a number of experiments where higher PM levels are formed than most of the experiments reported here. Since there appears to be a slight negative dependence of the decay rate on maximum particle diameter, the plot against run number only shows experiments in the smaller maximum diameter range where no such dependence is evident. It can be seen that the apparent PM wall loss rate varies from run to run, but in general is in the 7±1 day^{-1} range. There may be slight decline in the apparent chamber loss rates in the later experiments, but it is unclear whether this is significant.

In chamber experiments used to determine secondary PM yields, the general practice has been to add the aerosol volume deposited to the walls after commencement of the experiment to the aerosol volume of suspended aerosol. This was not done in the analyses discussed here because the wall loss rates could not be determined for all experiments, making it more difficult to determine trends based only on corrected data. Therefore, the PM volume numbers reported in this report reflect only the PM remaining suspended in the reactor at the various times of the experiment, without correction for wall losses.

In general, the PM volumes corrected for wall losses differ from the uncorrected values by a factor that depends only on the irradiation time. This is shown on Figure 23, which shows plots of corrected against corrected 5-hour PM volume results for all experiments where the wall loss rates could be determined. It can be seen that the corrected values for 5 hours irradiations are well predicted by applying a factor of ~2 to the uncorrected values when the PM volume is less than ~50 µg/m^3, which is the case for almost of the experiments discussed in this report. A lower factor appears to be more appropriate for runs with higher PM levels. Figure 23 also shows the correction factors for the different irradiation times for which it was determined, where it can be seen that the factor increases with
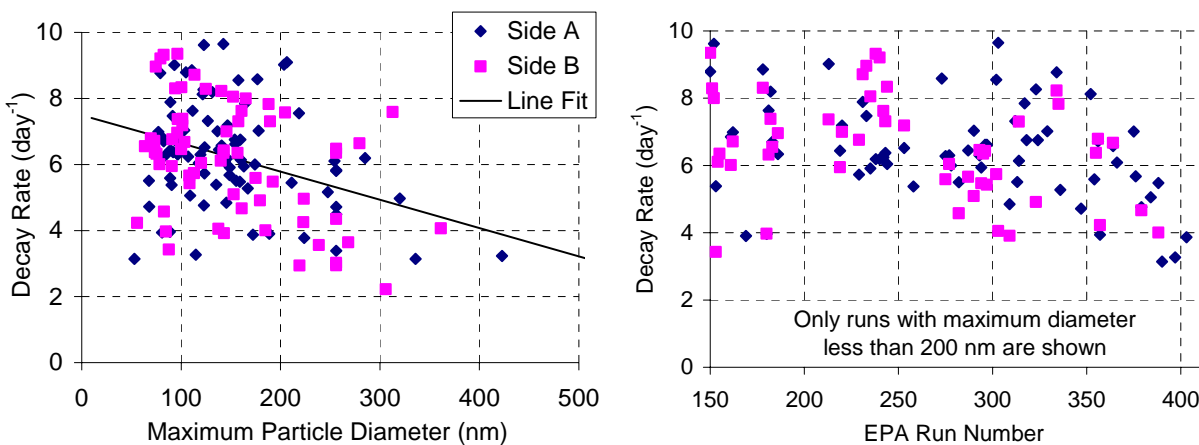
Figure 22.   Plots of PM wall loss rates against EPA run number and maximum particle diameter.
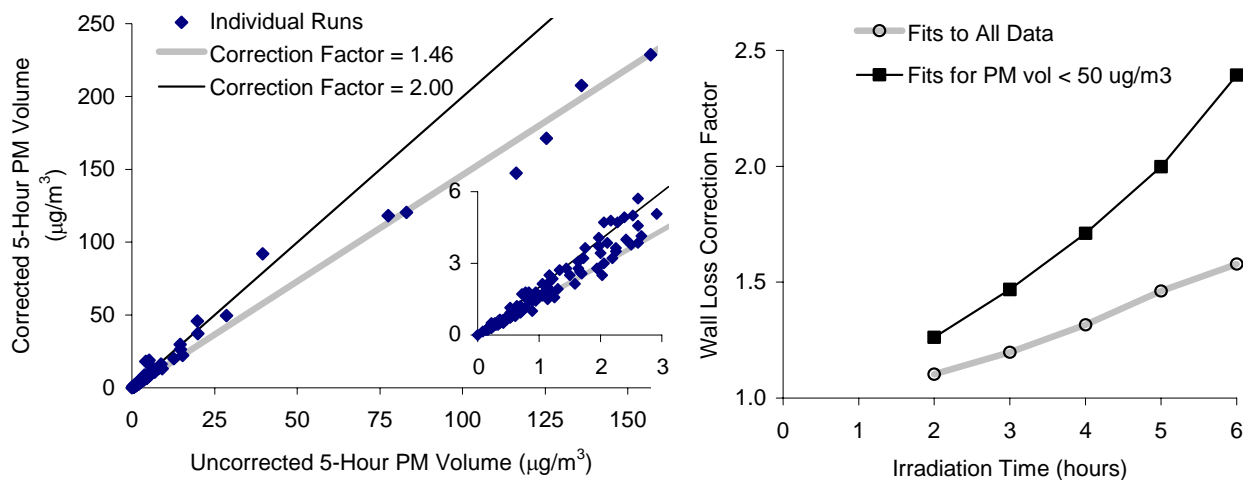
Figure 23. Plots of 5-Hour PM volume corrected for wall loss against the corresponding uncorrected measurements, and plots of the best fit wall loss correction factors against irradiation time for the chamber experiments where PM wall loss rates could be determined.

irradiation time, up to a factor of ~1.5 for 6 hours when the PM volume is in the range for most of the experiments in this report. Therefore, although only uncorrected PM volume data are given in this report, the corrected PM volume numbers can be estimated using the correction factors shown in Figure 23

PM Background Experiments

PM background experiments are experiments, such as pure air, CO - air, CO - NO_x or propene - NO_x irradiations, where condensable materials are not expected to be formed, and any PM formed in such experiments is taken as indicative of chamber background effects. The conditions and selected PM results for the PM background characterization experiments are summarized on Table 8, Figure 24 shows plots of 5-hour PM volume levels against run number for the PM background irradiation experiments, and Figure 25 shows time series plots of PM levels in replicate pure air runs carried out to assess PM background effects.

Essentially no PM formation was observed in the dark experiments, suggesting that PM is not present in the matrix air, or being released from the walls over time, at least in the dark. Background PM formation is also very low or unmeasurable in the CO - air or CO - NO_x irradiations, suggesting that PM is not released from the walls in the light due to physical heating. On the other hand, measurable PM formation is observed in almost all the pure air irradiations and also in the propene - NO_x runs, with significantly more PM always being formed in Side A compared to Side B. The PM levels in the propene - NO_x runs are not significantly different from those in the pure air runs, suggesting that the photooxidation products in the propene runs (which include HNO_3, PAN, formaldehyde and acetaldehyde) are probably not contributing significantly to this background PM.

The fact that higher PM formation occurs in the pure air and propene - NO_x irradiations than occur in the CO - air and CO - NO_x runs can be attributed to the fact that OH radicals are calculated to be significantly higher in the former types of runs than in the runs with CO. Apparently the OH radicals react with some contaminant (that is present in higher levels in Reactor A than B) to form condensable products. O_3 does not appear to play a significant role in this background, since the O_3 levels tend to be

63

Table 8.   Summary of conditions and PM measurement results of the PM background characterization experiments.

Run	Initial NO_x (ppb)	Initial VOC or CO (ppm)	5 Hr PM vol ($\mu g/m^3$)		Max PM Number (cm^{-3}) / 1000 [a]		5 Hr. Avg. PM Diam. (nm) [a]		Light [b]	Special Conditions and Notes [c]
			Side A	Side B	Side A	Side B	Side A	Side B		
Pure Air Dark										
342			0.0	0.0	0.0	0.0	-	-	D	
Pure Air Irradiation										
169			2.0	1.1	17.0	14.3	64	58	A	NR
172			1.5	0.2	16.4	3.4	60	51	A	
221			0.6	0.1	7.0	3.3	57	44	B	
263			0.5	0.1	6.6	3.0	53	42	B	CPA
264			0.2	0.1	3.9	1.8	49	40	B	CPA
265			0.2	0.0	3.4	1.9	48	39	B	CPA
266			0.1	0.0	2.8	1.5	46	38	B	CPA, HP
267			0.2	0.1	3.2	2.5	47	40	B	CPA, 3D
268			0.4 [d]	0.1 [d]	6.6	1.9	-	-	B	no CPA
269			0.4	0.0	4.4	1.1	54	39	B	R
270			0.3	0.0	4.8	1.5	52	42	B	R
271			0.3	0.0	2.4	0.1	64		A	R
274			0.3	0.1	6.0	2.3	45	40	B	NA
276			0.3	0.1	4.3	2.6	53	42	B	
295			0.5	0.1	7.2	3.4	53	43	B	
307			0.4	0.1	6.1	2.6	53	44	B	
311			0.4	0.2	7.0	3.7	49	44	B	
312			0.5	0.0	4.3	0.3	59	67	A	
317			0.7	0.0	5.4	0.2	68	65	A	
327			0.0	0.1	0.4	0.0	44		A	
333			0.0	0.0	0.0	0.0			A	
336			0.6	0.1	6.6	2.2	59	41	A	
339			0.2	0.0	2.5	0.1	56		A	
340			0.0	0.0	1.7	0.0	44		A	
347			0.7	0.0	5.2	0.2	68	64	A	
378			0.5	1.7	6.4	11.7	52		B	
384			0.5	0.0	8.6	2.0	51	37	B	
CO - Air Irradiation										
160		95	0.0	0.0	0.0	0.0			A	
170		40		0.0	0.0	0.0			A	
173		44	0.0	0.0	0.0	0.0			A	
175		46	0.0	0.0	0.1	0.0			A	
205		44	0.0	0.0	0.0	0.0			A	
251		45	0.0	0.0	0.0	0.0			A	
285		47	0.0	0.0	0.0	0.0			B	
344		51	0.0	0.0	0.0	0.0			A	
CO - NO_x Irradiation										
174	23	47	0.0	0.0	0.1	0.0	90		A	
184	12	24	0.0	0.0	0.0	0.0			A	

Table 8 (continued)

Run	Initial NOx (ppb)	Initial VOC or CO (ppm)	5 Hr PM vol (µg/m³) Side A	Side B	Max PM Number (cm⁻³) / 1000 [a] Side A	Side B	5 Hr. Avg. PM Diam. (nm) [a] Side A	Side B	Light [b]	Special Conditions and Notes [c]
234	25	45	0.0	0.0	0.0	0.0			A	
345	27	47		0.0	0.0	0.0			A	
346	27	46	0.0	0.0	0.0	0.0			A	
362	21	33		0.0	0.0	0.0			A	
306	22	46	0.0	0.0	0.0	0.0			B	
401	29	49	0.0	0.0	0.0	0.0			B	
				Formaldehyde - CO - NOx Irradiation						
176	22	0.054	1.0	0.5	8.0	4.6	69	66	A	39 ppm CO
202	24	0.042	0.2	0.0	0.4	0.1	101		A	48 ppm CO
				Propene - NOx Irradiation						
177	10	0.32	1.1	1.2	16.5	17.9	58	58	A	
255	27	0.34	0.5	0.1	3.3	1.2	73	53	A	
260	29	0.43	0.4	0.0	1.5	0.0	87		A	
262	27	0.21	0.3		2.2		76		A	
329	20	0.31	0.3	0.0	2.8	0.1	66		A	
341	13	0.25	1.2	0.4	15.3	9.1	58	45	A	
348	28	0.35	1.2	0.3	13.3	7.7	62	43	A	
259	15	0.41	0.2	0.0	2.2	0.6	61	46	B	NF
281	28	0.09	0.1		2.7		47		B	
281	28	0.09		0.1		1.1		45	B	28 ppm CO
				Ozone Light and Dark Exposure						
158	~0.24 ppm O₃		0.0	0.1	0.3	0.2	43	78	D	
179	~0.22 ppm O₃		0.1	0.1	1.4	1.4	54	57	D,A	[e]
328	~0.16 ppm O₃		0.0	0.0	0.0	0.0			D	[f]
256	~0.16 ppm O₃		0.2	0.0	1.9	0.1	59		A	[g]

[a] Calculated from average PM volume per particle (from ration of total PM volume to PM number), assuming spherical particles, at 5 hours irradiation time. Not given if PM number is below 100 cm⁻³.

[b] A = arc light; B = blacklights; D = dark.

[c] Codes for special conditions:
   NR ....New Reactors
   CPA ....Mixing ports covered with Teflon® (Side A only)
   no CPA ......Port covers on Side A removed; reactor entered. Back to standard conditions.
   HP ....Higher positive pressure in reaction bags
   3D ....Air kept in reactor 3 days before irradiation
   NA ....Pure air replaced in reactor immediately before irradiation
   NF ....No mixing fans used
   R ....Replicate of run on previous day (except as noted, if applicable)

[d] 5-Hour PM values are not available. Values given are for 4 hours.

[e] Lights turned on for about 1 hour after about 6 hours. PM volume increased to 0.2 ug/m₃ on Side A and 0.15 ug m3 on Side B.

[f] 50 ppm CO also present. No measurable PM formation in either reactor.

[g] O₃ injected ~3 hours prior to start of irradiation. No dark PM formation observed in either reactor during that time.
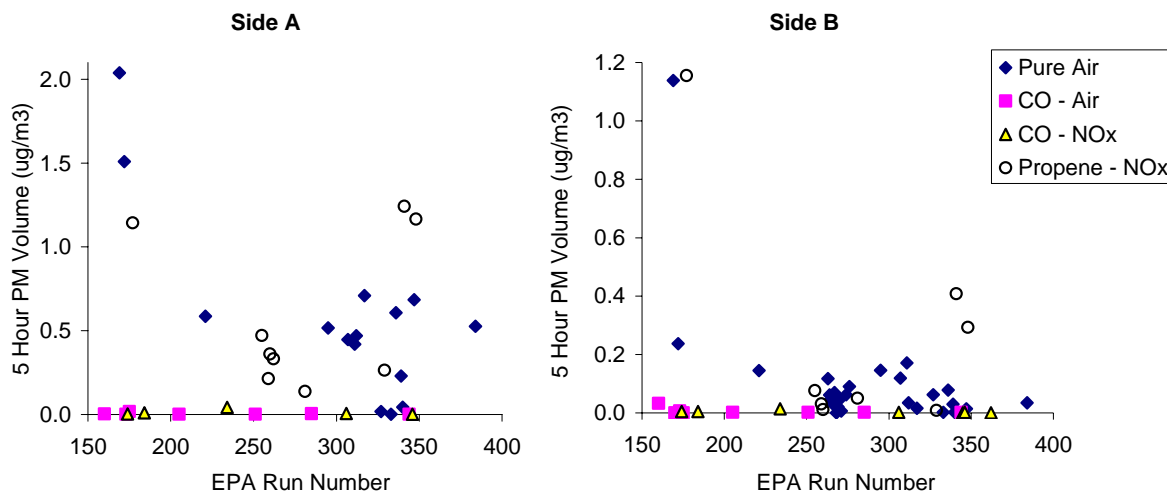
Figure 24.   Plots of 5 hour PM volume against run number for the pure air, CO - air, CO - NO$_x$, and propene - NO$_x$ characterization runs.
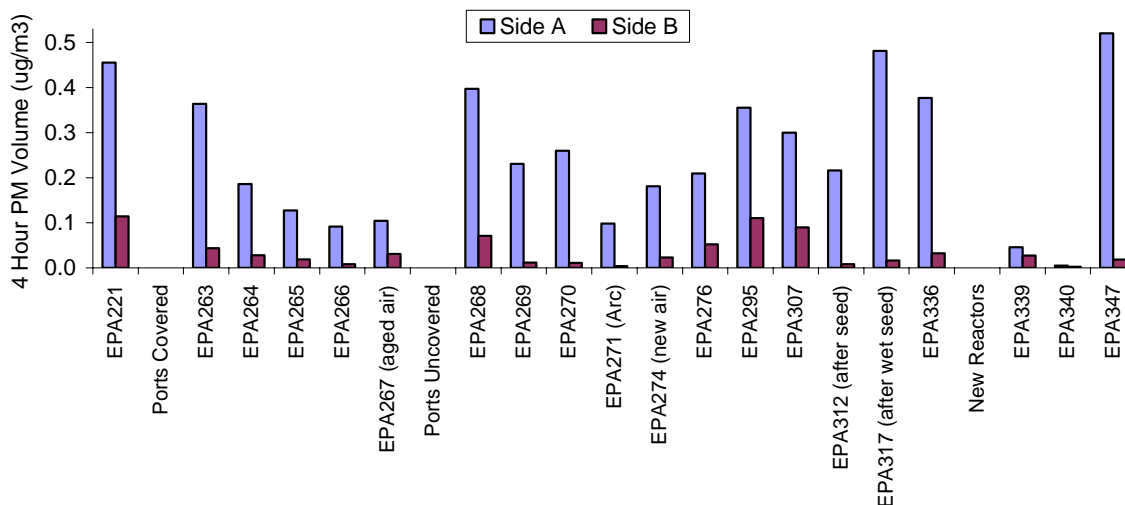
Figure 25.   Time series plots of PM volume levels after 4 hours in pure air experiments carried out to assess background PM levels.

higher in CO - air runs than in pure air runs, and PM formation when the chamber is exposed to O$_3$ in the dark is generally small. The formation of PM when O$_3$ is irradiated can be attributed to OH radials formed in the photolysis. Although this background PM is relatively small compared to PM levels generally formed in previous chamber studies, as discussed below it is non-negligible compared to the PM levels observed in the base case and many of the added VOC reactivity experiments, so it needs to be taken into account when interpreting the results of these experiments.

Despite various attempts and tests, we have been unable to determine the source of the contamination that causes the formation of background PM in experiments where OH radicals are formed, or why the contamination is always higher in Reactor A than B. As indicated on footnotes to Table 8, the tests that were carried out included (1) changing the Teflon® film reactors; (2) covering the Teflon®-coated metal mixing ports that are not changed when the reactors are changed; (3) changing whether the mixing fans are used prior to the experiments; and (4) changing the amount of time the pure air is in the reactors prior to the irradiation. As indicated on Figure 25, these changes do not clearly implicate any source for this background PM, or why the background PM is always higher in Side A than B. The sampling ports were also switched from side to side to eliminate the possibility that the differences would be due to sampling artifacts. The only indications obtained from the various tests is that the background PM levels tend to go up when the reactors are somehow disturbed, such as entering them to cover or uncover the mixing ports (see Figure 25).

Because the two reactors have significantly different background effects, the two reactors cannot be considered to be equivalent for the purpose of assessing PM impacts, so experiments in each of the reactors have to be considered separately. For example, when determining how a particular test compound affects PM formation in the reactivity experiments, it is necessary to compare the results of the added with a base case experiment carried out in the same reactor. Since it is obviously not possible to carry out a test experiment and a base case experiment in the same reactor at the same time, one cannot take advantage of the dual-reactor feature of the chamber when assessing PM effects in the same way as done for the gas-phase reactivity experiments discussed in the previous sections.

Base Case ROG Surrogate Experiments

Table 9 summarizes the initial concentrations and selected PM measurement results for the MIR and MOIR/2 base case reactivity experiments where PM measurements were made. This includes base case experiments carried out for the CARB coatings project (Carter and Malkina, 2005) as well as those carried out for this project. The gas-phase results for the experiments for the CARB project are given by Carter and Malkina (2005) and for the experiments for this project are summarized in Table 7, above, for the experiments in this project, and are generally consistent from run to run.

The amount of PM formation in the base case experiments was relatively small but was higher than in the background runs. As with the background runs, higher PM levels were consistently observed in side A compared to Side B, with the average 5-hour PM volumes (in $\mu g/m^3$) being as follows:

Run Type	Side A	Side B
MIR Surrogate - NO$_x$	3.0±0.8	0.7±0.3
MOIR/2 Surrogate - NO$_x$	1.9±0.8	0.6±0.2
Non Aromatic Surrogate - NO$_x$	0.4±0.3	
Pure air irradiation	0.4±0.2	0.06±0.05

(The average for the pure air runs excluded the first two experiments, which had significantly higher PM than subsequent runs.) As shown in plots Table 9 and also in plots given in the next section, the PM volumes in the base case experiments tended to decline over time in Side B, but remained consistently high in Side A.

It is interesting to note that the difference in PM formation between Side A and Side B in base case surrogate - NO$_x$ experiments is greater than the difference in PM formation in the background run. This cannot be attributed to differences in OH radical levels because the two sides are generally equivalent in terms of gas-phase processes that affect O$_3$ and OH. Apparently, the presence of the

Table 9.   Summary of conditions and PM measurement results of base case incremental reactivity experiments.

Run	Initial NOx (ppb)	Initial ROG (ppmC)	5 Hr PM vol (µg/m³) Side A	Side B	Max PM Number (cm⁻³) / 1000 [a] Side A	Side B	5 Hr. Avg PM Diam. (nm) [a] Side A	Side B

$\text{Max PM Number } (cm^{-3}) / 1000 \text{ [a]}$, $\text{5 Hr. Avg PM Diam. (nm) [a]}$

Run	Initial NO$_x$ (ppb)	Initial ROG (ppmC)	5 Hr PM vol (µg/m³) Side A	Side B	Max PM Number Side A	Side B	5 Hr Avg PM Diam Side A	Side B
MIR Base Case								
151	30	0.56		1.2		2.9		112
163	24	0.53		0.7		3.6		90
167	30	0.56	4.3		5.7		136	
168	28	0.55		1.1		2.5		109
226	31	0.56	2.9		7.8		96	
229	32	0.66		0.6		2.6		81
230	33	0.60	2.4		4.6		115	
235	32	0.55	2.2	0.5	5.1	2.7	107	79
238	33	0.56		0.8		8.1		72
244	32	0.63	2.5		6.6		104	
257	33	0.63			3.7		-	
277	32	0.59		0.4		2.2		72
278	33	0.62	2.6		4.4		122	
323	27	0.53	3.4		8.1		110	
352	31	0.58	4.1		6.7		122	
MOIR/2 Base Case								
152	25	0.93	3.6		13.0	152	110	
159	22	1.02			14.0	9.8	-	-
231	27	1.12	1.7		8.5		89	
232	27	1.12		0.7		5.9		73
233	27	1.11	1.6	0.8	11.7	9.0	81	69
237	26	1.13	1.7		10.9		84	
239	27	1.20		0.7		7.7		71
240	27	1.16		0.7		8.0		71
242	26	1.16	2.6		10.3		97	
243	27	1.17	1.6		9.8		83	
245	27	1.17	1.3		8.1		85	
250	27	1.21	1.5		9.7		80	
252	27	1.23		0.5		6.7		61
253	27	1.16		0.6		7.0		66
334	28	1.28	0.8	0.2	8.0	4.8	71	54
335	28	1.24		0.5		5.3		68
353	26	1.18	2.9		12.8		88	
Non-Aromatic MIR Base Case								
404	27	0.59	0.2		0.4		90	
415	27	0.59	0.7		8.0		55	

[a] Calculated from average PM volume per particle (from ration of total PM volume to PM number), assuming spherical particles, at 5 hours irradiation time.

background PM source affects PM formation from the gas-phase processes. This may be consistent with the predictions of the equilibrium partitioning theory for secondary organic aerosol (SOA) formation where the amount of aerosol formed is dependent on the mass of aerosol present (Pankow 1994a,b). Gas-particle equilibrium of semi-volatile species is described by a partitioning parameter K (m^3 μg^{-1}) (analogous to Henry's coefficient) in terms of the organic mass concentration, defined as:

$$K_i = \frac{F_{i,om}}{A_i M_o} \tag{III}$$

where $F_{i,om}$ is the particle-phase concentration of compound i (ng m^{-3}), A_i is the gas-phase concentration of compound i (ng m^{-3}), and M_o is the organic mass concentration of suspended particulate (μg m^{-3}). However, this explanation can only hold if the background material is organic in nature. The differences between sides would therefore be expected to be give correspondingly different PM impacts of test VOCs whose reactions also form SOA, although this effect is likely minimized for systems with significant organic aerosol formation.

It should be noted that the PM formation in the base case experiments should be occurring primarily from the reactions of the aromatics in the base ROG, since the other base ROG components are not expected to form significant levels of condensable products. This is consistent with the fact that the PM levels formed in the non-aromatic surrogate MIR experiments, also shown on Table 9, are considerably lower than observed in the MIR full surrogate experiments essentially within the variability observed for the background experiments, discussed above.

Added Test VOC Experiments

Table 10 summarizes the conditions and selected PM results for the incremental reactivity experiments with PM measurements that were carried out for this and the CARB coatings project. The compounds studied and the gas-phase results from the CARB coatings projects are discussed by Carter and Malkina (2005), and the gas-phase results from this project are discussed above (e.g., see Table 7). The compounds studied for the CARB coatings project consisted of various C_8-C_{12} hydrocarbon solvents with varying aromatic content and Texanol® (isobutyrate monoesters of 2,2,4-trimethyl-1,3-pentanediol) (Carter and Malkina, 2005), and as discussed above the compounds studied for this project were ethylene and propylene glycol, 2-(2-butoxyethoxy)-ethanol (DGBE), and benzyl alcohol. The table shows the change in the 5-hour PM volume in the added test compound experiment compared to the average (for Side A) or linear regression against run number (for Side B) for the corresponding measurement in the base case experiments. The 5-hour average PM diameter for the test VOC experiment are also shown in the table. The PM impacts for the various types of compounds are discussed below.

Plots of averages of the 5-hour PM volume results for the various types of incremental reactivity experiments are shown on Figure 26, where the PM formation impacts of the various types of compounds can be compared. Plots of 5-hour PM volume and average PM diameter for the individual experiments against EPA run number are shown on Figure 27 and Figure 28, respectively. These results are discussed below for the various types of test compounds that were studied.

Table 10 also shows approximate estimates of the overall percentage yield of PM after five hours of irradiation, for those compounds or mixtures where the PM formation in the added test compounds experiment were consistently higher than the base case results in the same reactor. These were calculated based on the measured differences in PM volume between the added VOC and the base case experiment in the same reactor, estimated amounts of PM lost to the walls, estimated molecular weights of PM formed, and estimated amounts of test VOC reacted. For the purpose of these highly approximate

Table 10. Summary of selected conditions and PM results for the incremental reactivity experiments for this project and for the CARB Coatings project.

Run	Test Side	Type	Added	Base Conc NOx (ppb)	Base Conc ROG (ppmC)	Side B PM vol Change (5 Hr) (µg/m³) [a]	Side A PM vol Change (5 Hr) (µg/m³) [a]	5-Hr Avg. PM Diam. [b] (nm)	5-Hr Est'd PM yield [c]
					Texanol® (measured ppm added)				
230	B	MIRa	0.09	33	0.60	-0.2		137	
231	B	MOIR/2a	0.11	27	1.12	0.2		113	
229	A	MIRa	0.08	32	0.66		-0.8	123	
232	A	MOIR/2a	0.14	27	1.12		-0.7	118	
					VMP Naphtha solvent (calculated ppmC added)				
243	B	MOIR/2a	0.90	27	1.17	0.2		91	0.1%
238	A	MIRa	1.20	33	0.56		4.0	133	0.7% [d]
					ASTM-1C solvent (calculated ppmC added)				
152	B	MOIR/2	0.91	25	0.93	1.6		153	0.2%
168	A	MIR	0.90	28	0.55		1.6	193	0.2%
					ASTM-1B solvent (calculated ppmC added)				
242	B	MOIR/2a	0.90	26	1.16	4.0		149	0.6%
151	A	MIR	0.90	30	0.56		4.4	198	0.7%
					ASTM-1A solvent (calculated ppmC added)				
167	B	MIR	0.90	30	0.56	3.6		165	0.3%
153	A	MOIR/2	0.97	24	1.02		5.7	126	0.8%
240	A	MOIR/2a	1.21	27	1.16		4.3	134	0.5%
					Aromatic 100 solvent (calculated ppmC added)				
244	B	MIRa	0.31	32	0.63	1.7		91	0.3%
239	A	MOIR/2a	0.76	27	1.20		3.3	109	0.4%
					ASTM-3C1 solvent (calculated ppmC added)				
150	B	MOIR/2	0.84	23	1.03	0.1		88	
237	B	MOIR/2a	1.20	26	1.13	0.2		79	
163	A	MIR	0.89	24	0.53		-0.5	115	
					Propylene glycol (calculated ppm added)				
257	B	MIRa	0.40	33	0.63	0.0		-	
245	B	MOIR/2a	0.40	27	1.17	-0.6		63	
273	A	MIRa	0.20	32	0.60		-2.0	75	
277	A	MIRa	0.20	32	0.59		-1.4	84	
252	A	MOIR/2a	0.40	27	1.23		-2.0	61	
404	B	MIR-NA	0.20	27	0.59		~0 [e]		
					Ethylene glycol (calculated ppm added)				
278	B	MIRa	0.30	33	0.62	-0.4		66	
250	B	MOIR/2a	0.40	27	1.21	-0.4		55	
253	A	MOIR/2a	0.40	27	1.16		-1.7	68	
415	B	MIR-NA	0.20	27	0.59		0.1 [e]	54	

Table 10 (continued)

Run	Test Side	Type	Added	Base Conc NOx (ppb)	ROG (ppmC)	Side B PM vol Change (5 Hr) (μg/m³) [a]	Side A	5-Hr Avg. PM Diam. [b] (nm)	5-Hr Est'd PM yield [c]
2-(2-Butoxyethoxy)-Ethanol (measured ppm added)									
352	B	MIRa	0.050	31	0.58	8.9		313	16%
353	B	MOIR/2a	0.050	26	1.18	14.1		241	26%
335	A	MOIR/2a	0.050	28	1.24		8.7	-	14% [d]
Benzyl alcohol (measured ppm added)									
323	B	MIRa	0.066	27	0.53	28.3		173	28%
319	A	MIRa	0.098	31	0.56		37.1	197	29%
320	B	MOIR/2	0.102	21	1.09	38.6 [f]		-	

[a] Change relative to the average 5-hour PM volume for the base case experiments for Side A or relative to the 5-hour PM volume from the linear regression of the base case results against run number for Side B. The MIR and MOIR/2 base case runs are not distinguished in this analysis.

[b] Calculated from average PM volume per particle (from ration of total PM volume to PM number), assuming spherical particles, at 5 hours irradiation time.

[c] Estimated as discussed in the text.

[d] IntOH estimated from model calculation and average experimental / calculated IntOH ratio for other runs.

[e] No PM data for non-aromatic surrogate base case on Side B. Assume the base case is approximately the same as in pure air runs for this side, which is 0.06±0.05 μg/m³.

[f] Result for t=3 hours.
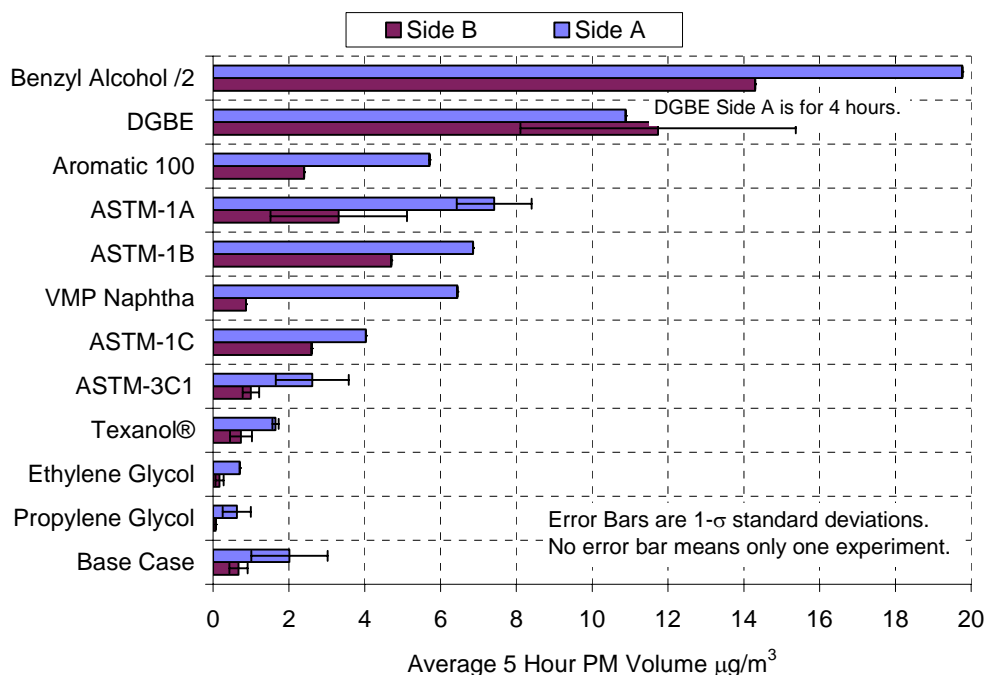
Figure 26. Summary of average 5-hour PM volume results for the incremental reactivity experiments.
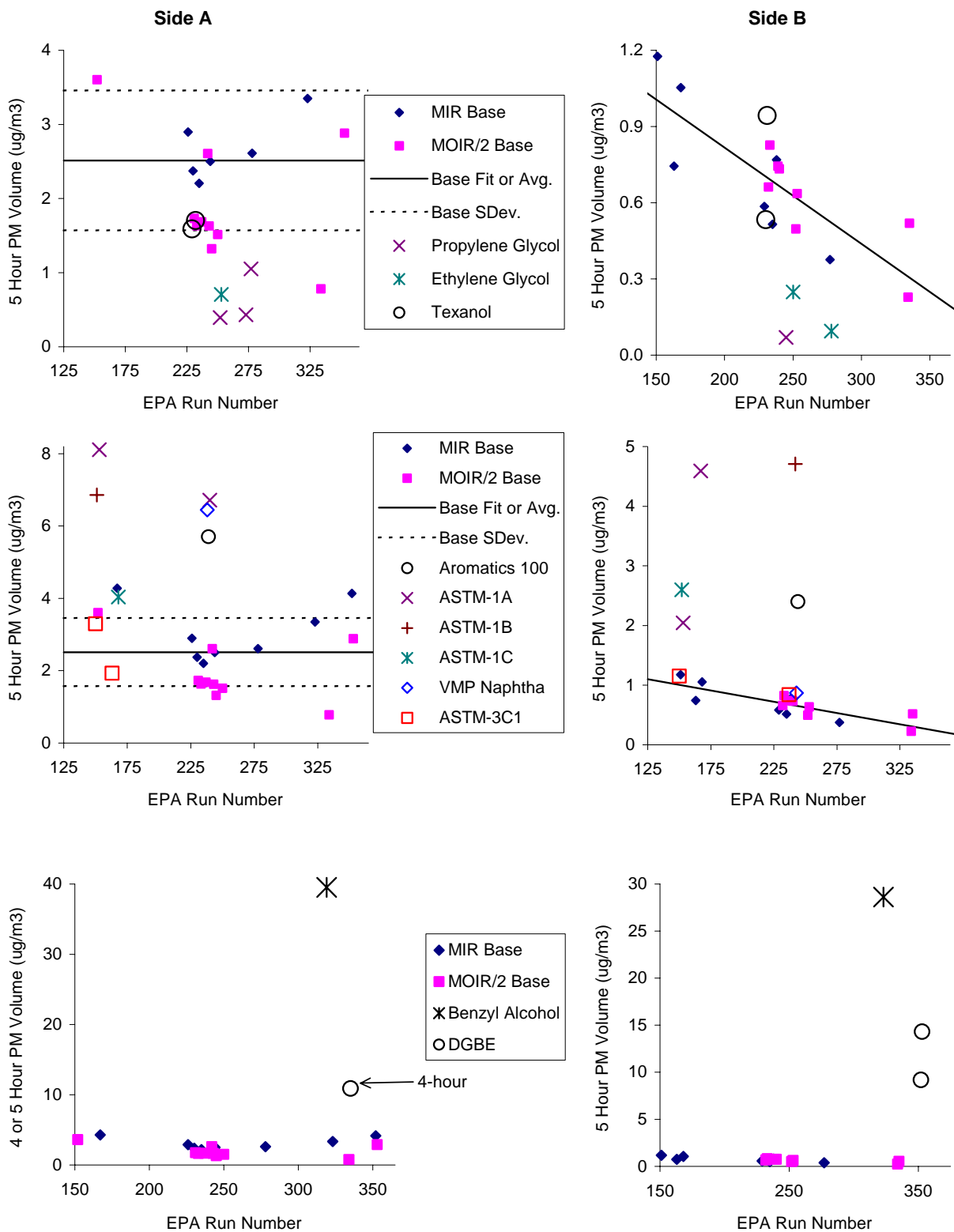
71

Side A

Side B

Figure 27.   Plots of 5 hour PM volume against run number for the base case and the incremental reactivity experiments with the various test compounds.
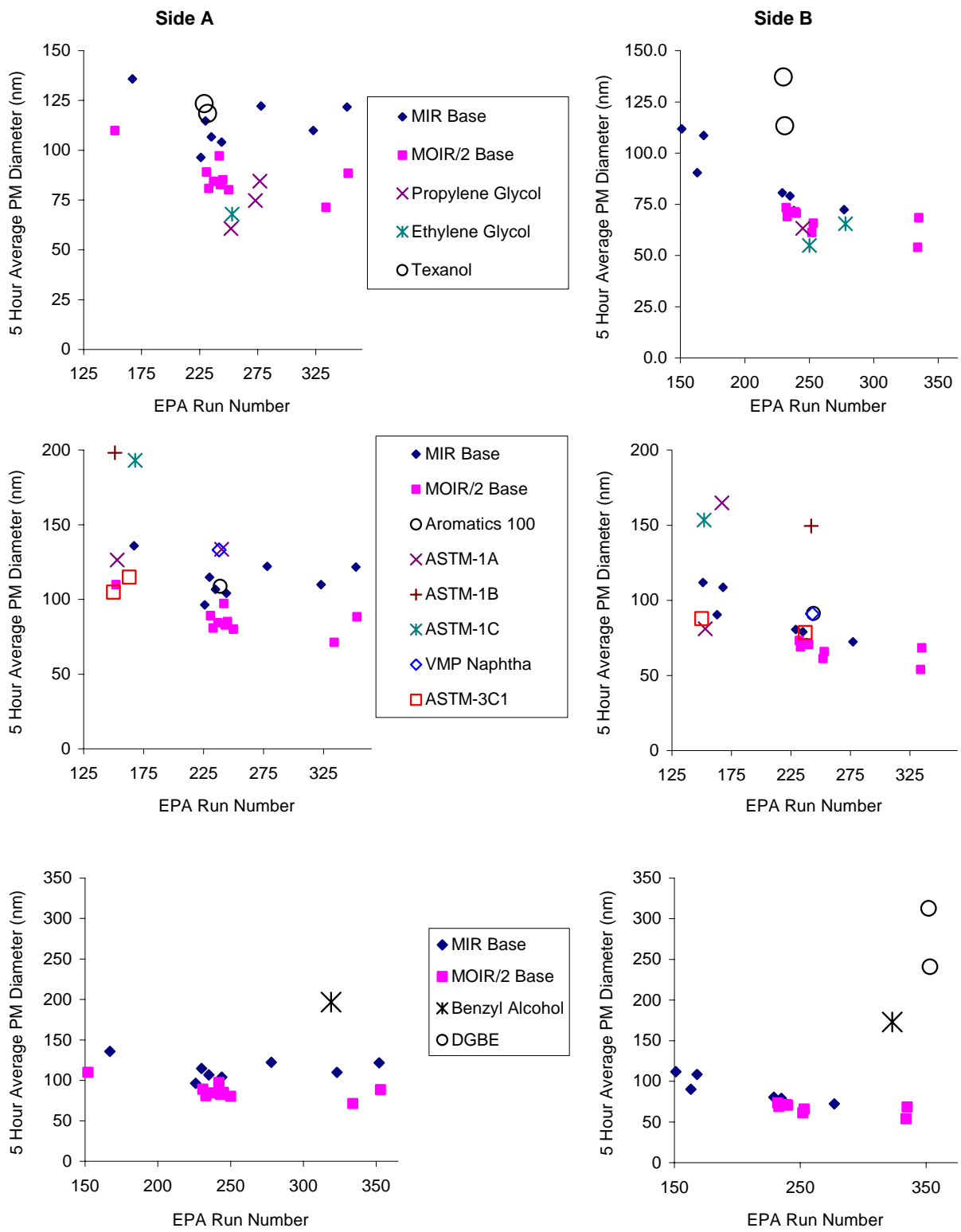
Figure 28.   Plots of 5 hour average PM diameter against run number for the base case and the incremental reactivity experiments with the various test compounds.

estimates, a wall loss correction factor of 2 was assumed to be applicable for PM yields at 5 hours of irradiation (see Figure 23), the molecular weight of the PM was assumed to be the same as the molecular weight of the added VOC, and the amount of test VOC reacted is estimated from

$$[\text{VOC reacted}] = [\text{Initial Test VOC}] \, (1 - e^{-\text{IntOH kOH}}) \qquad (IV)$$

Where IntOH is the integrated OH radical levels in the experiments, estimated from the m-xylene data as shown in Equation (II), above, and kOH is the OH radical rate constant for the test compound. For the hydrocarbon mixtures, the molecular weight used for the PM was the average molecular weight for the constituents, and the kOH values were for selected compounds chosen as representative of the mixture, as follows: ASTM 1A, 1B, and 1C: n-undecane; Aromatic-100: m-xylene. Although these estimated PM yields are highly approximate, they are useful in useful in indicating the approximate magnitudes involved.

Before discussing the results for the various types of compounds, it is useful to discuss the relationship between the final PM volume and average PM diameter data that are used as the measure of the PM impacts of the various compounds. The results on Figure 27 and Figure 28 are generally similar, suggesting that, as expected, there should be a correlation between final PM volume and average PM diameter. This is examined further on Figure 29, which shows plots of the 5-hour average PM diameter against the 5-hour PM volume for the various types of experiments (background, base case, and added test compound) that were carried out. It can be seen that the PM volume and average PM diameter results are indeed reasonably well correlated and do not depend significantly on the reactor or type of experiment, at least for PM volume levels up to ~5 μg/m^3. However, there is more scatter in the data for the added test VOC experiments, particularly for those at the higher PM levels, which might be attributed to the differences in the SOA formed from the test compounds. At the higher PM levels the average PM diameter tends to become independent of the PM volume, leveling off at ~200-300 nm. While average PM diameter should correlate fairly well with final volume, other factors such as the number of particles formed during nucleation and the total wall loss rate will reduce the quality of the correlation.
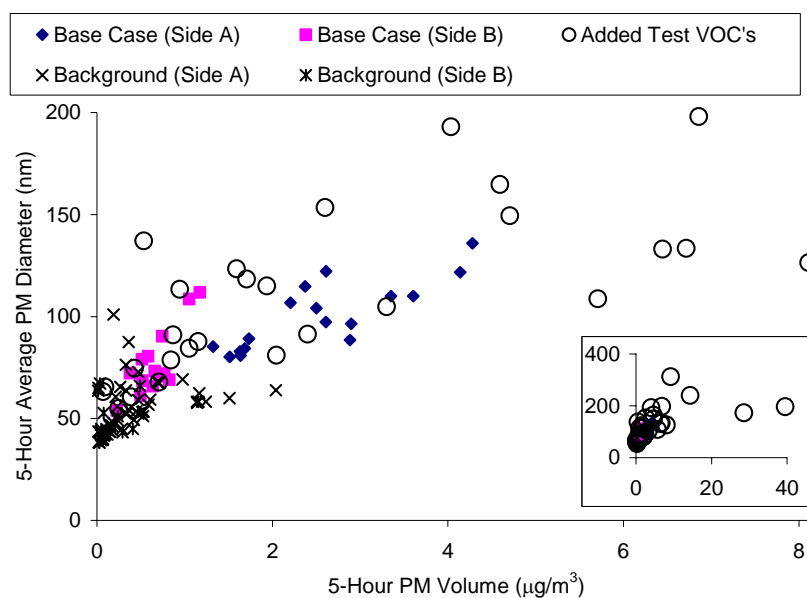

Figure 29.   Plots of 5 hour average PM diameter against 5 hour PM volume for the base case and added test compound reactivity experiments.

74

Glycols. Figure 26 and the top plots on Figure 27 and Figure 28 show that ethylene and propylene glycols have small or somewhat negative effects on PM volume and average PM diameter. This suggests that there is relatively little secondary aerosol formation occurring from the reactions of these glycols. A negative effect of a added test compound on PM could occur if the compound decreases overall OH radical levels, and thus the amount of PM formed from the reactions of OH with the aromatics in the base ROG. This is consistent with the fact that the glycols have negative effects on IntOH levels in the full surrogate experiments, as discussed in the previous section. A small amount of PM formation was observed in the non-aromatic surrogate experiment with ethylene glycol, but the amount formed was not outside the variability in chamber background PM.

Texanol®. Figure 26 and the top plots on Figure 27 and Figure 28 also show that Texanol® has no measurable effect on PM volume in the reactivity experiments. Since the addition of Texanol® inhibits OH radical levels (Carter and Malkina, 2005), one would expect that if it did not form any secondary organic aerosol (SOA) one would expect that the addition of this solvent would cause somewhat reduced PM levels because of reductions of the reactions of the aromatic PM precursors in the base ROG. The fact that there is no net effect of Texanol® on PM formation suggests that there may be a small amount of SOA being formed from the reactions of the Texanol® isomers. However, this amount is apparently small and difficult to quantify for these experiments.

ASTM-3C1 Synthetic Hydrocarbon Solvent. Figure 26 and the middle plots on Figure 27 and Figure 28 show the PM effects of the additions of the various hydrocarbon solvents that were studied in the CARB project. The results for the ASTM-3C1 solvent are discussed separately because this is a synthetic mixture while the other solvents are petroleum distillates, and because its PM impacts appear to be somewhat lower than those for the petroleum distillates that were studied. Like Texanol® this mixture was found to have no measurable effect on PM volume. This mixture also has a tendency to inhibit OH radicals in these surrogate experiments (Carter and Malkina, 2005), so one would expect it to have a negative effect on PM formation if the reactions of its components formed no SOA. The fact that it has no net effect on PM suggests that the reactions of the components of this mixture may be forming at least some SOA, but the amount is small and difficult to quantify.

Petroleum Distillate Hydrocarbon Solvents. Figure 26 and the middle plots on Figure 27 show that the petroleum distillate hydrocarbon solvents have measurable effects on PM volume, indicating that the reactions of their components must be forming at least some SOA. However, the PM yields under the conditions of these experiments are estimated to be low, being less than 1% after 5 yours of irradiation in all cases. One might expect the PM impacts of these solvents to correlate with their aromatic contents, but such an obvious correlation is not seen. As discussed by Carter and Malkina (2005) the aromatic contents of these solvents are 100% for Aromatics-100, ~20% for ASTM-1A, ~6% for ASTM-1B, small but nonzero for VMP-Naphtha, and negligible for ASTM-1C. While the relative PM impacts vary from run to run, in general the PM impacts of ASTM-1A, ASTM-1B and Aromatic 100 do not appear to be significantly different, and the PM impacts of the ASTM-1C, which contains no aromatics, is only slightly smaller. The PM impacts of VMP-Naphtha, a lighter solvent than the others which also has very low aromatics, is variable, with the one experiment in Side A having as much PM impact as the higher PM impact petroleum distillates, while the one experiment in Side B has very low PM impact. More data would be needed to make conclusions about the relative PM impact of that solvent.

2-(2-Butoxyethoxy)-ethanol (DGBE). . Figure 26 and the bottom plots on Figure 27 and Figure 28 show that DGBE has a considerably higher PM impact than the other compounds or solvents discussed above, though not as high as benzyl alcohol. A comparison with Texanol® is of interest, because the Texanol® isomers are larger molecules than DGBE (having 12 carbons compared to 8 carbons for DGBE), and one would expect more SOA formation from larger molecules. However, the Texanol® isomers are more branched molecules and the reactions of more branched molecules tend to involve

75

formation of radicals that favor more decomposition processes to smaller molecules, while DGBE is a straight chain molecule whose reactions tend to form radicals that favor internal H-shift isomerizations, which result in more highly substituted products that may tend to have lower vapor pressures. On the other hand, the SAPRC-99 mechanism generation system predicts ~50% of the DGBE reaction involves formation of lower molecular weight formates as products, with the remainder of the reaction involving formation of many different molecules, with no single highly substituted product dominating. Apparently, at least some of these smaller yield products are contributing to the SOA formation from this compound.

Table 10 shows that the estimated PM yields in the added DGBE experiments are on the order of 20%, which is considerably more than observed for the petroleum distillates. However, this is still relatively small compared to the amount of DGBE reacted, and indicates that most of DGBE products remain in the gas phase under the conditions of these experiments.

Benzyl Alcohol. Figure 26 and the bottom plots on Figure 27 and Figure 28 show that benzyl alcohol has a much higher PM impact than any other compound studied for this project. (Note that the PM volumes shown on Figure 26 for this compound are divided by two in order not to overwhelm the scale for the other compounds.) In addition, a qualitative comparison of the PM formed in the benzyl alcohol - NO_x experiments with PM formation in comparable experiments with m-xylene (Song et. al, 2005) shows that it also forms much more SOA than that compound. To investigate whether this high PM impact from benzyl alcohol may be due to secondary reactions of the benzaldehyde product, we conducted a separate reactivity experiments with benzaldehyde, but found that its PM impact was small (unpublished results from this laboratory). Apparently, the SOA precursor from this compound is either the -CH_2OH substituted phenols or the hydroxy-substituted ring-opening products that result from the OH addition to the aromatic ring. More data would be needed to determine the reason for the relatively high PM formation potential for this compound.

Table 10 shows that the PM yields in the benzyl alcohol experiments are on the order of 30%, which, though significant, indicates that most of the products remain in the gas phase under the conditions of our experiments.

Seed Aerosol and Availability Experiments

One of the objectives of this project was to evaluate the potential utility of the environmental chamber to evaluate the availability of lower volatility and hydrophilic VOCs to react in the gas phase to promote ozone formation. For example, if such compounds have a significant tendency to partition onto atmospheric aerosols or other surfaces in the environment, then their tendency to react in the gas phase and promote atmospheric ozone formation would be correspondingly reduced. The proposal for this project called for holding discussions with the Reactivity Research Working Group (RRWG)'s Atmospheric Availability subgroup to design an appropriate set of exploratory experiments for this project. Accordingly, discussions were held with Dr. Jonathan J. Kurland, the leader of that subgroup, as to what experiments would be useful for this project. Discussions were also held with the SCAQMD and CARB staff and other members of the RRWG and RRAC regarding this project.

As a result of these discussions, it was decided to focus on conducting a limited number of experiments to investigate whether the presence of humidity and hydrophilic seed aerosol affect the gas-phase decay rates and reactivities of ethylene and propylene glycol. These glycols are highly hydrophilic and have a tendency to be absorbed on surfaces, so they are probably the most likely of the coatings VOCs we were studying for the CARB and SCAQMD to partition into wet seed aerosols and have their availability to react in the gas phase correspondingly reduced. The experiments carried out consisted of determining whether the presence of humidity and $(NH_4)_2SO_4$ or NH_4HSO_4 seed aerosol (1) enhances the dark decay rate of these glycols, (2) affects their rates of consumption when irradiated in the presence of

the ROG surrogate and NO$_x$, and (3) affects their impact on the glycols on O$_3$ formation and other measures of gas-phase reactivity. For control purposes, we also carried out an experiment to determine whether a small amount of the (NH$_4$)$_2$SO$_4$ seed aerosol affects the results of a standard base case MOIR/2 surrogate - NO$_x$ experiment. The special procedures employed with these experiments were discussed above in the "Experimental Methods" section of this report. The results obtained are discussed below.

<u>Effect of Seed Aerosol on a Base Case Surrogate - NO$_x$ Experiment</u>. In order to determine whether the presence of a small amount of (NH$_4$)$_2$SO$_4$ seed aerosol will affect gas-phase results of a base case surrogate - NO$_x$ experiment in the chamber, and MOIR/2 side equivalency test experiment was carried out with ~1.5-2 µg/m^3 seed aerosol added to each reactor. Essentially the same gas-phase and PM results were observed on both sides, indicating good side equivalency. Experimental and calculated concentration-time plots for selected gas-phase species and experimental total PM number and volume data for that experiment are shown on Figure 30. For comparison purposes, results of an experiment with comparable conditions but without added seed aerosol are also shown on that figure.

The O$_3$ formation and NO oxidation results of both of these MOIR/2 surrogate - NO$_x$ base case experiments were in excellent agreement with the predictions of the standard SAPRC-99 mechanism, and the correspondence between experimental data and model calculation for consumptions of the reacting
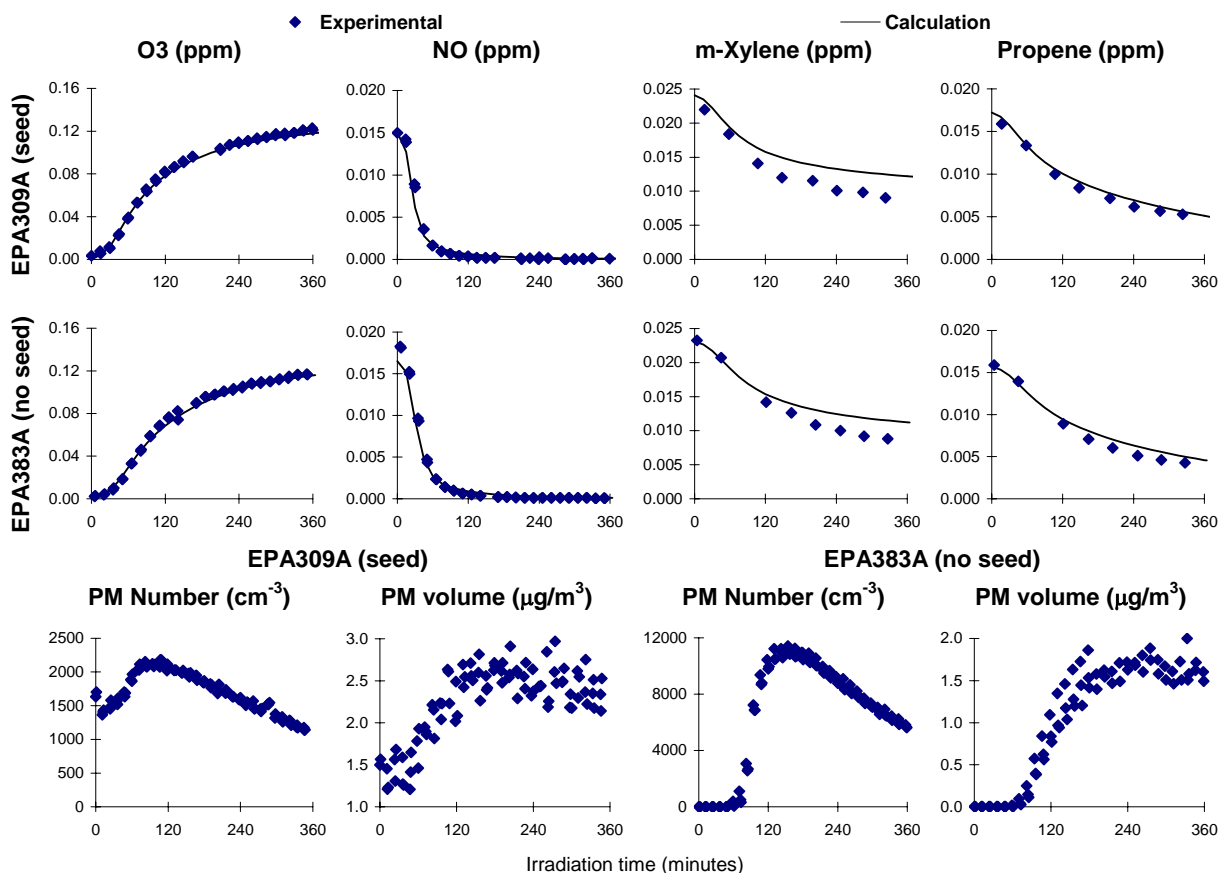

Figure 30.   Comparison of selected results of the blacklight surrogate - NO$_x$ experiment with seed aerosol, EPA309A with those for a comparable experiment, EPA393A, without added seed aerosol. Calculations used the standard SAPRC-99 mechanism.

77

surrogate components was comparable. This indicates that the presence of the low amount of this seed aerosol does not affect the gas-phase results of these experiments, since if it did the correspondence between the model calculation and the experimental data would be different when the seed is present. In addition, the amount of new aerosol formation in the two experiments was comparable; the final PM volume in the added seed aerosol experiment was higher than in the comparable no added seed experiment by approximately the amount of initial seed aerosol in the experiment where it was added.

These results were not unexpected, since the amounts of added aerosol was relatively low, and the VOCs in the base surrogate are relatively volatile and do not have strong affinities for surfaces. Unfortunately, because of limited aerosol generating capacity at the time the experiment was conducted we were not able to conduct experiments with significantly higher seed aerosol levels. However, the experiment is still a useful control in indicating no unexpected chamber effects or other impacts resulting when the $(NH_4)_2SO_4$ is added to the system.

Glycol Dark Decay Experiment. In order to determine whether the presence of humidity and $(NH_4)_2SO_4$ seed aerosol have measurable effects on the atmospheric lifetimes of the glycols in the dark, an experiment was carried out where ethylene and propylene glycol were injected into each of the dual reactors, Side A was humidified to 35% and 10 $\mu g/m^3$ seed aerosol was added, Side B was kept dry with no aerosol added, and the glycols were monitored in the dark for 6 hours. The glycol measurements made during this experiment are shown on Figure 31. It can be seen that the glycol dark decay rates were negligible, to within the precision of the GC measurements, in both reactors. Therefore, these glycols do not appear to go to the walls to a significant extent in our chamber during the course of our 6-hour irradiation experiments, and the presence of humidity and seed aerosol at the level employed in this experiment had no measurable effect on enhancing glycol dark decay.

Glycol Reactivity Experiments. One experiment each was carried out to determine if the presence of humidify and seed aerosol would affect results of incremental reactivity experiments with the glycols. Both of these were MIR experiments because these are most sensitive to the effects of added VOCs. Because of limited humidification and aerosol generation capacity at the time the experiments were carried out, only one reactor was employed in each case, so simultaneous base case experiments could not
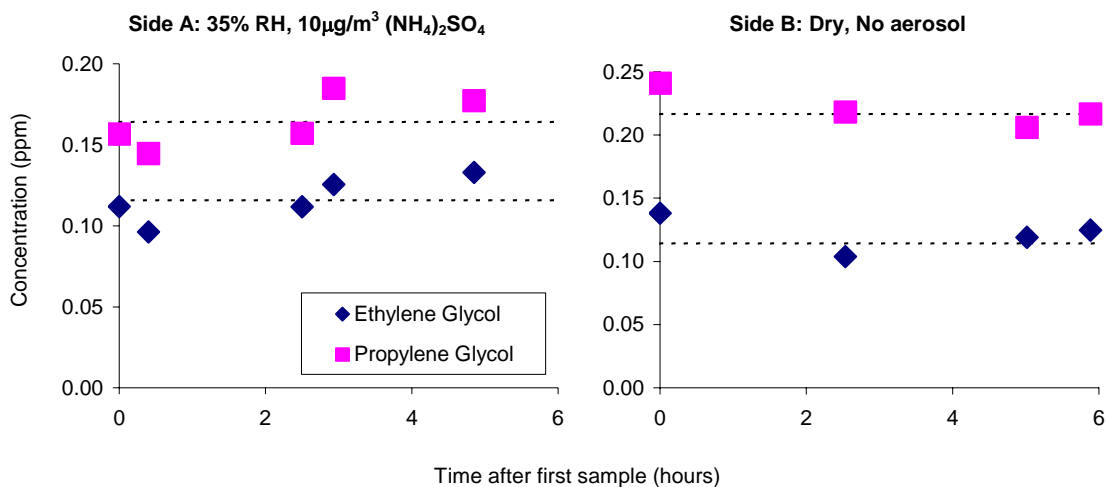
Figure 31.   Concentration-time plots for the glycols measured during the glycol dark decay experiment.

be carried out. Therefore, the effects of humidity and seed aerosol on the results have to be assessed by comparing the results of comparable reactivity experiments with the compounds in the absence of humidity and seed aerosol.

The propylene glycol experiment was carried first, and involved humidification to 25% RH and addition of 9 μg/m³ of $(NH_4)_2SO_4$ seed aerosol to an experiment where 0.4 ppm of glycol was added to an otherwise standard MIR surrogate - NO_x experiment. The results are shown on Figure 32, where they are compared with the most comparable propylene glycol reactivity experiment with no added seed aerosol. Results of model calculations are also shown, to serve as a basis for comparing the experiments with the differences in initial reactant concentrations taken into account. It can be seen that the correspondence between the experimental gas-phase measurement and the model calculation is the same for both experiments, indicating no evidence for the humidity or seed aerosol affecting the gas-phase results. Figure 32 also shows that the PM volume declined during the added seed aerosol experiment, which is consistent with the results of the other reactivity experiments that indicated little or no SOA formation from propylene glycol.

Because there was no apparent effect of humidity and seed aerosol in the propylene glycol experiment, it was decided to use an aqueous seed aerosol in the experiment with ethylene glycol, so

Figure 32.   Comparison of selected results of the propylene glycol + MIR surrogate - NO_x experiment with wet seed aerosol, EPA316A with those for a comparable experiment, EPA273A, without added seed aerosol.

NH$_4$HSO$_4$ (added to an already humid chamber, with the diffusion dryer removed from the seed generator) was used instead of (NH$_4$)$_2$SO$_4$ for the seed aerosol. This experiment involved humidification to 30% RH and adding ~7 μg/m^3 NH$_4$HSO$_4$ seed aerosol and 0.3 ppm ethylene glycol to an otherwise standard MIR surrogate - NO$_x$ mixture. The results are shown on Figure 33, where they are compared with the results of the most comparable ethylene glycol reactivity experiment without humidity and seed aerosol. Model calculations are shown to serve as a basis for comparing the gas-phase results of the different experiments with the differences in initial reactant concentrations taken into account. Again, the results show essentially the same correspondence between experimental and calculated results for both experiments, giving no indication that the presence of the humidity and the seed is affecting the results.

The presence of the humidity and seed aerosol also had no measurable effect on the relative rates of decay of the glycols in these experiments. If the humidity and seed aerosol was enhancing the rates of decay of these compounds, their consumption rates, relative to the m-xylene that was also present in the experiments, would be different than predicted by the ratios of OH radical rate constants for the two compounds, since reaction with OH is their major gas-phase loss process. As discussed in the "OH Radical Rate Constant Determination" section, above, the relative rates of consumption of the glycols and m-xylene in the glycol reactivity experiments without humidity and seed aerosol were in reasonably good
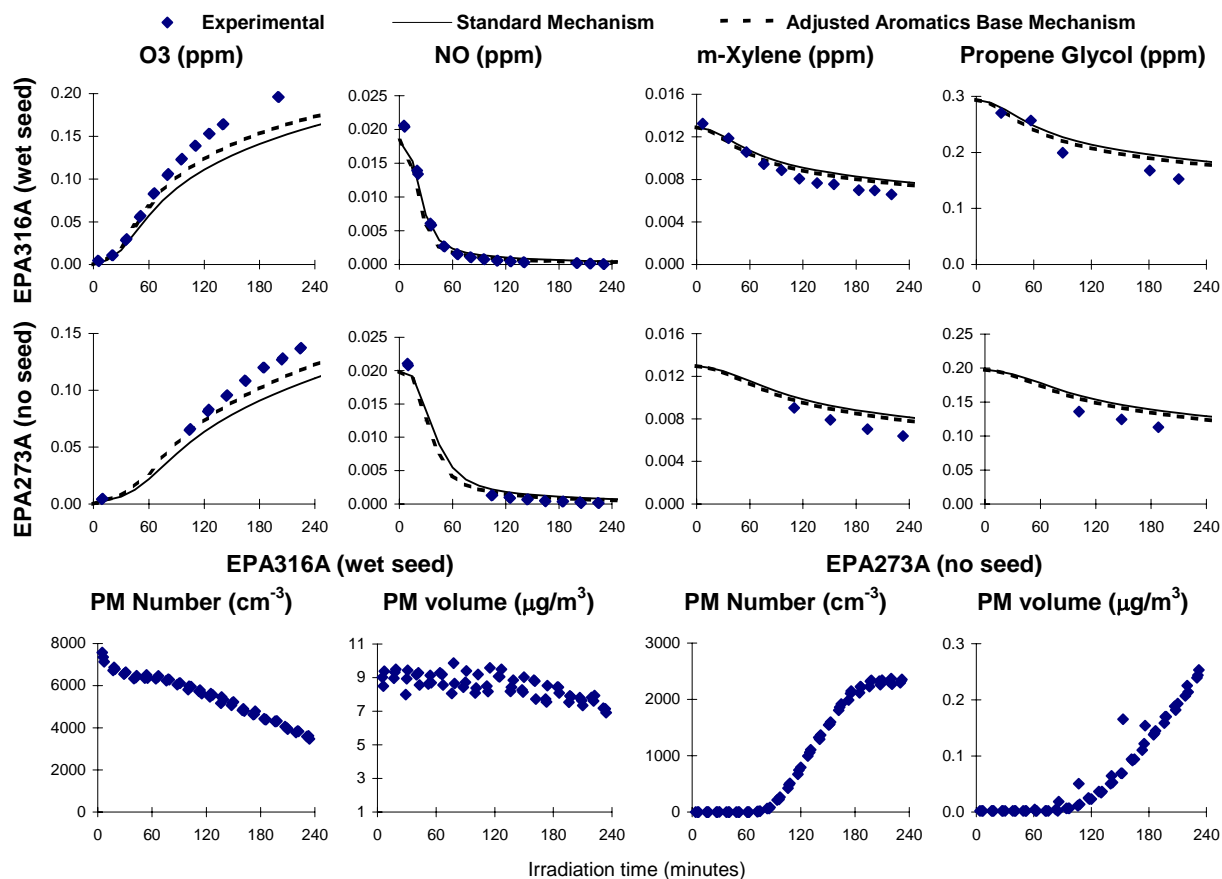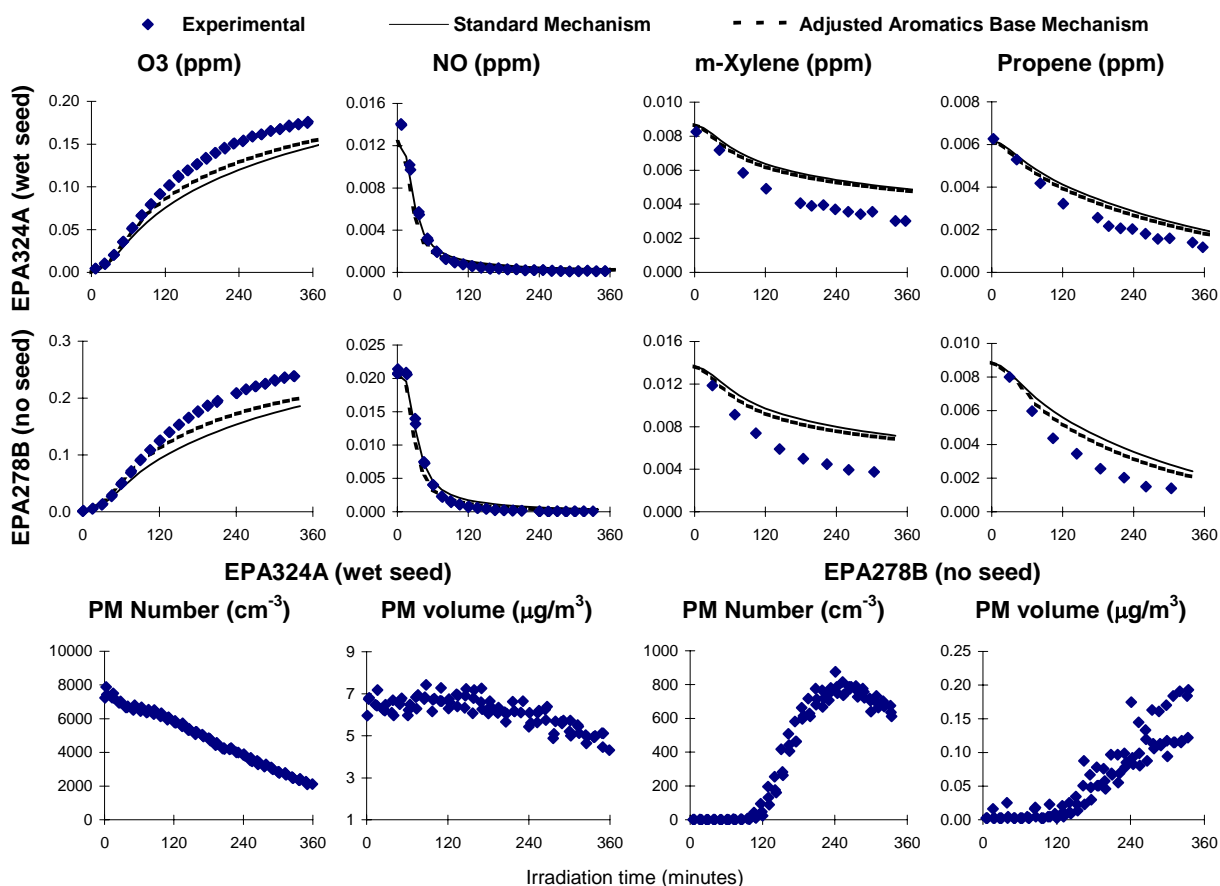

Figure 33.   Comparison of selected results of the ethylene glycol + MIR surrogate - NO$_x$ experiment with wet seed aerosol, EPA324A with those for a comparable experiment, EPA278B, without added seed aerosol.

agreement with those predicted using their OH radical rate constants as used in the mechanism. This is also seen in the added seed aerosol experiments, as shown in Figure 34, which give plots of the relative decay rates of the glycols and m-xylene in these experiments, compared to the line predicted by their OH radical rate constants as used in the mechanism ("Literature kOH line"). Therefore, there is no indication of humidity or seed aerosol affecting the consumption rates of these glycols in the experiments.

It should be noted that dry ammonium sulfate or even aqueous ammonium bisulfate are insufficient by themselves to simulate ambient aerosol. Different results may occur in the presence of an acidic seed or an organic seed particle. Further study on the atmospheric availability of VOCs including glycols for other seed types is still required.

Another problem with these experiments is that the total mass of added seed aerosol was orders of magnitude less to the mass of glycols present in the gas phase in these experiments. The amount of gas-phase glycols in the seed aerosol experiments discussed in this section ranged from ~600 - 800 $\mu g/m^3$, while the maximum amount of seed aerosol was ~10 $\mu g/m^3$. Therefore, the possibility that measurable effects of added aerosol may have been observed if the amount of aerosol was comparable to the amount of gas-phase material cannot be ruled out. Unfortunately, the aerosol generation capability available at the times of these experiments was insufficient for this to be investigated.
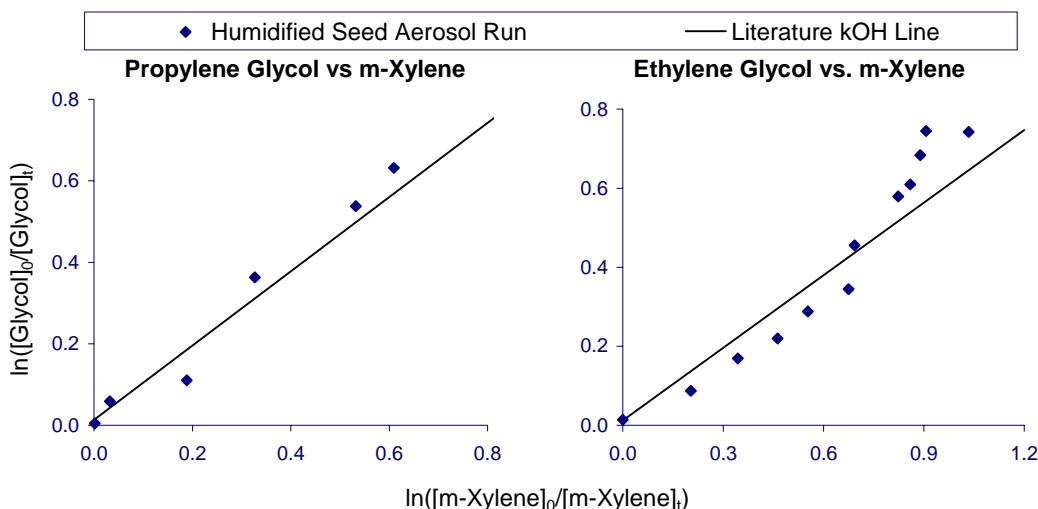
Figure 34.   Plots of Equation (I) for apparent relative OH radical determinations from the data from the ethylene and propylene glycol wet seed aerosol experiments.

CONCLUSIONS AND RECOMMENDATIONS

This project had variable success in achieving its several objectives. One of the objectives was to conduct chamber experiments with reactive organic gas (ROG) surrogates that best represent current mobile source and other emissions into ambient atmospheres, to serve as a basis for updating the ROG surrogate used in experiments and models for VOC reactivity assessments and other purposes. However, this objective could not be addressed in this project because there was insufficient time and resources available to derive a target ROG composition to serve as a basis for such a study. On the other hand, this project was successful in obtaining high-quality environmental chamber data to reduce the uncertainties in ozone impact predictions for several important water-based coatings VOCs, though issues were encountered in evaluating the results for the glycols that were not completely resolved. This project was also successful in demonstrating the utility of the new UCR EPA environmental chamber for assessing relative aerosol formation potentials for VOCs, and obtained useful qualitative information concerning the relative PM impacts of the coatings VOCs studied for this and the CARB project. However, additional work is needed before such data can be used for quantitative SOA model evaluation. This project also demonstrated the potential utility of the chamber for evaluating the effects of aerosol and humidity on availabilities of VOCs to react in the gas phase, at least in terms of demonstrating the lack of effects of humidity and low levels of seed aerosol on glycol availability. The conclusions and recommendations resulting from the work for this project, and from related work on the previous CARB project (Carter and Malkina, 2005), on these various objectives are discussed in more detail below.

Need for an Updated Reactive Organic Gas (ROG) Surrogate

The impacts of volatile organic compounds on ozone and PM formation depends on the environment where they react, and one of the factors affecting their chemical environment is the mixture of reactive organic compounds from other sources. The composition of the reactive organic gas (ROG) surrogate is in important input not only to calculation of ozone reactivity scales such as MIR (Carter, 1994a), but also for conducting environmental chamber experiments to evaluate chemical mechanism for predicting reactivity (Carter et al, 1995a). The ROG surrogate mixture used to represent ambient ROG emissions in the Carter (1995a, 2000a) reactivity scales, and used as the basis for designing the ROG surrogates used in the environmental chamber reactivity experiments (Carter et al, 1995a) is based primarily on ambient measurements made in the 80's (Carter, 1994a, Jeffries et al, 1989, and references therein) and is probably out-of-date. Emissions from mobile sources make an important contribution to this base ROG mixture, and potentially significant changes in the chemical composition of these emissions may have occurred in recent years as a result of control measures and fuel modification efforts. In addition, the base ROG mixture used in the chamber experiments was not derived for the purpose of assessing PM formation potentials, and does not contain the higher molecular weight compounds that may impact SOA formation. For this reason, we included in the proposal an effort to evaluate updating the ROG surrogate used for environmental chamber reactivity experiments, and conducting chamber experiments necessary to support this evaluation. This is discussed in Appendix A to this report.

Addressing this objective requires that a consensus be reached among the relevant regulatory agencies and the experts in the field as to the target composition to serve as the basis for developing new ROG surrogates. Unfortunately, this consensus was not reached in the time frame needed for this project, and therefore we were unable to make progress on this element of the program. However, the need to update the ambient ROG surrogate remains, both from the perspective of updating the methods used to calculate VOC reactivity scales affecting all sources, mobile as well as stationary, and updating the experimental methods used to evaluate models for ozone and PM reactivity. Therefore, we recommend

that the CARB, SCAQMD, and EPA make a concerted effort to reach a consensus as to the appropriate target composition for ambient ROG surrogates to use for reactivity assessment experiments and modeling, which can serve as a basis for developing and evaluating updated surrogates for this purpose.

Atmospheric Ozone Impacts of Selected Coatings VOCs

A major effort for this project was carrying out environmental chamber experiments to provide data needed to develop or evaluate mechanisms to predict the ozone impacts of the representative water-based coatings VOCs ethylene and propylene glycol, 2-(2-butoxyethoxy)-ethanol (DGBE), and benzyl alcohol. These compounds were studied because of their importance in the inventory and because (except for propylene glycol) there were no chamber data available to evaluate their mechanisms. In addition, no mechanism had previously been developed to assess the atmospheric ozone impact of benzyl alcohol. The conclusions and recommendations that can be drawn concerning the mechanisms and ozone impact predictions for these compounds are as summarized below.

Ethylene and Propylene Glycols. The atmospheric chemical mechanisms for these compounds appear to be reasonably well understood, and the measured relative consumption rates for these glycols in the chamber experiments for these compounds were consistent with their currently accepted OH radical rate constants. Nevertheless, the SAPRC-99 mechanism appears to have a tendency to underpredict the ozone impacts of these compounds in some in the chamber experiments at low concentrations and with aromatic-containing base ROG surrogates. In particular, the measured ozone impacts of these compounds in the new environmental chamber data using the complete ROG surrogate were about 20% higher than model predictions in the case of propylene glycol, and 25-30% higher in the case of ethylene glycol. On the other hand, the model predictions were consistent with results of the experiments with these two glycols using a ROG surrogate with the aromatics removed, and also with results of higher concentration surrogate experiments carried out previously for Philip Morris (Carter et al, 1997). Given that the mechanisms and rate constants for these compounds are reasonably well established, and the results do not appear to be highly sensitive to uncertainties in the mechanisms for the glycol oxidation products, it is unclear what modifications to the mechanism for these compounds would be appropriate to improve the fits to these data.

The fact that better fits of model calculations to the reactivity data are obtained if the aromatics are removed from the ROG surrogate in the reactivity experiments suggests that the problem may not necessarily be the glycol mechanisms but may be in the mechanisms for the aromatics in the base surrogate. A similar (if not entirely analogous) situation occurs in the case of CO, where the model underpredicts, by about a factor of 2, the effects of adding CO to aromatics - NO_x irradiations. This is despite the fact that the rate constant for CO has been measured numerous times and is well established, it has only one possible reaction, and that forms no reactive products other than HO_2. This problem does not appear to be as evident for other compounds for which chamber reactivity data are available, particularly those with strong radical sinks, such as hydrocarbon solvents and the higher molecular weight glycols ethers and esters studied for the coatings projects, or those with strong radical sources, such as aromatics. It also does not appear to be as evident in the higher concentration reactivity experiments carried out previously, where the model underprediction bias at low ROG/NO_x ratios is also not seen (Carter, 2000a, 2004). However, the reason for this apparent problem with the base case mechanism is unknown, and the possibility that there may indeed be problems with the glycol mechanism cannot be ruled out.

The recommendation in this regard is to continue to use the current mechanism for these glycols to predict their atmospheric ozone impacts for the time being, but to re-examine them using the data from this project when the aromatics mechanisms have been updated. A project to update and hopefully address the problems with current aromatics mechanisms is underway for the CARB. When the mechanisms are re-evaluated using improved aromatics mechanisms that, for example, correctly predict

radical levels and the effects of added CO, the reactivity data from this project can be used to indicate whether there are indeed problems with the glycol mechanisms that need further study. The updated data will then be made available to the SCAQMD, CARB, and others. If the problems persist, then there will be a need to verify the currently assumed product yields from these glycols, and to study the atmospheric reactivities of these products.

2-(2-Butoxyethoxy)-ethanol (DGBE). Despite the fact that there are no known kinetic and product data concerning the atmospheric reactions of DGBE, and that the current representation of this compound in the SAPRC-99 mechanism is based entirely on estimates, the results of the experiments for this project were entirely consistent with the predictions of the mechanism. This is true not only for predictions of its ozone impacts, but also for its OH radical rate constant, where the rate constant derived from the data in from this project, 5.04×10^{-11} cm^3 $molec^{-1}$ s^{-1}, was only 17% higher than the estimated rate constant used in the mechanism. Therefore, the data obtained in this project tended to validate the mechanism already used for this compound, and indicated no need to change the mechanism or its estimated reactivity in the MIR scale.

A similar result was observed in our previous experiments with the Texanol® isomers, where the OH radical rate constant and reactivity data derived from our experiments were entirely consistent with predictions of the estimated mechanism. Together, these data tend to support the predictive capabilities of mechanisms derived using the SAPRC-99 mechanism estimation and generation methods (Carter, 2000a), at least for these higher molecular weight glycol ethers and esters. However, the estimated mechanisms for these compounds are relatively complex, having many modes of reaction and competing processes involved in their photooxidations. Therefore, the relatively good performance in predicting rate constants and reactivities for these compounds may be due, at least in part, to cancellations of errors in the estimations of the many branching ratios and rate constants that go into the derivations of these mechanisms.

Benzyl Alcohol. This project resulted in the development of a new mechanism for the atmospheric reactions of benzyl alcohol, a compound that was not previously represented in the SAPRC mechanisms. Benzyl alcohol appears to be similar to other aromatic hydrocarbons in having relatively large internal radical sources and tending to enhance O_3 formation under MIR conditions, but inhibiting, or at least not enhancing, O_3 when NO_x is limited. As with other aromatics, many of the details of its atmospheric reactions are uncertain and difficult to estimate, but a suitably modified version of the existing parameterized SAPRC-99 mechanism for toluene was found to simulate the data at least as well as mechanisms for other aromatics. The benzaldehyde formation observed in benzyl alcohol - NO_x experiments indicated a higher fraction of the reaction occurs by OH radicals abstracting from the side group than is the case for toluene (~30% vs. ~9%), which is expected given the tendency for α-OH substitution to increase H-atom abstraction reactions by OH. A higher overall nitrate yield from the reactions of peroxy radicals with NO (~5% vs 0.8%) was also necessary to improve the model fits to the data. The relative consumption rate of benzyl alcohol in the reactivity experiments indicated an OH radical rate constant of 2.56×10^{-11} cm^3 $molec^{-1}$ s^{-1}, which is in good agreement with the previously reported value of 2.29×10^{-11} that is used in the mechanism.

Since the new benzyl alcohol mechanism is reasonably consistent with the data obtained in this project and is consistent with the representation used for other aromatics, it represents our current best estimate for the purpose of calculating atmospheric ozone impacts of this compound. However, it suffers from the same problems as aromatic mechanisms in general. In particular, it represents the ring-opening processes using a parameterized approach that simplifies the processes that actually occurs; it tends to underpredict OH levels in NO_x -air irradiations of the compounds; and it does not correctly predict the effects of adding CO. Therefore, this mechanism will also need to be updated when we have new mechanisms for aromatics that can serve as a better basis for deriving a more explicit mechanism for this

compound. The data obtained in this project will then be useful for evaluating and if necessary improving the updated mechanism for this compound once it is developed.

Summary of Atmospheric Reactivity Predictions. Table 11 gives a summary of the previous (Carter, 2003) and (where applicable) revised atmospheric reactivity predictions in the MIR scale for the various coatings compounds that were studied for this project. The results for the compounds studied for the CARB coatings reactivity project are also included, for completeness. The comments on the table indicate the reasons for the revisions (or lack thereof) that were made. The uncertainty classification codes used with the most recent complete MIR tabulation (Carter, 2003) is also given. These represent our current best estimates for the MIRs for these compounds until the reactivity scale is updated.

PM Formation Potentials of Coatings VOCs

This program was successful in addressing its second major objective, which was to obtain measurements of relative PM impacts of the representative coatings VOCs that were studied for this and the CARB coatings reactivity project. As far as we are aware, there are no previous environmental chamber data concerning relative PM impacts of these particular compounds, nor are we aware of PM impact data for any VOCs under conditions as closely approximating atmospheric pollutant levels as these experiments and that also sufficiently well characterized for gas-phase mechanism evaluation.

Table 12 lists the compounds whose PM impacts were studied for this project, and gives the ranges and averages of the estimated SOA yields for the compounds found to have positive PM impacts. Note that the estimated SOA yields are approximate, since they are based on assumed SOA densities and molecular weights that may not be appropriate, and the estimated amounts of test compound reacted are highly approximate for the hydrocarbon mixtures. Note also that the SOA yields shown on the table are calculated from differences between PM levels in the base case and added test compound experiments, and do not take into account the effect of the added test compound on SOA formation from the VOCs in the base ROG mixture and the background PM source. Since most of these coatings VOCs tended to suppress OH radical levels (see Table 7 and Carter and Malkina, 2005), and thus decrease the amount of reaction of the base ROG constituents or background PM source, the effect of the added test VOC on SOA formation from the base ROG would tend to be negative. Therefore, the actual SOA yields of the test compounds under the conditions of these experiments would probably be somewhat higher than shown on Table 12, particularly for the compounds with the lowest SOA yields..

In addition to depending on the yields of condensable products, the SOA yields will also depend on the amount of condensable product that partitions into the gas phase. According to equilibrium partitioning theory (Pankow 1994a,b), this will depend on the amount of organic aerosol mass present, as well as the compound and the temperature. Therefore, the SOA yields shown in Table 12 are strictly speaking applicable for the conditions of these experiments, which had relatively low background and base case organic aerosol (typically less than ~3 $\mu g/m^3$, depending on the reactor). The maximum PM levels in the added test compound experiments were typically less than 10 $\mu g/m^3$, except for some runs with DGBE or benzyl alcohol where the 5-hour PM levels were as high as ~30 $\mu g/m^3$. This can be compared to the 24-hour PM 2.5 standard of 65 $\mu g/m^3$ (EPA, 2005), of which ~40% would be organic carbon during peak PM periods in California (Motallebi et al, 2003). Therefore, the highest PM experiments in this study correspond approximately to organic aerosol content of the 24-hour PM 2.5 standard. Most chamber experiments for this project have organic PM levels and therefore potentially lower SOA yields than would occur in highly PM polluted atmospheres in California.

To completely characterize the SOA formation potential it would be necessary to measure SOA yields at a variety of organic aerosol levels, and also at differing temperatures, humidities, and reactant

Table 11.   Maximum incremental reactivity (MIR) values for the coatings compounds studied for the coatings reactivity projects.

Compound or mixture	MIR (gm O_3 /gm VOC) [a]		Unc'y Class [b]	Comments
	Previous	Revised		
Ethylene Glycol	3.36	3.63	2a	Revised as a result of representing glycolaldehyde explicitly. This mechanism still underpredicts glycol reactivity by 25-30% in some experiments, but there is no mechanistic justification for adjustments.
Propylene Glycol	2.74	No change	2a	This mechanism underpredicts glycol reactivity by ~20% in some experiments, but there is no mechanistic justification for adjustments.
Texanol® (2,2,4-trimethyl-1,3-pentanediol isobutyrate monoesters) [c]	0.88	No change	2a	Current estimated mechanism fits the new data satisfactorily
2-(2-butoxyethoxy)-ethanol (DGBE)	2.86	No change	2a	Current estimated mechanism fits the new data satisfactorily
Benzyl Alcohol	Not repre-sented	4.89		Mechanism developed for this work and adjusted to fit the new chamber data.
Petroleum distillates studied for the CARB project [d]				
VMP Naphtha, Primarily C_7-C_9 mixed alkanes	1.41	1.35	2a	Current mechanisms and compositional assignments fit the data satisfactorily.
Dearomatized Mixed Alkanes, Primarily C_{10}-C_{12} (ASTM-1C)	0.91	0.96	2a	Current mechanisms and compositional assignments fit the data satisfactorily.
Reduced Aromatics Mineral Spirits, Primarily C_{10}-C_{12} mixed alkanes with 6% aromatics (ASTM-1B)	1.21	1.26	2a	Current mechanisms and compositional assignments fit the data satisfactorily.
Regular mineral spirits, Primarily C_{10}-C_{12} mixed alkanes with 19% aromatics (ASTM-1A)	1.82	1.97	2a	Current mechanisms and compositional assignments fit the data satisfactorily.
Synthetic isoparaffinic alkanes, primarily C_{10}-C_{12} branched alkanes (ASTM-3C1)	0.81	1.1 - 1.5	4	The current assignments and mechanism for this mixture underestimates its reactivity. MIRs given are ranges of values using mechanisms adjusted to fit the data.

Table 11 (continued)

Compound or mixture	MIR (gm O$_3$ /gm VOC) [a]		Unc'y Class [b]	Comments
	Previous	Revised		
Aromatic 100 (Primarily C$_9$-C$_{10}$ alkylbenzenes)	7.51	7.70	2c	Change in MIR when aromatics mechanisms are updated is uncertain but probably less than ~50%. Reactivities in MOIR and other lower NOx scales are much more uncertain and probably are overestimated.

[a] Previous value is from Carter (2003), unless indicated otherwise. Revised value is value derived as a result of this or the CARB coatings reactivity study.

[b] Uncertainty classification code as used in tabulation by Carter (2003)

[c] Compound studied for CARB project (Carter and Malkina, 2005).

[d] See Carter and Malkina (2005) for more details concerning the results of the experiments with these hydrocarbon solvents. The MIR value in "previous" column is that calculated using the CARB "bin" method for hydrocarbon solvent reactivities (Kwok et al, 2000)

Table 12.   Summary of ranges of estimated SOA yields for coatings VOCs whose PM formation potentials were studied for this project

Compound or Mixture	Approx. 5-hour SOA Yield Range	Comments
Ethylene Glycol	-	PM lower than base case
Propylene Glycol	-	PM lower than base case
Texanol® (2,2,4-trimethyl-1,3-pentanediol isobutyrate esters)	-	Net effect on PM small
Synthetic isoparaffinic alkanes, primarily C$_{10}$-C$_{12}$ branched alkanes (ASTM-3C1)	-	Net effect on PM small
Dearomatized Mixed Alkanes, Primarily C$_{10}$-C$_{12}$ (ASTM-1C)	0.2%	Similar yields in 2 runs
Aromatic 100 (Primarily C9-C10 alkylbenzenes)	0.3 - 0.4%	Avg. for 2 runs = 0.3%
VMP Naphtha, Primarily C$_7$-C$_9$ mixed alkanes	0.1 - 0.7%	Avg. for 2 runs = 0.4%
Regular mineral spirits, Primarily C$_{10}$-C$_{12}$ mixed alkanes with 19% aromatics (ASTM-1A)	0.3 - 0.8%	Avg. for 3 runs = 0.5%
Reduced Aromatics Mineral Spirits, Primarily C$_{10}$-C$_{12}$ mixed alkanes with 6% aromatics (ASTM-1B)	0.6 - 0.7%	Avg. for 2 runs = 0.6%
2-(2-butoxyethoxy)-ethanol (DGBE)	14 - 26%	Avg. for 3 runs = 20%
Benzyl Alcohol	30%	Similar yields in 2 runs

concentrations, etc. It would also be necessary to characterize PM formation from the base ROG constituents and the background PM sources, particularly to assess SOA formation from VOCs with relatively little SOA formation potentials. Nevertheless, at a minimum the results obtained from this study can be used for a relative ranking the relative PM impacts of the compounds or mixtures studied, and will eventually be useful for quantitative PM model evaluation once more comprehensive data are available, and the PM formation mechanisms and PM chamber effects model are sufficiently well developed.

In terms of relative PM impacts, Table 12 indicates that the ordering was found to be benzyl alcohol > DGBE >> petroleum distillate-derived hydrocarbon solvents > a synthetic hydrocarbon solvent consisting primarily of branched alkanes ≈ Texanol® ≥ ethylene and propylene glycols. In some respects these results are qualitatively as expected, but in others they are not. This is discussed further below.

Benzyl alcohol had the highest PM impact of the compounds studied, and it apparently it also has higher PM impacts than most other aromatics that have been studied. The reason for this is unknown, except that it is apparently not due to reactions of benzaldehyde, which was found not to have a large PM impact in separate reactivity experiments carried out for another project. Apparently the OH substitution on either the phenolic or ring-opening products decreases the volatility of at least some of these products sufficiently that they participate significantly in the formation of SOA. It would be worthwhile to investigate which of the products are involved.

Although the PM formation impact of DGBE in our experiments was less than that of benzyl alcohol, it was significantly higher than any of the other compounds or mixtures studied for this project. This is despite the fact that the molecular weight of Texanol®, which had no measurable PM impact, is 33% higher than that of DGBE. The main difference between DGBE and the Texanol® isomers is that DGBE is a straight chain compound while the Texanol® isomers have a relatively high degree of branching. As a general rule, long chain compounds tend to react to a greater extent by increasing oxidation on the molecule, while branched compounds tend to have a greater tendency to fall apart as they react. However, more data are needed before generalizations of predictive utility can be derived, and probably the SOA formation potentials of these complex molecules will need to be looked at on a case-by case basis.

While it is not surprising that the petroleum distillate solvents used in architectural coatings have some PM impacts, it is surprising that the ordering of the PM impacts of these solvents was not well predicted by their aromatic contents. In particular, the "ASTM-1A" and "ASTM-1B" solvents, which are respectively 20% and 6% aromatics and the rest C_9-C_{12} mixed alkanes, had approximately the same, and in some experiments even greater, PM impacts than the 100% aromatic Aromatic-100 solvent. The chemical compositions of the aromatics in these solvents are very similar (Carter and Malkina, 2005), so the difference is unlikely to be due to different types of aromatics in the two solvents. Therefore, the alkanes in these solvents appear to be contributing to the PM impacts of these solvents, and may be more important as SOA precursors relative to aromatics than previously realized. It is likely that the normal and cyclic alkanes are more important contributors than the branched alkanes, given the increased tendency for branched compounds to break apart when they react. This is consistent with the fact that the primarily branched alkane synthetic hydrocarbon solvent "ASTM-3C1" had the lowest PM impact of all the hydrocarbon solvents that were studied.

Texanol® was found to have essentially no measurable effect on the volume of PM formed in the chamber experiments. However, Texanol® is also a radical inhibitor, and the decreased OH radical levels in the experiments where Texanol® is added should cause decreased PM formation from the reactions of the aromatics in the base ROG surrogate. Indeed, the addition of ethylene or propylene glycol did decrease PM formation in the experiments, which can be attributed to this effect. The fact that Texanol® did not decrease PM formation suggests that it may have some small amount of SOA formation, that is

counteracting its inhibition of SOA formation from the aromatics in the base mixture. However, improved characterization of background effects and the mechanism of SOA formation in the base case experiments is needed to quantitatively assess this.

Both ethylene and propylene glycols were found to reduce PM formation in the experiments where they were added, which can be attributed to their inhibiting radicals and SOA formation from the reactions of the base case VOCs. This is not surprising since they are not predicted to form high molecular weight condensable products, and the availability experiments, discussed below, do not indicate that the glycols themselves are interacting with or partitioning into the aerosol phase.

Utilization of Environmental Chamber to Investigate Glycol Availability

The exploratory glycol availability experiments carried out for this project do not indicate that there is any tendency for ethylene or propylene glycol to interact with or partition into ammonium sulphate or ammonium bisulphate seed aerosol, at least for humidities up to ~30% and inorganic aerosol loadings up to ~10 $\mu g/m^3$. However, this does not rule out the possibility for interactions affecting glycol availability at higher humidities or aerosol loadings, or for different seed compositions (organic or acidic). The different seed compositions would most likely have the most significant impact as the organic layer may lead to enhanced gas-particle partitioning through sorption into the organic layer and the acidic seed may catalyze heterogeneous surface reactions. Although the capacity of the humidification and aerosol generation system limited the scope of what could be carried out for this project, these systems are currently being enhanced under funding from an EPA earmark, to permit studies of the effects of humidity on SOA. Therefore, our chamber should be capable of carrying out more comprehensive studies of effects of aerosol and humidity on availability and reactivity in the future.

In order to more comprehensively determine whether interactions with PM in the atmosphere significantly affect atmospheric availability of VOCs, it is necessary to carry out experiments with the full range of types of aerosol material that occur in the atmosphere, and with a greater range of humidity. Although chamber experiments are ultimately data needed to evaluate models for the atmosphere, they are expensive and may not be the most useful or sensitive screening tool. A potentially more sensitive approach that may be more useful for screening purposes would be to determine whether exposure to gas-phase coatings or other VOCs causes growth of aerosol particles under simulated atmospheric conditions. This would indicate partitioning of the VOC onto the particle, which may be occurring to a sufficient extent to affect ozone formation potential. This could be determined in flow experiments at much lower cost, and with a much greater variety of types of aerosol, that would be feasible environmental chamber experiments. However, once an effect of the VOC exposure to the aerosol is observed, then chamber experiments such as described in this report would be needed to investigate the system further, and to determine whether the effect the PM on reactivity is indeed significant.

Overall Conclusions and Recommendations

This project expanded the ozone mechanism evaluation database to several VOC compounds that are important in water-based coatings, which is important to reducing uncertainties in predictions of atmospheric impacts of these compounds. However, uncertainties exist in the mechanisms of aromatic hydrocarbons emitted from mobile and other sources that affect the results of the atmospheric simulation experiments with these compounds, and the atmosphere in which these VOCs react, that increase uncertainties in mechanism evaluation and atmospheric reactivity predictions for these and other compounds. Work is underway to improve the aromatics mechanisms, which should ultimately reduce these uncertainties. This is being covered by an ongoing CARB project, though additional work may be needed to resolve these problems. Once improved mechanisms for the compounds in the ambient VOC

mixture, then the results of these experiments can then be used to more comprehensively evaluate the mechanisms for the compounds of specific interest in this project. Therefore, the mechanism evaluation discussed in this report should not be considered the final result for this project.

Despite the uncertainties in the current mechanism and mechanism evaluation, we believe that the mechanism and reactivity estimates for the compounds presented in this report represent the current best estimate, and are appropriate for ozone reactivity assessments for regulatory and research at the present time.

Impacts on ground level ozone formation are not the only potential areas of concern for architectural coatings VOCs. Exceedences of PM standards are becoming an increasing concern and focus of research because of the known or suspected health impacts of atmospheric PM. Although SOA formation from the reactions of VOCs is not the only source of PM, it is an important PM source that will need to be included in any PM attainment strategies, particular for the finer PM that is if particular concern. The data obtained in this project, as well as previous studies in other chambers, clearly indicate that VOCs can differ significantly in their impact on secondary PM, and these differences will eventually have to be taken into account in any PM control strategy.

The results of this study indicate the difficulties that will be encountered when attempting to predict, even qualitatively, the relative PM impacts of different types of VOCs. For example, the PM impacts of two different water-based coatings VOCs were found to be different than predicted by their relative molecular weights, the aromatic contents of petroleum distillate hydrocarbon solvents were found to be poor predictors of their relative PM impacts, and benzyl alcohol was found to have an unexpectedly high PM impact compared to other aromatic compounds. Well-characterized environmental chamber data will be needed to develop *predictive* models for the affects of VOCs on PM formation, and this includes not only the characterization of the PM but also characterization of the gas-phase processes that lead to SOA precursor formation. Since PM formation is a highly nonlinear process, it is also essential that it be studied under the concentration ranges and chemical conditions that occur in ambient atmospheres. This project represents a beginning of the process of obtaining the types of well-characterized and low concentration data that are needed for PM mechanism evaluation.

A necessary component of the needed work to develop and evaluate predictive models for PM formation is characterization of PM background effects in chamber experiments. Previous chamber experiments have focused primarily on conducting experiments at much higher concentration ranges, where background effects are not as evident, or at least are easier to overlook. For that reason, there is little evidence in the literature for previous attempts to characterize PM background effects in chambers used for PM studies. However, the data obtained in this project indicate that measurable background effects exist in experiments simulating ambient concentrations, and "chamber models" for PM background effects will be needed when using such data for PM mechanism evaluation in low concentration. We suspect that these background effects are equal or larger in the other chambers that have been used for PM research, but because of the higher concentrations employed this has been less of a concern in the analysis of the results. But it would be useful if suitable characterization data were made available for the other chambers, so these effects can be appropriately assessed.

The current situation for PM mechanism evaluation is roughly analogous to the state of gas-phase mechanism evaluation in the mid 1970's, when the database needed for *quantitative* mechanism evaluation was extremely limited. In the case of SOA formation, it is important not only that the PM (and PM background effects) be adequately characterized, but that the gas-phase processes that lead to SOA precursors be as well characterized as they are for gas-phase evaluation experiments. Development of predictive mechanisms for SOA formation requires well-characterized experiments with different types of VOCs under a range of conditions, including varying reactant concentrations, PM levels, temperatures,

and humidities. This chamber, which was developed for gas-phase as well as PM mechanism evaluation in mind, is particularly well suited for this purpose. The work discussed this report represents an important beginning of this effort, but clearly significant additional work is needed before mechanisms for SOA formation have the predictive capability of current mechanisms for ozone formation.

Environmental chambers can also play a role in assessing and testing models for the interactions of gas-phase VOCs with PM and other surfaces, and therefore the availability of VOCs to react in the gas phase and promote ozone and SOA formation. The work for this project represents only a beginning in this regard, and additional work is clearly needed.

REFERENCES

Aschmann, S. M. and R. Atkinson (1998): "Kinetics of the Gas-Phase Reactions of the OH Radical with Selected Glycol Ethers, Glycols, and Alcohols," Int. J. Chem. Kinet, 30, 533-540.

ASTM (2003): "Standard Specification for Mineral Spirits (Petroleum Spirits) (Hydrocarbon Dry Cleaning Solvent)," ASTM Committee D01 on Paints and Related Coatings, Materials, and Applications, and Subcommittee D01.35 on Solvents, Plasticizers, and Chemical Intermediates. Approved Dec. 10, 2002 and published February 2003.

Atkinson, R. (1989): "Kinetics and Mechanisms of the Gas-Phase Reactions of the Hydroxyl Radical with Organic Compounds," J. Phys. Chem. Ref. Data, Monograph no 1.

Atkinson, R. (1997): "Gas Phase Tropospheric Chemistry of Volatile Organic Compounds: 1. Alkanes and Alkenes," J. Phys. Chem. Ref. Data, 26, 215-290.

Carter, W. P. L. (1994a): "Development of Ozone Reactivity Scales for Volatile Organic Compounds," J. Air & Waste Manage. Assoc., 44, 881-899.

Carter, W. P. L. (1994b): "Calculation of Reactivity Scales Using an Updated Carbon Bond IV Mechanism," Report Prepared for Systems Applications International Under Funding from the Auto/Oil Air Quality Improvement Research Program, April 12.

Carter, W. P. L. (2000a: "Documentation of the SAPRC-99 Chemical Mechanism for VOC Reactivity Assessment," Report to the California Air Resources Board, Contracts 92-329 and 95-308, May 8. Available at http://cert.ucr.edu/~carter/absts.htm#saprc99 and http://www.cert.ucr.edu/~carter/reactdat.htm.

Carter, W. P. L. (2000b): "Implementation of the SAPRC-99 Chemical Mechanism into the Models-3 Framework," Report to the United States Environmental Protection Agency, January 29. Available at http://www.cert.ucr.edu/~carter/absts.htm#s99mod3.

Carter, W. P. L. (2002): "Development of a Next Generation Environmental Chamber Facility for Chemical Mechanism and VOC Reactivity Research," Draft Research Plan and First Progress Report to the United States Environmental Protection Agency Cooperative Agreement CR 827331-01-0, January 3. Available at http://www.cert.ucr.edu/~carter/epacham.

Carter, W. P. L. (2003): "The SAPRC-99 Chemical Mechanism and Updated VOC Reactivity Scales, Updated and Corrected Data as of February 5, 2003," Available at http://www.cert.ucr.edu/~carter/reactdat.htm.

Carter, W. P. L. (2004): "Evaluation of a Gas-Phase Atmospheric Reaction Mechanism for Low NO_x Conditions," Final Report to California Air Resources Board Contract No. 01-305, May 5. Available at http://www.cert.ucr.edu/~carter/absts.htm#lnoxrpt.

Carter, W. P. L., R. Atkinson, A. M. Winer, and J. N. Pitts, Jr. (1982): "Experimental Investigation of Chamber-Dependent Radical Sources," Int. J. Chem. Kinet., 14, 1071.

Carter, W. P. L. and R. Atkinson (1987): "An Experimental Study of Incremental Hydrocarbon Reactivity," Environ. Sci. Technol., 21, 670-679

Carter, W. P .L., and Lurmann, F. W. (1991) Evaluation of a detailed gas-phase atmospheric reaction mechanism using environmental chamber data. Atmos. Environ. 25A:2771-2806.

Carter, W. P. L., J. A. Pierce, I. L. Malkina, D. Luo and W. D. Long (1993): "Environmental Chamber Studies of Maximum Incremental Reactivities of Volatile Organic Compounds," Report to Coordinating Research Council, Project No. ME-9, California Air Resources Board Contract No. A032-0692; South Coast Air Quality Management District Contract No. C91323, United States Environmental Protection Agency Cooperative Agreement No. CR-814396-01-0, University Corporation for Atmospheric Research Contract No. 59166, and Dow Corning Corporation. April 1. Available at http://www.cert.ucr.edu/~carter/absts.htm#rct1rept

Carter, W. P. L., D. Luo, I. L. Malkina, and J. A. Pierce (1995a): "Environmental Chamber Studies of Atmospheric Reactivities of Volatile Organic Compounds. Effects of Varying ROG Surrogate and NO_x," Final report to Coordinating Research Council, Inc., Project ME-9, California Air Resources Board, Contract A032-0692, and South Coast Air Quality Management District, Contract C91323. March 24. Available at http://www.cert.ucr.edu/~carter/absts.htm#rct2rept.

Carter, W. P. L., D. Luo, I. L. Malkina, and D. Fitz (1995b): "The University of California, Riverside Environmental Chamber Data Base for Evaluating Oxidant Mechanism. Indoor Chamber Experiments through 1993," Report submitted to the U. S. Environmental Protection Agency, EPA/AREAL, Research Triangle Park, NC., March 20..

Carter, W. P. L., D. Luo, and I. L. Malkina (1997): "Investigation of the Atmospheric Ozone Formation Potential of Propylene Glycol," Report to Philip Morris, USA, May 2. Available at http://www.cert.ucr.edu/~carter/absts.htm#pgrept

Carter, W. P. L., J. H. Seinfeld, D. R. Fitz and G. S. Tonnesen (1999): "Development of a Next-Generation Environmental Chamber Facility for Chemical Mechanism and VOC Reactivity Evaluation," Research Proposal to the United States Environmental Protection Agency, February 22. (Available at http://www.cert.ucr.edu/~carter/epacham/proposal.htm.)

Carter, W. P. L. and I. L. Malkina (2005): "Evaluation of Atmospheric Impacts of Selected Coatings VOC Emissions," Final report to the California Air Resources Board Contract No. 00-333, March 15. Available at http://www.cert.ucr.edu/~carter/absts.htm#coatrpt.

Cocker, D. R., R. C. Flagan, and J. H. Seinfeld. (2001). "State-of-the-Art Chamber Facility for Studying Atmospheric Aerosol Chemistry," Environ. Sci. Technol. 35, 2594-2601.

EPA (2005): "National Ambient Air Quality Standards (NAAQS)," http://www.epa.gov/air/criteria.html, last modified June 13.

Hastie, D. R, Mackay, G. I., Iguchi, T., Ridley, B. A.; and Schiff, H. I. (1983): "Tunable diode laser systems for measuring trace gases in tropospheric air," Environ. Sci. Technol. 17, 352A-364A.

IUPAC (2002a): IUPAC Subcommittee for Gas Kinetic Data Evaluation, data sheets for individual files of reaction data, available at http://www.iupac-kinetic.ch.cam.ac.uk. Data sheet HOX_VOC17. Dated August 9, 2002.

IUPAC (2002b): IUPAC Subcommittee for Gas Kinetic Data Evaluation, data sheets for individual files of reaction data, available at http://www.iupac-kinetic.ch.cam.ac.uk. Data sheet P5, dated May 16, 2002.

Jacobsen, N. W. and R. G. Dickinson (1994): "Spectrometric Assay of Aldehydes as 6-Mercapto-3-substituted-s-triazolo(4,3-b)-s-tetrazines," Analytical Chemistry 46/2 (1974) 298–299.

Johnson, G. M. (1983): "Factors Affecting Oxidant Formation in Sydney Air," in "The Urban Atmosphere -- Sydney, a Case Study." Eds. J. N. Carras and G. M. Johnson (CSIRO, Melbourne), pp. 393-408.

Kwok, E. S. C., C. Takemoto and A. Chew (2000): "Methods for Estimating Maximum Incremental Reactivity (MIR) of Hydrocarbon Solvents and their Classification," Appendix C to "Initial Statement of Reasons for the Proposed Amendments to the Regulation for Reducing Volatile Organic Compound Emissions from Aerosol Coating Products and Proposed Tables of Maximum Incremental Reactivity (MIR) Values, and Proposed Amendments to Method 310, 'Determination of Volatile Organic Compounds in Consumer Products'," California Air Resources Board, Liu, B. Y. H.; Lee, K. W (1975): "An aerosol generator of high stability," Am. Ind. Hyg. J. 1975, 861.

Motallebi N., C. A. Taylor, and B. E. Croes (2003): "Particulate matter in California: 2. Spatial, temporal, and compositional patterns of PM2.5, PM10-2.5, and PM10". J. Air Waste Manage. Assoc., 53 1517-1530.

NIOSH (1994): "Sulfite titration of formaldehyde stock solution: modified Method 3500," NIOSH Manual of Analytical Methods, NMAM, fourth edition, August 15.

Notling, F., F. Witte, and C. Zetzsch (1988): Report to the Umweltbundesamt, December, 1987; Private communication to R. Atkinson.

Pankow J. F (1994): "An absorption-model of gas-particle partitioning of organic-compounds in the atmosphere," Atmos. Environ. 1994, Vol. 28, No. 2, 185-188.

Pankow J. F. (1994): "An absorption-model of the gas aerosol partitioning involved in the formation of secondary organic aerosol," Atmos. Environ. 1994, Vol. 28, No. 2, 189-193.

Quesenberry, M. S. and Y. C. Lee (1996): "A Rapid Formaldehyde Assay Using Puprald Reagent: Application under Periodation Conditions," Analytical Biochemistry. 234, 50–55.

RRWG (1999): "VOC Reactivity Science Assessment", Prepared by the Reactivity Research Working Group Science Team, May 5, Available at http://www.cgenv.com/Narsto/reactinfo.html.

Schiff, H.. I., Mackay, G. I. and Bechara, J. (1994): "The Use of Tunable Diode Laser Absorption Spectroscopy for Atmospheric Measurements", Res. Chem. Intermed. 20, 1994, pp 525-556.

Song, C., K. Na, and D.R. Cocker (2005): "Impact of the Hydrocarbon to NOx Ratio on Secondary Organic Aerosol Formation," Environ. Sci. Technol. 39(9):3143-3149.

Wang SC and Flagan RC (1990): "Scanning Electrical Mobility Spectrometer," Aerosol Science and Technology. 13(2): 230-240 1990

Zafonte, L., P. L. Rieger, and J. R. Holmes (1977): "Nitrogen Dioxide Photolysis in the Los Angeles Atmosphere," Environ. Sci. Technol. 11, 483-487.

APPENDIX A. PROPOSED AMBIENT SURROGATE EVALUATION WORK

Environmental chamber experiments with ambient ROG surrogates are used for testing model predictions for ozone and (eventually) PM formation under controlled but chemically realistic conditions and also to serve as the "base case" in the incremental reactivity experiments where effects of VOCs on O_3 and (eventually) PM formation is determined. Experiments with base case ROG surrogates are also highly relevant to assessing the impacts of mobile source emissions because the base case ROG mixture currently employed (Carter et al, 1995b) is based on mixtures derived ambient air analyses (Jeffries et al, 1989) that detect primarily mobile source VOCs. Therefore, providing data to evaluate mechanisms for the base case also provided needed data to test models for mobile source impacts in the atmosphere. Although there is an extensive database of experiments from previous chambers that have been used for evaluating mechanisms for mobile source VOCs (e.g., Carter, 2000 and references therein), most of the experiments were conducted at higher than current ambient concentrations and contain no information on PM impacts. The base case assessment experiments for this project would be an important addition to the mechanism evaluation database, in addition to providing the base case data needed for VOC reactivity assessment studies.

The experiments we have carried out thus far employed a simplified 8-component surrogate that we determined was adequate for use in a base case for incremental reactivity experiments for testing mechanisms for effects of VOCs on O_3. This employed essentially the same degree of lumping in terms of representing VOC classes as current airshed models (each compound corresponding to a model species), which means that use of a more complex surrogate would not necessarily be represented by more complex models. Use of a simplified surrogate such as this was an advantage for this purpose, since it simplified the experiments and the mechanism evaluation process. The relative composition of this surrogate was derived based on analysis of air quality data carried out by Jeffries in 1989[5], which in turn was based on morning measurements in various cities by Lonneman in the 1980's[6].

Although probably suitable for as a base case mixture for mechanism evaluation of O_3 reactivities of added VOCs, there is a concern about whether this adequately represents the mixture of VOCs in actually emitted into urban atmospheres today. Also, when designing this surrogate no effort has been made to obtain a mixture that represents the PM forming potential of ambient VOCs, and probably it doesn't adequately represent this because generally the lowest molecular weight compound is used to represent all compounds of a given type. Therefore, one of the objectives of this project as proposed was to evaluate the organic surrogates we use in environmental chamber experiments to represent the reactive organic gas (ROG) in urban atmospheres.

Accordingly, as a component of this SCAQMD project we proposed to design a new, more complex ROG surrogate to more closely represent current emissions, both in term PM formation potential as well as reactivity to form ozone. The plan included conducting a limited number of chamber experiments using the new surrogate to determine to evaluate the performance of the SAPRC-99 mechanism in predicting O_3 formation at various ROG, NO_x, and ROG/NO_x is comparable to or different than the results obtained with the larger body of experiments with the simpler surrogate. Incremental

---

[5] Jeffries, H. E., K. G. Sexton, J. R. Arnold, and T. L. Kale (1989): "Validation Testing of New Mechanisms with Outdoor Chamber Data. Volume 2: Analysis of VOC Data for the CB4 and CAL Photochemical Mechanisms," Final Report, EPA-600/3-89-010b

[6] Lonneman, W. A. (1986): "Comparison of 0600-0900 AM Hydrocarbon Compositions Obtained from 29 Cities," Proceedings APCA/U.S. EPA Symposium on Measuremtns of Toxic Air Pollutants, Raleigh, NC

reactivity experiments would also be carried out with selected compounds, to determine whether there is any difference in mechanism performance in simulating incremental reactivities of these different types of VOCs, compared to the experiments with the simpler surrogate. PM formation was also to be measured during these experiments, with the results being compared with the PM formed in the experiments with the simpler surrogate. The ozone and gas-phase reactivity data would be useful to assess the relevance of the larger data of ambient surrogate and incremental reactivity experiments that have already been conducted. The PM data may be potentially more useful for evaluating mechanisms for PM formation under more chemically realistic atmospheric conditions.

In order that the experiments with any new base ROG surrogate be useful and credible, it is important that consensus be obtained as to the ambient ROG mixture that this mixture is intended to represent. For this purpose, we sought guidance from the SCAQMD and the CARB staff whether it is better to base the surrogate on ambient air measurements or emissions data, and which emissions or ambient measurement data should be used as the basis for the design composition. The consensus was that the surrogate should be based on ambient air data, and that the CARB and SCAQMD staff should provide guidance on the best dataset to use. Unfortunately, the CARB and SCAQMD staff were not able to provide recommendations as to which ambient measurement datasets to use as a basis for deriving a new base ROG surrogate in the time frame required for this project, apparently because of a lack of necessary time and resources.

Because recommendations about the composition of a new base ROG surrogate was not provided when needed for this project, it was decided that it was best to defer this study to a later date when consensus is reached concerning the target base ROG composition. Instead, the resources allocated to this task were used to conduct chamber experiments for an additional type of coatings VOC. Therefore, this work will need to be carried out in a subsequent project, which is beyond the scope of the present report.

APPENDIX B. CHAMBER EXPERIMENT LISTING

Table B-1.   Summary chamber experiments relevant to this project.

Run [a]	Date	Type [b]	Purpose and Applicable Conditions.	Results
245	1/30/04	MOIR/2 Surrogate + Propylene Glycol	Standard MOIR/2 Incremental reactivity experiment with 0.4 ppm propylene glycol added to Side B	Poor quality GC data for glycol. Experimental conditions and selected gas-phase results summarized on Table 7, PM results shown on Table 8, Table 10, Figure 27 and Figure 28, and model simulation results shown on Figure 10.
250	2/11/04	MOIR/2 Surrogate + Ethylene Glycol	Standard MOIR/2 Incremental reactivity experiment with 0.4 ppm ethylene glycol added to Side B	Poor quality GC data for glycol. Experimental conditions and selected gas-phase results summarized on Table 7, PM results shown on Table 8, Table 10, Figure 27 and Figure 28, and model simulation results shown on Figure 12.
251	2/12/04	CO - Air	Control experiment to test for NO_x offgasing effects. 50 ppm CO injected in both sides.	Data fit by HONO offgasing rate parameter (RN-I) of 15 and 10 ppt for Sides A and B, respectively, which is within normal range.
252	2/13/04	MOIR/2 Surrogate + Propylene Glycol	MOIR/2 reactivity experiment with 0.4 ppm glycol in Side B.	Experimental conditions and selected gas-phase results summarized on Table 7, PM results shown on Table 8, Table 10, Figure 27 and Figure 28, and model simulation results shown on Figure 10.
253	2/20/04	MOIR/2 Surrogate + Ethylene Glycol	Same as EPA250 except glycol on Side A.	Experimental conditions and selected gas-phase results summarized on Table 7, PM results shown on Table 8, Table 10, Figure 27 and Figure 28, and model simulation results shown on Figure 12.
257	3/11/04	MIR Surrogate + Propylene Glycol	Standard MIR reactivity experiment with 0.4 ppm of Propylene glycol on side B	Arc was off for ~20 minuets in the middle of the run. Experimental conditions and selected gas-phase results summarized on Table 7, PM results shown on Table 8, Table 10, Figure 27 and Figure 28, and model simulation results shown on Figure 9.
258	3/12/04	MOIR/2-like Surrogate + Ethylene Glycol	Attempted to run standard MIR surrogate experiment but non-standard base case conditions used because of injection error. 0.95 ppmC surrogate mixture and 30 ppb NOx injected in both reactors, making conditions closer to MOIR/2. 0.3 ppm of Ethylene glycol on side B.	Experimental conditions and selected gas-phase results summarized on Table 7, PM results shown on Table 8, Table 10, Figure 27 and Figure 28, and model simulation results shown on Figure 12.

Run [a]	Date	Type [b]	Purpose and Applicable Conditions.	Results
260	3/17/04	Propene-NOx (Blacklights)	Control experiment to test side equivalency for PM. Mixing fans not used.	Good side equivalency and gas-phase results reasonably consistent with model predictions. PM results summarized on Table 8 and Figure 24.
262	3/19/04	Propene-NOx (Side A and Chamber Enclosure)	Approximately 0.5 ppm propene and 25 ppb NOx injected in Side A and chamber enclosure to test for contamination leading to PM formation in enclosure.	Approximately 180 ppb O3 in Side A but only ~30 ppb O3 formed in enclosure because of dilution. PM volume in enclosure less than 1 $\mu g/m^3$ at start of experiment and declined during run. Reactor PM data summarized on Table 8 and Figure 24.
			Mixing system and dump openings covered with panels with Teflon film.	
263	3/22/04	Pure Air Irradiation	Test for background PM formation with mixing system openings covered.	PM formation in both reactors comparable to previous pure air experiments, and still higher on Side A. See Table 8, Figure 24 and Figure 25.
264	3/23/04	Pure Air Irradiation	Repeat background PM test with mixing system openings covered.	Somewhat less PM formation than previous run. Problems with PM analyzer at end of experiment
265	3/24/04	Pure Air Irradiation	Repeat background PM test with mixing system openings covered.	Somewhat less PM formation than previous runs. See Table 8, Figure 24 and Figure 25.
266	3/25/04	Pure Air Irradiation (Blacklights)	Repeat background PM test with mixing system openings covered. Reactors under higher pressure to reduce leakage	Comparable PM formation as previous run. See Table 8, Figure 24 and Figure 25.
267	3/29/04	Pure Air Irradiation (Blacklights)	Repeat background PM test with mixing system openings covered. Air aged 3 days after final fill to determine if wall offgasing over time before experiment is affecting results.	Comparable PM formation as previous runs. See Table 8, Figure 24 and Figure 25.
			Covers on mixing system and dump openings removed. (Back to standard configuration)	
268	3/30/04	Pure Air Irradiation (Blacklights)	Repeat background PM test with chamber returned to standard conditions	Higher PM levels in both reactors. PM results comparable to run immediately after covers added (EPA263). See Table 8, Figure 24 and Figure 25.
269	3/31/04	Pure Air Irradiation (Blacklights)	Repeat background PM test to see if background PM decreases with time.	Lower PM levels than previous run. See Table 8, Figure 24 and Figure 25.
270	4/1/04	Pure Air Irradiation (Blacklights)	Repeat background PM test to see if background PM decreases with time.	Similar PM levels as previous run. See Table 8, Figure 24 and Figure 25.

Run [a]	Date	Type [b]	Purpose and Applicable Conditions.	Results
271	4/2/04	Pure Air Irradiation (Arc lights)	Repeat background PM test to see if background PM decreases with time, and see if different with arc lights.	Somewhat less PM than previous runs. See Table 8, Figure 24 and Figure 25.
272	4/6/04	Pure Air Irradiation	Repeat previous background PM experiment to check for trend over time.	PM data could not be processed.
273	4/7/04	MIR Surrogate + Propylene Glycol (Blacklights)	Standard MIR reactivity experiment for propylene glycol except blacklights used (arc lights inoperative). 0.2 ppm glycol added to Side A.	Experimental conditions and selected gas-phase results summarized on Table 7, PM results shown on Table 8, Table 10, Figure 27 and Figure 28, and model simulation results shown on Figure 9.
274	4/9/04	Pure air irradiation	Repeat previous background PM experiment to check for trend over time.	Similar PM levels as previous blacklight runs. See Table 8, Figure 24 and Figure 25.
276	4/12/04	Long term pure air irradiation (Blacklights)	Determine background PM formation over longer time period. Irradiated for ~22 hours.	Similar PM levels during first 6 hours as previous runs. See Table 8, Figure 24 and Figure 25. PM volume corrected for wall losses increased approximately linearly with time after formation began.
277	4/15/04	MIR Surrogate + Propylene Glycol	Standard MIR reactivity experiment with 0.2 ppm glycol added to Side A. Arc lights used.	Experimental conditions and selected gas-phase results summarized on Table 7, , PM results shown on Table 8, Table 10, Figure 27 and Figure 28, and model simulation results shown on Figure 9.
278	4/16/04	MIR Surrogate + Ethylene Glycol	MIR reactivity experiment with 0.3 ppm ethylene glycol added to Side B.	Experimental conditions and selected gas-phase results summarized on Table 7, PM results shown on Table 8, Table 10, Figure 27 and Figure 28, and model simulation results shown on Figure 12.
285	4/26/04	CO - Air (Blacklights)	Characterize NO_x offgasing ~50 ppm CO injected into both reactors.	Results indicate HONO offgasing parameters of 12.5 and 8 ppt for Sides A and B, respectively, consistent with chamber effects model.
295	5/7/04	Pure Air Irradiation (Blacklights)	Determine background PM formation over time	Somewhat higher PM than the previous pure air irradiations but within the normal range. See Table 8, Figure 24 and Figure 25.
306	5/26/04	CO - NO_x (Blacklights)	Characterize chamber radical source. ~25 ppb NO_x and ~50 ppm CO injected into both reactors.	Results indicate HONO offgasing parameters of 8 and 4 ppt for Sides A and B, respectively, somewhat lower than predicted by chamber effects model.
307	5/27/04	Pure Air Irradiation (Blacklights)	Determine background PM formation over time	Similar PM levels as EPA295. See Table 8, Figure 24 and Figure 25.

Run [a]	Date	Type [b]	Purpose and Applicable Conditions.	Results
308	6/2/04	CO - Air with seed aerosol	Injected ~75 ppm CO and 1.5 $\mu g/m^3$ ammonium sulfate seed aerosol into both reactors. (Capacity of aerosol generation system limited output.)	PM levels declined during the irradiation. O_3 data fit by HONO offgasing parameter (RN-I) value of 20 ppt for Side A and 15 ppt for Side B. This is somewhat larger than the standard chamber model values of 13 and 9 ppt for Side A and B, respectively, but not outside the normal variability.
309	6/3/04	MOIR/2 Surrogate - NOx with Seed Aerosol (Blacklights)	Standard MOIR/2 Surrogate - NO_x experiment in both reactors, except that ~1.5 $\mu g/m^3$ NH_4SO_4 seed aerosol added to both reactors.	Gas-phase reactivity results comparable to normal experiments and fit by standard mechanism; see Figure 30. PM volume increased to 2.5 and 2 $\mu g/m^3$ in Side A and B, respectively.
312	6/8/04	Pure Air Irradiation	Determine background PM formation over time. Arc light used	PM levels comparable to previous pure air experiments. See Table 8, Figure 24 and Figure 25.
313	6/10/04	Pure Air Irradiation with Wet Seed Aerosol	Determine PM formation and gas-phase background effects in presence of humidity and seed aerosol. Only Side A used because of limited humidification capacity. Humidified to ~30% RH. ~8 $\mu g/m^3$ NH_4SO_4 seed aerosol added.	PM volume and number declined slowly during experiment. O_3 formation consistent with model prediction using standard chamber model.
314	6/11/04	CO-NO_x with Wet Seed Aerosol on side A	Determine NOx offgasing background effects in presence of humidity and seed aerosol. Only Side A used. Humidified to ~25% RH. ~8 $\mu g/m^3$ NH_4SO_4 seed aerosol added.	PM volume and number declined slowly during experiment. O_3 formation indicated HONO offgasing parameter of 12.5 ppt, consistent with standard chamber model.
315	6/16/04	Glycol Dark Decay	Determine if presence of humidity and seed aerosol affects loss of glycols in the dark. Injected 0.3 ppm each ethylene and propylene glycols. Side A humidified to 35%, and 9 $\mu g/m^3$ NH_4SO_4 seed aerosol added. No humidity or aerosol in Side B.	Essentially no measurable decay of either glycol in either reactor. See Figure 31.
316	6/17/04	MIR Surrogate + Propylene Glycol with Wet Seed Aerosol	Determine if humidity and seed aerosol affects surrogate + glycol experiment. Standard MIR surrogate and 0.4 ppm propylene glycol, ~25% RH and ~9 $\mu g/m^3$ NH_4SO_4 seed aerosol added to Side A. Side B not used.	PM levels declined slowly during irradiation. Gas-phase results consistent with results without humidity or added aerosol. See Figure 32.

Run [a]	Date	Type [b]	Purpose and Applicable Conditions.	Results
317	6/18/04	Pure Air Irradiation	Determine background PM formation over time. Arc light used. No humidity or seed aerosol.	PM levels higher than previous pure air experiments but not far outside normal range. See Table 8, Figure 24 and Figure 25.
319	6/21/04	MIR Surrogate + Benzyl Alcohol	Standard MIR reactivity experiment with 0.1 ppm Benzyl alcohol added to Side A.	Experimental conditions and selected gas-phase results summarized on Table 7, PM results shown on Table 10, , Figure 27 and Figure 28, and model simulation results shown on Figure 19.
320	6/22/04	MOIR/2 Surrogate + Benzyl Alcohol	Standard MOIR/2 reactivity experiment with 0.1 ppm Benzyl alcohol added to Side B.	Very high PM formation on added benzyl alcohol side compared to other reactivity experiments. No PM data for last part of experiment. Experimental conditions and selected gas-phase results summarized on Table 7, PM results shown on Table 10 , Figure 27 and Figure 28, and model simulation results shown on Figure 19.
321	6/23/04	Benzyl Alcohol - NO_x (Blacklights)	Mechanism evaluation experiment for benzyl alcohol. 0.4 ppm benzyl alcohol added to both sides, 40 ppb NO on Side A and 20 on Side B. Blacklights used.	Similar PM formation (~120 ug/m3) on both sides, but earlier PM formation on low NO_x side. Experimental conditions and selected gas-phase results summarized on Table 7 and model simulation results shown on Figure 17.
322	6/24/04	Benzyl Alcohol - NO_x	Mechanism evaluation experiment for benzyl alcohol, but using different light source. Same injections as EPA321, except arc used.	Results similar to arc light experiment. Experimental conditions and selected gas-phase results summarized on Table 7 and model simulation results shown on Figure 17.
323	6/25/04	MIR Surrogate + Benzyl Alcohol	Standard MIR reactivity experiment with 0.05 ppm benzyl alcohol on Side B.	High PM formation on benzyl alcohol side. Experimental conditions and selected gas-phase results summarized on Table 7, PM results shown on Table 10 , Figure 27 and Figure 28, and model simulation results shown on Figure 19.
324	6/28/04	MIR Surrogate + Ethylene Glycol with Wet Seed Aerosol	Determine if humidity and a more hydroscopic seed aerosol affects surrogate + ethylene glycol experiment. Standard MIR surrogate and 0.3 ppm ethylene glycol, ~30% RH and ~7 $\mu g/m^3$ $(NH_4)_2HSO_4$ seed aerosol added to Side A. Side B not used.	PM levels declined slowly during irradiation. Gas-phase results consistent with results without humidity or added aerosol. See Figure 33.

Run [a]	Date	Type [b]	Purpose and Applicable Conditions.	Results
325	6/29/04	Benzyl Alcohol - NO_x + CO	Mechanism evaluation experiment with benzyl alcohol. Determine if effect of adding CO similar to observed with other aromatics. 0.25 ppm benzyl alcohol and 40 ppb NO_x added to both sides, with 24 ppm CO on Side B.	Added CO caused higher O_3 formation but somewhat reduced formation of PM. Experimental conditions and selected gas-phase results summarized on Table 7 and model simulation results shown on Figure 17 and Figure 18.
326	6/30/04	CO- NO_x	Evaluate chamber effects related to background radical source.	No PM formation. Gas-phase data fit by HONO offgasing parameter (RN-I) value of 20 ppt for Side A and 25 ppt for Side B. This is somewhat larger than the standard chamber model values of 13 and 9 ppt for Side A and B, respectively, and probably outside general variability for Side B.
327	7/1/04	Pure Air Irradiation	Determine background PM formation over time. Arc light used. Possible contamination of reactor with propane.	Very little PM formation, even on Side A. Results considered to be anomalous, and may be problem with instrument. Data not included in summaries.
328	7/2/04	Ozone Decay	Determine O_3 wall loss rate. 50 ppm CO and 0.3 ppm O_3 added to both sides.	O_3 decayed at ~0.6%/hour in both reactors, which is in the expected range. However, CO decayed at ~0.3 %/hour in both reactors, and if this reflects dilution then the O_3 decay rate is about half the expected value.
329	7/7/04	Propene - NOx	Standard propene - NOx control experiment. 25 ppb NOx and 0.25 ppm propene injected into both reactors.	Some propane contamination observed, but that should not affect gas-phase results significantly. Somewhat higher propene levels measured in Side A, and consequently higher O3 formed in that side. Results consistent with model predictions.
330	7/8/04	Actinometry	Quartz tube actinometry experiment inside Reactor A. Used both blacklights and arc light.	NO_2 photolysis rate with arc light was 0.28 min^{-1}, about 7% higher than previous in-reactor actinometry results. NO_2 photolysis rate with black lights was anomalously low and was not used.
331	7/9/04	Actinometry	Repeated quartz tube actinometry experiments inside both reactors with both arc and blacklights	NO_2 photolysis rate with arc light was 0.29 and 0.28 min^{-1} inside Reactors A and B, respectively, consistent with previous experiment. NO_2 photolysis rates with black lights were 0.16 and 0.17 min^{-1} in Reactors A and B, respectively, consistent with trend from previous experiments.
332	7/12/04	Pure Air Irradiation	Test whether entering the reactors for in-chamber actinometry measurements affected PM measurements.	PM instrument failed so no PM data obtained.

Run [a]	Date	Type [b]	Purpose and Applicable Conditions.	Results
333	7/13/04	Pure Air Irradiation	Repeat previous experiment	Results of subsequent experiments indicated that there was possible propane contamination (~0.5 ppm) in the reactor. Essentially no PM formation observed. Since the presence of this amount of propane would suppress OH and therefore possibly PM formation, the results of the experiment are considered to be inconclusive.
334	7/14/04	MOIR/2 Surrogate Side Equivalency Test	Test for side equivalency of gas-phase results and obtain additional base case PM data in each reactor.	GC data indicated propane contamination (~0.5 ppm) from outside source, but presence not expected to significantly affect results of this type of experiment. Good side equivalency observed and results consistent with model predictions.
335	7/16/04	MOIR/2 Surrogate + DGBE	MOIR/2 reactivity experiment with 50 ppb diethylene glycol butyl ether (DGBE) added to Side A.	Experimental conditions and selected gas-phase results summarized on Table 7, PM results shown on Table 8, Table 10, Figure 27 and Figure 28, and model simulation results shown on Figure 16.
336	7/19/04	Pure Air Irradiation	Test for background PM over time	PM levels in both reactors relatively high but consistent with previous pure air experiments with useable PM data. See Table 8, Figure 24 and Figure 25.
		Replaced Both Reactors		
338	8/16/04	Pure Air Irradiation	Test for background PM in new reactor	PM levels may be approximately the same range as previous pure air runs but results rejected because of instrument problems.
339	8/17/04	Pure Air Irradiation	Repeat test for background PM in new reactor	PM levels much lower than observed in previous experiments, but still higher on Side A. See Table 8, Figure 24 and Figure 25.
340	8/18/04	Pure Air Irradiation	Repeat test for background PM in new reactor	Results similar to EPA339. See Table 8, Figure 24 and Figure 25.
341	8/19/04	Propene - NO_x	Control experiment and background PM determination. ~15 ppb NO_x and 0.25 ppm propene injected into both reactors.	Good side equivalency and results consistent with model predictions. PM results summarized on Table 8 and Figure 24.
342	9/20/04	Dark PM background test	PM measured with pure air in dark in both reactors.	No significant PM formation observed. See Table 8.
344	8/25/04	CO - Air	Test for NO_x offgasing in new reactor. ~50 ppm CO added bo both sides.	Data fit using HONO offgasing parameter (RN-I) of 1 and 2 ppt for Side A and B, respectively, which are much lower than in previous experiments.
345	8/26/04	CO - NO_x	Test for background radical source in new reactor. ~25 ppb NO_x and ~50 ppm CO injected in both reactors.	Data fit using HONO offgasing parameter (RN-I) of 2.5 and 1.8 ppt for Side A and B, respectively, which are consistent with results of EPA345.

Run [a]	Date	Type [b]	Purpose and Applicable Conditions.	Results
346	8/27/04	CO - NO$_x$	Repeated previous experiment using new NO tank. (Some previous NO tanks had apparent HONO contamination that affected results of radical source characterization runs.)	Data fit using HONO offgasing parameter (RN-I) of 2.5 for both reactors, which is consistent with previous runs. No effect of changing NO tank seen.
347	8/30/04	Pure Air Irradiation	Test for background PM in reactor after several experiments	Relatively high PM levels in Side A. See Table 8, Figure 24 and Figure 25.
352	9/9/04	MIR Surrogate + DGBE	MIR reactivity experiment with 50 ppb DGBE added to Side B.	Experimental conditions and selected gas-phase results summarized on Table 7, PM results shown on Table 8, Table 10, Figure 27 and Figure 28, and model simulation results shown on Figure 16.
353	9/10/04	MOIR/2 Surrogate + DGBE	MOIR/2 reactivity experiment with 50 ppb DGBE added to Side B.	Experimental conditions and selected gas-phase results summarized on Table 7, PM results shown on Table 8, Table 10, Figure 27 and Figure 28, and model simulation results shown on Figure 16.
362	9/23/04	CO-NO$_x$	Character NO$_x$ offgasing. ~35 ppb CO and ~10 ppb NO$_x$ injected into both reactors.	Results indicate a HONO offgasing parameters (RN-I) of 6 and 4.5 for Sides A and B, respectively, slightly higher than previous experiments but still relatively low.
401	12/11/04	CO-NO$_x$ (Blacklights)	Characterize NO$_x$ offgasing. 50 ppm CO and ~15 ppb NOx added to both reactors.	Data fit using HONO offgasing parameter (RN-I) of 6 and 4 ppt for Side A and B, respectively, which is very similar to results of EPA362.
404	12/15/04	Non-aromatic surrogate + Propylene Glycol	Reactivity experiment with no aromatics in base case experiment to see if this may affect biases in simulations of glycol reactivity experiments. 0.6 ppmC surrogate mixture with aromatics removed and 30 ppb NOx injected into both reactors, with 0.2 ppm propylene glycol added to Side B.	Experimental conditions and selected gas-phase results summarized on Table 7 and model simulation results shown on Figure 9.
405	12/16/04	CO-Air (Blacklights)	Characterize NO$_x$ offgasing in reactor at time of non-aromatic surrogate experiments. ~100 ppm CO added to both reactors.	Data fit using HONO offgasing parameter (RN-I) of 5 and 2 ppt for Side A and B, respectively, which are consistent with the results of EPA401.
	1/05	Replaced Bottom of Side A Reactor, which was damaged in an accident.		

Run [a]	Date	Type [b]	Purpose and Applicable Conditions.	Results
411	1/26/05	CO-NO$_x$ (Blacklights)	Characterize radical source. First run after maintenance in chamber. ~50 ppm CO and ~25 ppb NO$_x$ injected in both reactors.	Results indicate HONO offgasing parameters (RN-I) of 20 ppt in Side A and 12 ppt in Side B, which are significantly higher than previously in this reactor, but within the range observed with earlier reactors. May be anomalously high because of maintenance.
414	2/7/05	CO-Air	Characterize NO$_x$ offgasing. ~50 ppm CO injected in both reactors.	Results indicate HONO offgasing parameters (RN-I) of 5 and 4 ppt in Sides A and B, respectively, which is within the normal range for the present reactor. This suggests that the high results for EPA411 are anomalous.
415	2/8/05	Non-aromatic surrogate + Ethylene Glycol	Same purpose and procedures as with EPA404 except with ethylene glycol.	Experimental conditions and selected gas-phase results summarized on Table 7 and model simulation results shown on Figure 13.
437	3/14/05	CO-NO$_x$	Characterize radical source. ~50 ppm CO and ~30 ppb NO$_x$ injected into both reactors.	Results indicate HONO offgasing parameters (RN-I) of 4 and 2.5 ppt in Sides A and B, respectively, which is within the normal range for the present reactor.

[a] EPA Run number. Gaps in run numbers reflect experiments carried out for other projects, or experiments that were aborted because of equipment or instrumentation problems, and that are not expected to affect the characterization results.

[b] Unless indicated otherwise, "Surrogate" refers to the 8-component "Full Surrogate" as used in previous environmental chamber incremental reactivity studies in our laboratories, except that formaldehyde was removed and the other ROG components were increased by 10% to yield approximately the same reactivity as discussed by Carter and Malkina (2005). The designation "MIR Surrogate" refers to experiments with 0.55 ppmC base case surrogate and 30 ppb NO$_x$, The designation "MOIR/2 Surrogate" refers to experiments with 1.1 ppmC base case surrogate and 25 ppb NO$_x$.